

# On Approximate Inference for Generalized Gaussian Process Models

**Lifeng Shang**

*Department of Computer Science  
City University of Hong Kong*

LSHANG@CITYU.EDU.HK

**Antoni B. Chan**

*Department of Computer Science  
City University of Hong Kong*

ABCHAN@CITYU.EDU.HK

(This manuscript was submitted for review on July 12, 2013)

**Editor:**

## Abstract

A generalized Gaussian process model (GGPM) is a unifying framework that encompasses many existing Gaussian process (GP) models, such as GP regression, classification, and counting. In the GGPM framework, the observation likelihood of the GP model is itself parameterized using the exponential family distribution (EFD). In this paper, we consider efficient algorithms for approximate inference on GGPMs using the general form of the EFD. A particular GP model and its associated inference algorithms can then be formed by changing the parameters of the EFD, thus greatly simplifying its creation for task-specific output domains. We demonstrate the efficacy of this framework by creating several new GP models for regressing to non-negative reals and to real intervals. We also consider a closed-form Taylor approximation for efficient inference on GGPMs, and elaborate on its connections with other model-specific heuristic closed-form approximations. Finally, we present a comprehensive set of experiments to compare approximate inference algorithms on a wide variety of GGPMs.

**Keywords:** Gaussian processes, Bayesian generalized linear models, non-parametric regression, exponential family, approximate inference

## 1. Introduction

In recent years, Gaussian processes (GPs) (Rasmussen and Williams, 2006), a non-parametric Bayesian approach to regression and classification, have been gaining popularity in machine learning and computer vision. For example, recent work Kapoor et al. (2010) has demonstrated promising results on object classification using GP classification and active learning. GPs have several properties that are desirable for solving complex regression tasks, such as those found in computer vision. First, due to the Bayesian formulation, GPs can be learned robustly from small training sets, which is important in tasks where the amount of training data is sparse compared to the dimension of the model (e.g., large-scale object recognition, tracking, 3d human pose modeling). Second, GP regression produces a predictive distribution, not just a single predicted value, thus providing a probabilistic approach to judging confidence in the predictions, e.g., for active learning. Third, GPs are based on kernel functions between the input examples, which allows for both a diverse set of image representations (e.g., bag-of-words, local-feature descriptors), and incorporation of prior knowledge about the computer vision task (e.g., modeling object structure). Finally, in the GP framework, the

kernel hyperparameters can be learned by maximizing the marginal likelihood, or evidence, of the training data. This is typically more efficient than standard cross-validation (which requires a grid search), and allows for more expressive kernels, e.g., compound kernels that model different trends in the data, or multiple kernel learning, where features are optimally combined by weighting the kernel function of each feature.

Because of these advantages, GP regression and classification have been applied to many computer vision problems, such as object classification (Kapoor et al., 2010), human action recognition (Han et al., 2009), age estimation (Zhang and Yeung, 2010), eye-gaze recognition (Noris et al., 2008), tracking (Raskin et al., 2007), counting people (Chan et al., 2008; Chan and Vasconcelos, 2009), crowd flow modeling (Ellis et al., 2009), anomaly detection (Loy et al., 2009), stereo vision (Williams, 2006; Sinz et al., 2004), interpolation of range data (Plagemann et al., 2007), non-rigid shape recovery (Zhu et al., 2009), 3d human pose recovery (Bo and Sminchisescu, 2010; Urtasun and Darrell, 2008; Fergie and Galata, 2010; Zhao et al., 2008), and latent-space models of 3d human pose (Urtasun et al., 2005; Wang et al., 2008; Chen et al., 2009). However, despite their successes, many of these methods attempt to “shoe-horn” their computer vision task into the standard GP regression framework. In particular, while the standard GP regresses a continuous *real-valued* function, it is often used to predict *discrete* non-negative integers (crowd counts Chan et al., 2008 or age Zhang and Yeung, 2010), non-negative real numbers (disparity Williams, 2006; Sinz et al., 2004 or depth Plagemann et al., 2007), and real numbers on a fixed interval (pose angles Bo and Sminchisescu, 2010; Urtasun and Darrell, 2008; Fergie and Galata, 2010; Zhao et al., 2008 or squashed optical flow Loy et al., 2009). Hence, heuristics are often required to convert the real-valued GP prediction to a *valid task-specific output*, which is not optimal in the Bayesian setting. For example in Chan et al. (2008), the real-valued GP prediction must be truncated and rounded to generate a proper count prediction, and it is not obvious how the predictive distribution over real-values can be converted to one over counts.

Developing a new GP model for each of the above regression tasks requires first finding a suitable distribution for the output variable (e.g., Poisson distribution for counting numbers, Gamma distribution for positive reals, Beta distribution for a real interval), and then deriving an approximate inference algorithm. This task can be simplified considerably with recourse to a unifying framework, which we call a *generalized Gaussian process model* (GGPM) (Chan and Dong, 2011). The GGPM is inspired by the *generalized linear model* (GLM) (McCullagh and Nelder, 1989), which aims to consolidate parametric regression methods (e.g., least-squares regression, Poisson regression, logistic regression) into a unifying framework. Similarly, the GGPM unifies many Bayesian non-parametric regression methods using GP priors (e.g., GP regression, GP classification, and GP counting) through the *exponential family*.

With the GGPM, the observation likelihood of the output is itself parameterized using the *generic form* of the exponential family distribution. Approximate inference algorithms can then be derived that depend only on these EFD parameter functions, elucidating the terms (e.g., derivatives, moments) needed for each algorithm. Different GP models are then created by simply changing the parameters of the likelihood function, thus *easing the development of new GP models for task-specific output domains*. Note that this is analogous to GLMs (McCullagh and Nelder, 1989), where a common iteratively reweighted least-squares (IRLS) algorithm was derived to estimate all associated regression models.

This paper is intended to both survey existing GP regression models, as well as develop a unifying regression framework for GP models and its associated approximate inference algorithms.

Besides further formalizing the GGPM framework, the contributions of this paper are 4-fold: 1) we derive a closed-form approximate inference method for GGPMs, based on a Taylor approximation, and show that model-specific closed-form approximations from Kapoor et al. (2010); Chan and Vasconcelos (2009); Heikkinen et al. (2008) are special cases; 2) we analyze existing approximate inference algorithms (Laplace approximation, expectation propagation, variational approximations) using the generic form of the exponential family distribution; 3) using the GGPM framework, we propose several new GP models for regressing to non-negative and interval real outputs; 4) we conduct comprehensive experiments comparing the efficacy of the approximate inference algorithms on both synthetic and real data sets. The remainder of the paper is organized as follows. In Section 2, we first review Gaussian process regression and related work. In Section 3, we introduce the GGPM framework, in Section 4, we discuss existing novel GP models within the GGPM framework. In Section 5, we derive efficient approximate inference algorithms. Next, we compare approximate posteriors in Section 6, and discuss initialization strategies for hyperparameter estimation in Section 7. Finally, in Section 8, we present experiments to compare the approximate inference algorithms, as well as demonstrate the efficacy of the new proposed models.

## 2. Gaussian processes and related work

In this section we review Gaussian process regression and other related work.

### 2.1 Gaussian process regression

Gaussian process regression (GPR) (Rasmussen and Williams, 2006) is a Bayesian approach to predicting a real-valued function  $f(\mathbf{x})$  of an input vector  $\mathbf{x} \in \mathbb{R}^d$  (also known as the regressor or explanatory variable). The function value is observed through a noisy observation (or measurement or output)  $y \in \mathbb{R}$ ,

$$y = f(\mathbf{x}) + \epsilon, \quad (1)$$

where  $\epsilon$  is zero-mean Gaussian noise with variance  $\sigma_n^2$ , i.e.,  $\epsilon \sim \mathcal{N}(0, \sigma_n^2)$ . A zero-mean *Gaussian process* (GP) prior is placed on the function, yielding the GPR model

$$f \sim \mathcal{GP}(\mathbf{0}, k(\mathbf{x}, \mathbf{x}')), \quad y|f(\mathbf{x}) \sim \mathcal{N}(f(\mathbf{x}), \sigma_n^2). \quad (2)$$

A GP is a random process that represents a distribution over functions, and is completely specified by its mean and covariance functions,  $m(\mathbf{x})$  and  $k(\mathbf{x}, \mathbf{x}')$ . For simplicity, we assume the mean function is zero. The covariance (or kernel) function  $k(\mathbf{x}, \mathbf{x}')$  determines the class of functions that  $f$  can represent (e.g., linear, polynomial, etc). Given any set of input vectors  $\mathbf{X} = [\mathbf{x}_1, \dots, \mathbf{x}_n]$ , the GP specifies that the corresponding function values  $\mathbf{f} = [f(\mathbf{x}_1), \dots, f(\mathbf{x}_n)]^T$  are jointly Gaussian,  $\mathbf{f}|\mathbf{X} \sim \mathcal{N}(\mathbf{0}, \mathbf{K})$ , where  $\mathbf{K}$  is the covariance (kernel) matrix with entries  $k(\mathbf{x}_i, \mathbf{x}_j)$ .

The function  $f$  is estimated from a training set of input vectors  $\mathbf{X} = [\mathbf{x}_1, \dots, \mathbf{x}_n]$  and corresponding *noisy* observations  $\mathbf{y} = [y_1, \dots, y_n]^T$ . First, given the inputs and noisy outputs  $\{\mathbf{X}, \mathbf{y}\}$ , the posterior distribution of the corresponding function values  $\mathbf{f}$  is obtained with Bayes' rule,

$$p(\mathbf{f}|\mathbf{X}, \mathbf{y}) = \frac{p(\mathbf{y}|\mathbf{f})p(\mathbf{f}|\mathbf{X})}{\int p(\mathbf{y}|\mathbf{f})p(\mathbf{f}|\mathbf{X})d\mathbf{f}} \quad (3)$$

where  $p(\mathbf{y}|\mathbf{f}) = \prod_{i=1}^n p(y_i|f_i)$  is the observation likelihood, and the denominator is the marginal likelihood,  $p(\mathbf{y}|\mathbf{X}) = \int p(\mathbf{y}|\mathbf{f})p(\mathbf{f}|\mathbf{X})d\mathbf{f}$ . To predict a function value  $f_* = f(\mathbf{x}_*)$  from a novel input  $\mathbf{x}_*$ , the posterior distribution in (3) is marginalized to obtain the predictive distribution (i.e., an average over all possible latent function values),

$$p(f_*|\mathbf{X}, \mathbf{x}_*, \mathbf{y}) = \int p(f_*|\mathbf{f}, \mathbf{X}, \mathbf{x}_*)p(\mathbf{f}|\mathbf{X}, \mathbf{y})d\mathbf{f} \quad (4)$$

Finally, the distribution of the predicted noisy observation  $y_*$  is obtained by marginalizing over  $f_*$ ,

$$p(y_*|\mathbf{X}, \mathbf{x}_*, \mathbf{y}) = \int p(y_*|f_*)p(f_*|\mathbf{X}, \mathbf{x}_*, \mathbf{y})df_*. \quad (5)$$

Since the observation likelihood and posterior are both Gaussian, the predictive distributions in (4, 5) are both Gaussian, with parameters that can be computed in closed-form (Rasmussen and Williams, 2006),

$$\mu_* = \mathbf{k}_*^T(\mathbf{K} + \sigma^2\mathbf{I})^{-1}\mathbf{y}, \quad \sigma_*^2 = k_{**} - \mathbf{k}_*^T(\mathbf{K}^{-1} + \sigma^2\mathbf{I})^{-1}\mathbf{k}_*, \quad (6)$$

$$p(f_*|\mathbf{X}, \mathbf{x}_*, \mathbf{y}) = \mathcal{N}(f_*|\mu_*, \sigma_*^2), \quad p(y_*|\mathbf{X}, \mathbf{x}_*, \mathbf{y}) = \mathcal{N}(y_*|\mu_*, \sigma_*^2 + \sigma_n^2). \quad (7)$$

where  $\mathbf{k}_* = [k(\mathbf{x}_*, \mathbf{x}_1) \cdots k(\mathbf{x}_*, \mathbf{x}_n)]^T$  and  $k_{**} = k(\mathbf{x}_*, \mathbf{x}_*)$ .

The hyperparameters  $\alpha$  of the kernel function and the observation noise  $\sigma_n^2$  are typically estimated by maximizing the marginal likelihood, or evidence, of the training data (also called Type-II maximum likelihood),

$$\{\hat{\alpha}, \hat{\sigma}_n^2\} = \underset{\alpha, \sigma_n^2}{\operatorname{argmax}} \log p(\mathbf{y}|\mathbf{X}), \quad (8)$$

$$\log p(\mathbf{y}|\mathbf{X}) = -\frac{1}{2}\mathbf{y}^T(\mathbf{K} + \sigma_n^2\mathbf{I})^{-1}\mathbf{y} - \frac{1}{2} \log |\mathbf{K} + \sigma_n^2\mathbf{I}| - \frac{n}{2} \log 2\pi. \quad (9)$$

The marginal likelihood measures the data fit, averaged over all probable functions. Hence, the kernel hyperparameters are selected so that each probable latent function will model the data well.

## 2.2 GP classification and other GP models

For Gaussian process classification (GPC) (Nickisch and Rasmussen, 2008; Kuss and Rasmussen, 2005; Rasmussen and Williams, 2006), a GP prior is again placed on the function  $f$ , which is then “squashed” through a sigmoid function to obtain the probability of the class  $y \in \{0, 1\}$ ,

$$f \sim \mathcal{GP}(0, k(\mathbf{x}, \mathbf{x}')), \quad p(y = 1|f(\mathbf{x})) = \sigma(f(\mathbf{x})), \quad (10)$$

where  $\sigma(f)$  is a sigmoid function, e.g. the logistic or probit functions, which maps a real number to the range  $[0, 1]$ . However, since the observation likelihood is no longer Gaussian, computing the posterior and predictive distributions in (3, 4, 5) is no longer analytically tractable. This has led to the development of several approximate inference algorithms for GPC, such as Markov-chain Monte Carlo (MCMC) (Nickisch and Rasmussen, 2008), variational bounds (Gibbs and Mackay, 2000), Laplace approximation (Williams and Barber, 1998), and expectation propagation (EP) (Minka, 2001; Rasmussen and Williams, 2006). As an alternative to approximate inference, the classification task itself can be approximated as a GP *regression* problem, where the observations are set to

method	likelihood	$\mathcal{Y}$	inference methods					TA#
			MCMC	LA	EP	KLD	VB	
regression	Gaussian	$\mathbb{R}$	-	-	-	-	-	<b>RW06</b> (exact)
classification	logit/probit	$\{0, 1\}$	<b>N97</b>	<b>WB98</b> <b>KG06</b>	<b>M01</b>	<b>NR08</b>	<b>GM97</b>	<b>NR08</b> (label regression)
robust regression	Laplace	$\mathbb{R}$	-	-	<b>K06</b>	<b>MA09</b>	<b>RN10</b> <sup>†</sup>	-
counting	Poisson	$\mathbb{Z}_+^\infty$	<b>D98</b> <b>VV07</b> <b>S11</b>	<b>V10</b>	<b>V10</b>	#	-	<b>CV09</b> (BPR)
counting	COM-Poisson	$\mathbb{Z}_+^\infty$	-	#	#	#	-	#
robust counting	neg. binomial	$\mathbb{Z}_+^N$	<b>S11</b>	<b>V11</b> <sup>†</sup>	<b>V11</b> <sup>†</sup>	#	-	#
occurrence	binomial	$\mathbb{Z}_+^N$	<b>PS04</b>	<b>V11</b> <sup>†</sup>	<b>V11</b> <sup>†</sup>	#	-	#
range regression	beta	$[0, 1]$		#	#	#	-	#
non-negative	Gamma	$\mathbb{R}_+$		#	#	#	-	#
non-negative	Inv. Gaussian	$\mathbb{R}_+$		#	#	#	-	#
robust regression	student-t	$\mathbb{R}$	<b>N97</b> <b>K06</b>	<b>V09</b> <b>RN10</b>	<b>J11</b>	<b>K06</b> <b>MA09</b> *	<b>RN10</b> <sup>†</sup>	-

GGPMs

Table 1: Bayesian regression methods using GP priors.

Abbreviations – Inference: MCMC (Markov-chain Monte Carlo), LA (Laplace approximation), EP (expectation propagation); KLD (KL divergence minimization), VB (variational bounds), TA (Taylor approximation). Citations: **CV09** (Chan and Vasconcelos, 2009), **D98** (Diggle et al., 1998), **GM97** (Gibbs and Mackay, 2000), **J11** (Jylänki et al., 2011), **K06** (Kuss, 2006), **KG06** (Kim and Ghahramani, 2006), **M01** (Minka, 2001), **MA09** (Manfred and Archambeau, 2009), **N97** (Neal, 1997), **NR08** (Nickisch and Rasmussen, 2008), **PS04** (Paciorek and Schervish, 2004), **RN10** (Rasmussen and Nickisch, 2010), **RW06** (Rasmussen and Williams, 2006), **S11** (Savitsky et al., 2011), **V09** (Vanhatalo et al., 2009), **V10** (Vanhatalo et al., 2010), **V11** (Vanhatalo et al., 2011), **VV07** (Vanhatalo and Vehtari, 2007), **WB98** (Williams and Barber, 1998) Other:  $\mathbb{Z}_+^N = \{0, 1, 2, \dots, N\}$ , BPR (Bayesian Poisson regression); <sup>†</sup> part of a software toolbox. \* considered the Cauchy distribution (Student-t with 1 d.o.f.). # introduced in this paper by our model.

$y \in \{-1, +1\}$  and standard GPR is applied. This is a computationally efficient alternative called *label regression* (Nickisch and Rasmussen, 2008) (or *least-squares classification* in Rasmussen and Williams, 2006, and also discussed in Tresp, 2000 as a “fast version” for two-class classification), and has shown promising results in object recognition (Kapoor et al., 2010).

GPR has been extended in several ways for other regression tasks with univariate outputs. Robust GP regression can be obtained by replacing the Gaussian observation likelihood with the Laplace or Cauchy likelihood (Manfred and Archambeau, 2009), or with a student-t likelihood (Jylänki et al., 2011). Paciorek and Schervish (2004) uses a binomial likelihood to model event occurrence data. In spatial statistics, the *kriging* method was developed for interpolating spatial data, and essentially uses the same model as GP regression. Diggle et al. (1998); Vanhatalo and Vehtari (2007); Vanhatalo et al. (2010) extend this framework for modeling counting observations, by assuming a Poisson observation likelihood and a GP spatial prior. Similarly, Chan and Vasconcelos (2009) develops a method for Bayesian Poisson regression, by applying a Gaussian prior on the linear weights of Poisson regression. Using a log-gamma approximation and kernelizing yields a closed-form solution that resembles GPR with specific output-dependent noise. Finally, Savitsky et al. (2011); Savitsky and Vannucci (2010) presents a Bayesian formulation of the Cox hazard model, by replacing the linear covariate with a GP prior, and also studies GP counting models using the Poisson and negative binomial likelihoods, in the context of Bayesian variable selection.

Table 1 summarizes the previous work on Bayesian regression models using GP priors, along with the approximate inference algorithms proposed for them. The goal of this paper is to generalize many of these models into a unified framework.

Finally, GP models have also be extended to model *multivariate observations*, i.e., vector outputs. Chu and Ghahramani (2005) proposes GP ordinal regression (i.e., ranking) using a multi-

probit likelihood, while multiclass classification is obtained using a probit (Girolami and Rogers, 2006; Kim and Ghahramani, 2006) or softmax (Williams and Barber, 1998) sigmoid function. Teh et al. (2005) linearly mixes independent GP priors to obtain a *semiparametric latent factor model*. In this paper, we only consider a univariate outputs with a single GP prior; extending the GGPM to multivariate outputs is a topic of future work.

### 2.3 Related work on GGPMs

Previous works on GGPMs include Diggle et al. (1998), which focuses on geostatistics (extending kriging) using Poisson- and binomial-GGPMs, Paciorek and Schervish (2004), which uses binomial-GGPM in the context of testing non-stationary covariance functions, and Savitsky et al. (2011), which is mainly interested in variable selection by adding priors to the kernel hyperparameters of a GGPM. All these works (Diggle et al., 1998; Paciorek and Schervish, 2004; Savitsky et al., 2011) perform inference using MCMC, by plugging in different likelihood functions without exploiting the exponential family form. MCMC tends to be slow, and convergence problems were observed in Diggle et al. (1998). In contrast, this paper focuses on *efficient* algorithms for approximate inference, and derives their general forms by exploiting the exponential family form. By doing so, we can create a “plug-and-play” aspect to GP models, which we exploit later to create several novel GP models with very little extra work. Seeger (2004); Tresp (2000); Shi and Choi (2011) also briefly mention the connection between the assumed output likelihoods of GPR/GPC and the exponential family, but do not study approximate inference or new models in depth.

The GGPM can be interpreted as a Bayesian approach to *generalized linear models* (GLMs) (McCullagh and Nelder, 1989), where a Gaussian prior is placed on the linear weights (or equivalently a GP prior with linear kernel is placed on the systemic component, i.e., latent function). Previous works on Bayesian GLMs consider different priors. A typical approach is to form a Bayesian hierarchical GLM by applying a conjugate prior on the parameters (e.g., Albert, 1988; Das and Dey, 2007; Bedrick et al., 1996). Recent work focuses on inducing sparsity in the latent function, e.g., Seeger et al. (2007) and Nickisch and Seeger (2009) assume a factorial heavy-tailed prior distribution, but are not kernelizable due to the factorial assumption. Hannah et al. (2011) proposes a mixture of GLMs, based on a Dirichlet process, to allow different regression parameters in different areas of the input space, and performs inference using MCMC.

When used with a non-linear kernel, the GGPM is a Bayesian kernelized GLM for non-linear regression. Zhang et al. (2010) also proposes a Bayesian kernelized GLM using a hierarchical model with a sparse prior (a mixture of point mass and Silverman’s g-prior) and evaluates their models on classification problems. Finally, Cawley et al. (2007) proposes a non-Bayesian version of a GLM, called a *generalised kernel machines* (GKM), which is based on kernelizing the iterated-reweighted least-squares algorithm (IRWLS). The GGPM is a Bayesian formulation of the GKM.

With respect to our previous work (Chan and Dong, 2011), this paper presents more algorithms for approximate inference (e.g., variational methods), and in more depth. We also propose novel GP models for regression to non-negative reals and real intervals, and show more connections with heuristic methods using the Taylor approximation. Furthermore, comprehensive experiments are presented to compare the performance of the inference algorithms on a wide variety of likelihood functions.

### 3. Generalized Gaussian process models

In this section, we introduce the generalized Gaussian process model, a non-parametric Bayesian regression model that encompasses many existing GP models.

#### 3.1 Exponential family distributions

We first note that different GP models are obtained by changing the form of the observation likelihood  $p(y|f)$ . The standard GPR assumes a Gaussian observation likelihood, while GPC essentially uses a Bernoulli distribution, and Chan and Vasconcelos (2009) uses a Poisson likelihood for counting. These likelihood functions are all instances of the single-parameter *exponential family distribution* (Duda et al., 2001), with likelihood given by

$$p(y|\theta, \phi) = \exp \left\{ \frac{1}{a(\phi)} [T(y)\theta - b(\theta)] + c(\phi, y) \right\}, \quad (11)$$

where  $y \in \mathcal{Y}$  is the observation from a set of possible values  $\mathcal{Y}$  (e.g., real numbers, counting numbers, binary class labels),  $\theta$  is the natural parameter of the exponential family distribution, and  $\phi$  is the dispersion parameter.  $T(y)$  is the sufficient statistic (e.g. the logit function for beta distribution),  $a(\phi)$  and  $c(\phi, y)$  are known functions, and  $b(\theta) = \log \int \exp(\frac{1}{a(\phi)}T(y)\theta + c(\phi, y))dy$  is the log-partition function, which normalizes the distribution. The mean and variance of the sufficient statistic  $T(y)$  are functions of  $b(\theta)$  and  $a(\phi)$ ,

$$\mu = \mathbb{E}[T(y)|\theta] = \dot{b}(\theta), \quad \text{var}[T(y)|\theta] = \ddot{b}(\theta)a(\phi), \quad (12)$$

where  $\dot{b}(\theta)$  and  $\ddot{b}(\theta)$  are the first and second derivatives of  $b$  w.r.t.  $\theta$ . The exponential family generalizes a wide variety of distributions for different output domains, and hence a unifying framework can be created by analyzing a GP model where the likelihood takes the *generic form* of (11).

#### 3.2 Generalized Gaussian process models

We now consider a framework for a generic Bayesian model that regresses from inputs  $\mathbf{x} \in \mathbb{R}^d$  to outputs  $y \in \mathcal{Y}$ , which encompasses many popular GP models. Following the formulation of GLMs (McCullagh and Nelder, 1989), the model is composed of three components:

1. a latent function,  $\eta(\mathbf{x}) \sim \mathcal{GP}(0, k(\mathbf{x}, \mathbf{x}'))$ , which is a function of the inputs, modeled with a GP prior.
2. a random component,  $p(y|\theta, \phi)$ , that models the output as an exponential family distribution with parameter  $\theta$  and dispersion  $\phi$ .
3. a link function,  $\eta = g(\mu)$ , that relates the *mean* of the sufficient statistic with the latent function.

Formally, the GGPM is specified by

$$\eta(\mathbf{x}) \sim \mathcal{GP}(0, k(\mathbf{x}, \mathbf{x}')), \quad y \sim p(y|\theta, \phi), \quad g(\mathbb{E}[T(y)|\theta]) = \eta(\mathbf{x}). \quad (13)$$

The mean of the sufficient statistic is related to the latent function  $\eta(\mathbf{x})$  through the inverse-link function, i.e.  $\mu = g^{-1}(\eta(\mathbf{x}))$ . The advantage of the link function is that it allows *direct specification*

of *prior knowledge* about the functional relationship between the output mean and the latent function  $\eta(\mathbf{x})$ . On the other hand, the effect of the GP kernel function is to adaptively warp (or completely override) the link function to fit the data. While many trends can be represented by the GP kernel function (e.g., polynomial functions), it is important to note that some functions (e.g., logarithms) *cannot be naturally represented by a kernel function*, due to its positive-definite constraint. Hence, directly specifying the link function is necessary for these cases.

Substituting (12) for the mean, we obtain the parameter  $\theta$  as a function of the latent function,

$$\eta(\mathbf{x}) = g(\mathbb{E}[T(y)|\theta]) = g(\dot{b}(\theta)) \Rightarrow g^{-1}(\eta(\mathbf{x})) = \dot{b}(\theta) \Rightarrow \theta(\eta(\mathbf{x})) = \dot{b}^{-1}(g^{-1}(\eta(\mathbf{x}))), \quad (14)$$

where  $\dot{b}^{-1}$  is the inverse of the first derivative of  $b(\cdot)$ . Using (14), another form of GGPM that directly relates the latent function with the parameter is

$$\eta(\mathbf{x}) \sim \mathcal{GP}(0, k(\mathbf{x}, \mathbf{x}')), \quad y \sim p(y|\theta(\eta(\mathbf{x})), \phi), \quad \theta(\eta(\mathbf{x})) = \dot{b}^{-1}(g^{-1}(\eta(\mathbf{x}))). \quad (15)$$

The GGPM unifies many Bayesian regression methods using GP priors (e.g., all of Table 1 except the student-t distribution), with each model arising from a specific instantiation of the parameter functions,  $\mathcal{E} = \{a(\phi), b(\theta), c(\phi, y), \theta(\eta), T(y)\}$ . Given a set of training examples and a novel input, the predictive distribution is obtained by marginalizing over the posterior of the latent function  $\eta(\mathbf{x})$ , similar to standard GPR/GPC (Rasmussen and Williams, 2006). The dispersion  $\phi$  is treated as a hyperparameter, which can be estimated along with the kernel hyperparameters by maximizing the marginal likelihood.

### 3.3 Canonical link function

One common link function is to select  $g(\cdot)$  such that  $\theta(\eta(\mathbf{x})) = \eta(\mathbf{x})$ . This is called the *canonical link function*, and is obtained with  $g(\cdot) = \dot{b}^{-1}(\cdot)$  and  $g^{-1}(\cdot) = \dot{b}(\cdot)$ . For the canonical link function, the GGPM simplifies to

$$\eta(\mathbf{x}) \sim \mathcal{GP}(0, k(\mathbf{x}, \mathbf{x}')), \quad y \sim p(y|\theta = \eta(\mathbf{x}), \phi), \quad (16)$$

and the output mean is related to the latent function by  $\mu = \dot{b}(\eta(\mathbf{x}))$ .

### 3.4 Inference and prediction

Inference on GGPMs follows closely to that of standard GPR/GPC (Rasmussen and Williams, 2006). Given a set of training examples, input vectors  $\mathbf{X} = [\mathbf{x}_1, \dots, \mathbf{x}_n]$  and corresponding observations  $\mathbf{y} = [y_1, \dots, y_n]^T$ , the goal is to generate a *predictive distribution* of the output  $y_*$  corresponding to a novel input  $\mathbf{x}_*$ . The predictive distribution is obtained using two steps. The first step is to calculate a posterior distribution of the latent function values  $\boldsymbol{\eta}$ , which best explains the training examples  $\{\mathbf{X}, \mathbf{y}\}$ . This corresponds to the training or parameter estimation phase of a regression model. In the second step, the distribution of the latent function value  $\eta(\mathbf{x}_*)$  for the novel input  $\mathbf{x}_*$  is calculated, followed by the predictive distribution for  $y_*$ .

Formally, given the training inputs  $\mathbf{X} = [\mathbf{x}_1, \dots, \mathbf{x}_n]$ , the latent values  $\eta_i = \eta(\mathbf{x}_i)$  are jointly Gaussian, according to the GP prior,  $p(\boldsymbol{\eta}|\mathbf{X}) = \mathcal{N}(\boldsymbol{\eta}|0, \mathbf{K})$ , where  $\boldsymbol{\eta} = [\eta_1, \dots, \eta_n]^T$  and  $[\mathbf{K}]_{i,j} = k(\mathbf{x}_i, \mathbf{x}_j)$  is the kernel matrix. The posterior distribution of  $\boldsymbol{\eta}$  is obtained by further conditioning on the training outputs  $\mathbf{y}$ , and applying Bayes' rule,

$$p(\boldsymbol{\eta}|\mathbf{X}, \mathbf{y}) = \frac{p(\mathbf{y}|\boldsymbol{\eta})p(\boldsymbol{\eta}|\mathbf{X})}{p(\mathbf{y}|\mathbf{X})}, \quad (17)$$



where  $p(\mathbf{y}|\boldsymbol{\theta}(\boldsymbol{\eta}))$  is the observation likelihood<sup>1</sup>, and  $p(\mathbf{y}|\mathbf{X})$  is the marginal likelihood, or evidence,

$$p(\mathbf{y}|\mathbf{X}) = \int p(\mathbf{y}|\boldsymbol{\theta}(\boldsymbol{\eta}))p(\boldsymbol{\eta}|\mathbf{X})d\boldsymbol{\eta}. \quad (18)$$

The posterior  $p(\boldsymbol{\eta}|\mathbf{X}, \mathbf{y})$  in (17) is the distribution of the latent values for all inputs  $\mathbf{X}$  that can best describe the provided input/output pairs.

Next, the predictive distribution of  $y_*$  for a novel input  $\mathbf{x}_*$  is obtained by first predicting the latent function value  $\eta_* = \eta(\mathbf{x}_*)$ . Conditioned on all the inputs  $\{\mathbf{X}, \mathbf{x}_*\}$ , the joint distribution of the latent function values  $\{\boldsymbol{\eta}, \eta_*\}$  is also Gaussian, via the GP prior, and the conditional distribution is obtained using the conditional Gaussian theorem,

$$p(\eta_*|\boldsymbol{\eta}, \mathbf{X}, \mathbf{x}_*) = \mathcal{N}(\eta_*|\mathbf{k}_*^T \mathbf{K}^{-1} \boldsymbol{\eta}, k_{**} - \mathbf{k}_*^T \mathbf{K}^{-1} \mathbf{k}_*), \quad (19)$$

where  $\mathbf{k}_* = [k(\mathbf{x}_1, \mathbf{x}_*), \dots, k(\mathbf{x}_n, \mathbf{x}_*)]^T$  and  $k_{**} = k(\mathbf{x}_*, \mathbf{x}_*)$ . The predictive distribution of  $\eta_*$  is then obtained by marginalizing over the posterior distribution in (17) (i.e., averaging over all possible latent functions),

$$p(\eta_*|\mathbf{X}, \mathbf{x}_*, \mathbf{y}) = \int p(\eta_*|\boldsymbol{\eta}, \mathbf{X}, \mathbf{x}_*)p(\boldsymbol{\eta}|\mathbf{X}, \mathbf{y})d\boldsymbol{\eta}. \quad (20)$$

Finally, the predictive distribution of  $y_*$  is obtained by marginalizing over  $\eta_*$ ,

$$p(y_*|\mathbf{X}, \mathbf{x}_*, \mathbf{y}) = \int p(y_*|\boldsymbol{\theta}(\eta_*))p(\eta_*|\mathbf{X}, \mathbf{x}_*, \mathbf{y})d\eta_*. \quad (21)$$

Note that for most non-Gaussian likelihoods, the posterior and predictive distributions in (17, 18, 20, 21) cannot be computed analytically in closed-form. We will discuss efficient approximate inference algorithms in Section 5.

### 3.5 Learning the hyperparameters

As in GPR (Rasmussen and Williams, 2006), the kernel hyperparameters  $\boldsymbol{\alpha}$  and the dispersion  $\phi$ , can be estimated from the data by maximizing the marginal likelihood in (18),

$$\{\boldsymbol{\alpha}^*, \phi^*\} = \operatorname{argmax}_{\boldsymbol{\alpha}, \phi} \int p(\mathbf{y}|\boldsymbol{\eta}, \phi)p(\boldsymbol{\eta}|\mathbf{X}, \boldsymbol{\alpha})d\boldsymbol{\eta}, \quad (22)$$

where we now note the dependence on the hyperparameters. The marginal likelihood measures the data fit, averaged over all probable latent functions. Hence, the criteria selects the kernel hyperparameters such that each probable latent function will model the data well.

## 4. Example GGPMs

In this section, using the GGPM framework, we propose several *novel* models for GP regression on different output domains. We obtain Bayesian regression for non-negative real number outputs by adopting the Gamma and inverse-Gaussian distributions, and propose a Beta-GGPM that regresses to real numbers on the  $[0, 1]$  interval. We also consider existing GP models within the GGPM framework (e.g., Poisson- and binomial-GGPMs from Table 1). We also discuss the role of the link function and its selection criteria.

---

1. To reduce clutter, we will not write the dependency on the dispersion parameter  $\phi$  or the kernel hyperparameters, unless we are explicitly optimizing them.

## 4.1 Summary

Table 2 (top) presents some examples of EFDs (distributions and parameters), while Table 2 (bottom) shows their expectations and link functions of their corresponding GGPM. The table encompasses both existing and novel GP models. By changing the parameters of the EFD to form a specific observation likelihood (i.e., selecting the functions  $\{a(\phi), b(\theta), c(\phi, y), \theta(\eta), T(y)\}$ ), we can easily obtain a wide range of GP models with different types of outputs, e.g., Gamma and Inverse Gaussian for non-negative reals, Beta for  $[0, 1]$  interval reals, etc.

Model	$y$	$p(y)$	$\{\theta, \phi\}$	$T(y)$	$a(\phi)$	$b(\theta)$	$c(\phi, y)$
Gaussian	$\mathbb{R}$	$\frac{1}{\sqrt{2\pi\sigma^2}} e^{-\frac{1}{2\sigma^2}(y-\mu)^2}$	$\{\mu, \sigma^2\}$	$y$	$\phi$	$\frac{1}{2}\theta^2$	$-\frac{\log(2\pi\phi)}{2} - \frac{y^2}{2\phi}$
Gamma <sub>sh</sub>	$\mathbb{R}_+$	$\frac{(\nu/\mu)^\nu}{\Gamma(\nu)} y^{\nu-1} e^{-y\nu/\mu}$	$\{\frac{-1}{\mu}, \frac{1}{\nu}\}$	$y$	$\phi$	$-\log(-\theta)$	$\log \frac{y^{\phi-1} - 1}{\Gamma(\phi-1)}$
Gamma <sub>sc</sub>	$\mathbb{R}_+$	$\frac{s^{-\nu}}{\Gamma(\nu)} y^{\nu-1} e^{-y/s}$	$\{\nu, s\}$	$\log y$	$\phi$	$\theta \log \phi + \phi \log \Gamma(\frac{\theta}{\phi})$	$-y/\phi - \log y$
Inv. Gauss.	$\mathbb{R}_+$	$\left[\frac{\lambda}{2\pi y^3}\right]^{\frac{1}{2}} e^{-\frac{\lambda(y-\mu)^2}{2\mu^2 y}}$	$\{\frac{-1}{2\mu^2}, \frac{1}{\lambda}\}$	$y$	$\phi$	$-\sqrt{-2\theta}$	$\log\left(\frac{1}{2\pi y^3 \phi}\right)^{\frac{1}{2}} - \frac{1}{2y\phi}$
Neg. Bino.	$\mathbb{Z}_+$	$\frac{\Gamma(y+\alpha^{-1})p^{\alpha-1}(1-p)^y}{\Gamma(y+1)\Gamma(\alpha-1)}$	$\{\alpha \log(1-p), \alpha\}$	$y$	$\phi$	$-\log(1 - e^{\phi-1}\theta)$	$\log \frac{\Gamma(y+\phi-1)}{\Gamma(y+1)\Gamma(\phi-1)}$
Poisson	$\mathbb{Z}_+$	$\frac{1}{y!} \lambda^y e^{-\lambda}$	$\{\log \lambda, 1\}$	$y$	$\phi$	$e^\theta$	$-\log(y!)$
COM-Po.	$\mathbb{Z}_+$	$\frac{1}{S(\mu, \nu)} \left[\frac{\mu y}{y!}\right]^\nu$	$\{\log \mu, \nu\}$	$y$	$\frac{1}{\phi}$	$\phi^{-1} \log S(e^\theta, \phi)$	$-\phi \log(y!)$
Binomial	$\frac{1}{N} \mathbb{Z}_+$	$\binom{N}{Ny} \pi^{Ny} (1-\pi)^{N-Ny}$	$\{\log \frac{\pi}{1-\pi}, \frac{1}{N}\}$	$y$	$\phi$	$\log(1 + e^\theta)$	$\log\left(\frac{\phi-1}{\phi-1+y}\right)$
Beta	$[0, 1]$	$\frac{\Gamma(\nu) y^{\mu\nu-1} (1-y)^{(1-\mu)\nu-1}}{\Gamma(\mu\nu)\Gamma((1-\mu)\nu)}$	$\{\mu, \frac{1}{\nu}\}$	$\log \frac{y}{1-y}$	$\phi$	$\phi \log \Gamma(\frac{\theta}{\phi}) \Gamma(\frac{1-\theta}{\phi})$	$\log \frac{\Gamma(\frac{1}{\phi})(1-y)^{\frac{1}{\phi}-1}}{y}$

Model	$\hat{b}(\theta) = \mathbb{E}[T(y)]$	$\text{var}[T(y)]$	$g(\mathbb{E}[T(y)])$	$\theta(\eta)$
Gaussian	$\theta$	$\phi$	$\mu$	$\eta$
Gamma <sub>sh</sub>	$-\theta^{-1}$	$\theta^{-2}\phi$	$\log \mu$	$-e^{-\eta}$
Gamma <sub>sc</sub>	$\log \phi + \psi_0(\theta/\phi)$	$\psi_1(\theta/\phi)$	$\log \psi_0^{-1}(\mu - \log \phi) + \log \phi$	$e^\eta$
Inv. Gauss.	$(-2\theta)^{-\frac{1}{2}}$	$\phi(-2\theta)^{-\frac{3}{2}}$	$2 \log \mu + \log 2$	$-e^{-\eta}$
Neg. Bino.	$\frac{\phi^{-1} e^{\phi-1}\theta}{1 - e^{\phi-1}\theta}$	$\frac{\phi^{-1} e^{\phi-1}\theta}{(1 - e^{\phi-1}\theta)^2}$	$-\log\left[\left(\frac{\mu\phi}{1+\mu\phi}\right)^{-\phi} - 1\right]$	$-\log(1 + e^{-\eta})$
Poisson	$e^\theta$	$e^\theta$	$\log \mu$	$\eta$
Linear Poisson	$e^\theta$	$e^\theta$	$\log(e^\mu - 1)$	$\log(\log(1 + e^\eta))$
COM-Poisson	$e^\theta + \frac{1}{2\phi} - \frac{1}{2}$	$-$	$\log(\mu - \frac{1}{2\phi} + \frac{1}{2})$	$\eta$
Linear COM-Poisson	$e^\theta + \frac{1}{2\phi} - \frac{1}{2}$	$-$	$\log(e^{\mu - \frac{1}{2\phi} + \frac{1}{2}} - 1)$	$\log(\log(1 + e^\eta))$
Binomial	$\frac{e^\theta}{1+e^\theta}$	$\frac{\phi e^\theta}{(1+e^\theta)^2}$	$\log \frac{\mu}{1-\mu}$	$\eta$
Beta	$\psi_0(\frac{\theta}{\phi}) - \psi_0(\frac{1-\theta}{\phi})$	$\psi_1(\frac{\theta}{\phi}) + \psi_1(\frac{1-\theta}{\phi})$	$\mu$	$\frac{e^\eta}{1+e^\eta}$

Table 2: (top) Exponential family distributions; (bottom) expectations and link functions for GGPM

## 4.2 Binomial distribution

The binomial distribution models the probability of a certain number of events occurring in  $N$  independent trials, the event probability in an individual trial is  $\pi$ , and  $y \in \{\frac{0}{N}, \frac{1}{N}, \dots, \frac{N}{N}\}$  is the fraction of events. Assuming the canonical link function, then

$$\mu = \mathbb{E}[y|\theta] = g^{-1}(\eta) = \frac{e^\eta}{1+e^\eta}, \quad (23)$$

and hence the mean is related to the latent space through the logistic function. For  $N = 1$ , the binomial-GGPM (or Bernoulli-GGPM) is equivalent to the GPC model using the logistic function. For  $N > 1$ , the model can naturally accommodate uncertainty in the labels by using fractional  $y_i$ ,

e.g., for  $N = 2$  there are three levels  $y \in \{0, \frac{1}{2}, 1\}$ . Furthermore in the  $N = 1$  case, by changing the link function to the probit function, we obtain GPC using the probit likelihood,

$$g(\mu) = \Phi^{-1}(\mu) \quad \Rightarrow \quad \mu = g^{-1}(\eta) = \Phi(\eta)$$

where  $\Phi(\eta)$  is the cumulative distribution of a Gaussian. Substituting into the GGPM, we have

$$\theta(\eta) = \log \frac{\Phi(\eta)}{1-\Phi(\eta)}, \quad b(\theta(\eta)) = -\log(1 - \Phi(\eta)).$$

A common interpretation of the probit GPC is that the class probability arises from a noisy Heaviside step function (Seeger, 2004). Here, the GGPM framework provides further insight that the probit and logistic GPC models correspond to Bernoulli-GGPMs using different link functions.

### 4.3 Counting GP models

In this section, we consider counting regression models (Poisson, negative binomial, Conway-Maxwell Poisson), and show how the link function can be changed to better model the mean trend.

#### 4.3.1 POISSON DISTRIBUTION

The Poisson distribution is a model for counting data, where the outputs  $y \in \mathbb{Z}_+ = \{0, 1, \dots\}$  are counts, and  $\lambda$  is the arrival-rate (mean) parameter. For the canonical link function,

$$\mathbb{E}[y|\theta] = g^{-1}(\eta) = e^\eta = \lambda, \quad g(\mu) = \log \mu. \quad (24)$$

Hence, the mean of the Poisson is the exponential of the latent value. The Poisson-GGPM is a Bayesian regression model for predicting counts  $y$  from an input vector  $\mathbf{x}$ , and has been previously studied (Chan and Vasconcelos, 2009; Diggle et al., 1998; Vanhatalo and Vehtari, 2007).

#### 4.3.2 LINEARIZED MEAN

The canonical link function assumes that the mean is the exponential of the latent function. This may cause problems when the actual mean trend is different, as illustrated in Figure 1a, where the count actually follows a linear trend. One way to address this problem is to use a non-linear kernel function to counteract the exponential link function. In this case, the ideal kernel function should be a logarithm function. However, there is no such positive definite kernel, and hence changing the kernel cannot recover a linear trend exactly. Furthermore, using the RBF kernel has poor extrapolation capabilities due to the limited extent of the RBF function, as illustrated in Figure 2.

Alternatively, the mean can be *directly linearized* by changing the link function of the Poisson-GGPM to represent a linear trend. For this purpose, we use the logistic error function,

$$\mathbb{E}[y|\theta] = g^{-1}(\eta) = \log(1 + e^\eta) \quad \Rightarrow \quad g(\mu) = \log(e^\mu - 1), \mu > 0.$$

For large values of  $\eta$ , the link function is linear, while for negative values of  $\eta$ , the function approaches zero. The parameter function and new partition function are

$$\theta(\eta) = \log(\log(1 + e^\eta)), \quad b(\theta(\eta)) = \log(1 + e^\eta). \quad (25)$$

Figures 1a and 1b illustrate the difference between the standard and linearized Poisson GGPMs. The standard Poisson-GGPM cannot correctly model the linear trend, resulting in a poor data fit at the extremes, while the linearized Poisson follows the linear trend.

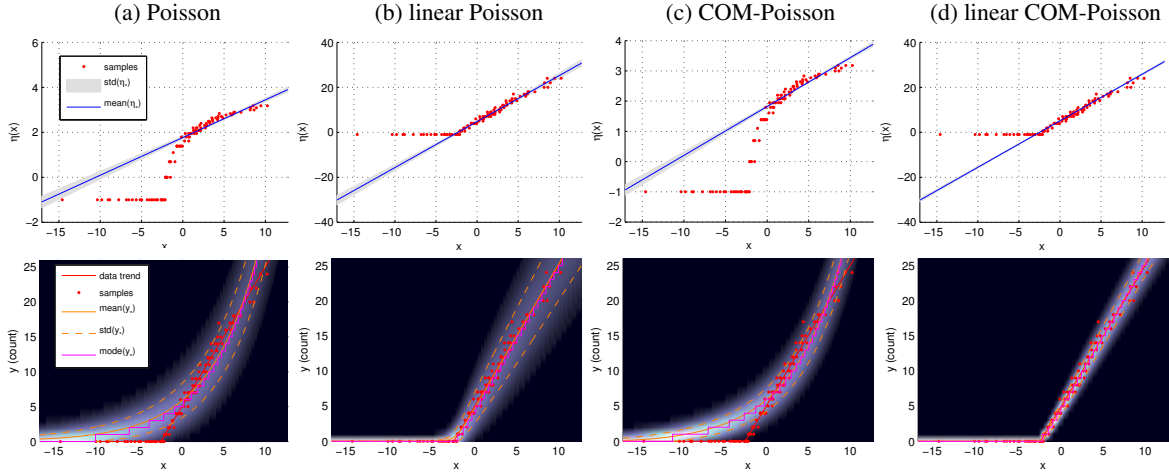


Figure 1: Examples of count regression using GGPM with linear kernel and different likelihood functions: a) Poisson; b) linearized Poisson; c) COM-Poisson; d) linearized COM-Poisson. The data follows a linear trend and is underdispersed. The top row shows the learned latent function, and the bottom row shows the predictive distributions. The background color indicates the count probability (white most probable, black least probable)

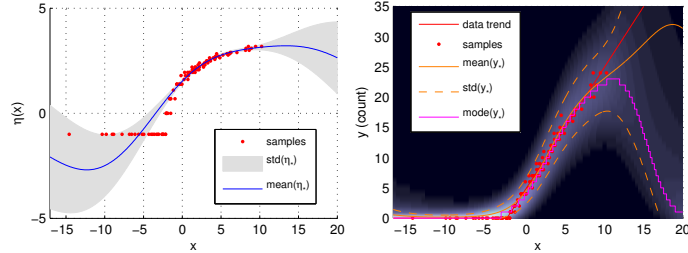


Figure 2: Example of regressing a linear trend using a Poisson-GGPM with RBF kernel.

One limitation with the Poisson distribution is that it models an equidispersed random variable, i.e. the variance is equal to the mean. However, in some cases, the actual random variable is *overdispersed* (with variance greater than the mean) or *underdispersed* (with variance less than the mean). We next consider two other counting distributions that can handle overdispersion and underdispersion.

#### 4.3.3 NEGATIVE BINOMIAL

The negative binomial distribution is a model for counting data, which is overdispersed (variance larger than the mean). The mean is given by  $\mu = \frac{1-p}{\alpha p}$ , where  $p \in (0, 1)$  and  $\alpha \geq 0$  is the scale parameter that adjusts the variance. The variance can be written as a function of mean, and always exceeds the mean,  $\text{var}(y) = \mathbb{E}[y] + \alpha \mathbb{E}[y]^2$ . When  $\alpha \rightarrow 0$ , the negative binomial reduces to the Poisson distribution.

Since  $\theta = \alpha \log(1 - p) < 0$  for valid parameters, the choice of  $\theta(\eta)$  must satisfy a non-positive constraint. Hence, we use a flipped log-loss function,

$$\theta(\eta) = -\log(1 + e^{-\eta}), \quad (26)$$

with the corresponding link function,

$$\mathbb{E}[y|\theta] = g^{-1}(\eta) = \frac{\alpha^{-1}(1 + e^{-\eta})^{-\alpha^{-1}}}{1 - (1 + e^{-\eta})^{-\alpha^{-1}}} \Rightarrow g(\mu) = -\log \left[ \left( \frac{\mu\alpha}{1 + \mu\alpha} \right)^{-\alpha} - 1 \right]. \quad (27)$$

When  $\alpha = 1$ , the link function reduces to  $\log \mu$ , and the negative binomial reduces to a Geometric distribution.

#### 4.3.4 CONWAY-MAXWELL-POISSON DISTRIBUTION

Another alternative distribution for count data, which represents different dispersion levels, is the Conway-Maxwell-Poisson (COM-Poisson) distribution (Conway and Maxwell, 1962; Shmueli et al., 2005; Guikema and Goffelt, 2008),

$$p(y|\mu, \nu) = \frac{1}{S(\mu, \nu)} \left[ \frac{\mu^y}{y!} \right]^\nu, \quad S(\mu, \nu) = \sum_{n=0}^{\infty} \left[ \frac{\mu^n}{n!} \right]^\nu, \quad (28)$$

where  $y \in \mathbb{Z}_+$ ,  $\mu$  is (roughly) the mean parameter, and  $\nu$  is the dispersion parameter. The COM-Poisson is a smooth interpolation between three distributions: geometric ( $\nu = 0$ ), Poisson ( $\nu = 1$ ), and Bernoulli ( $\nu \rightarrow \infty$ ). The distribution is overdispersed for  $\nu < 1$ , and underdispersed for  $\nu > 1$ . The partition function  $S(\mu, \nu)$  has no closed-form expression, but can be estimated numerically up to any precision (Shmueli et al., 2005). Note that  $b_\phi(\theta)$  is now also a function of  $\phi$ , which only affects optimization of the dispersion  $\phi$  (details in Appendix A.3.3 and Chan (2013)). For the canonical link function,

$$\mathbb{E}[y] \approx e^\eta + \frac{1}{2\nu} - \frac{1}{2} = g^{-1}(\eta) \Rightarrow g(\mu) = \log\left(\mu - \frac{1}{2\nu} + \frac{1}{2}\right). \quad (29)$$

Alternatively the parameter function in (25) can be used to model a linear trend in the mean.

The COM-Poisson GGPM includes a dispersion hyperparameter that decouples the variance of the Poisson from the mean, thus allowing more control on the observation noise of the output. Figures 1c and 1d show examples of using the COM-Poisson-GGPM on underdispersed counting data with a linear trend. Note that the variance of the prediction is much lower for the COM-Poisson models than for the Poisson models (Figures 1a and 1b), thus illustrating that the COM-Poisson GGPM can effectively estimate the dispersion of the data. A COM-Poisson GLM (with canonical link) was proposed in Guikema and Goffelt (2008), and thus the COM-Poisson GGPM is a non-linear Bayesian extension using a GP prior on the latent function.

## 4.4 GP regression to non-negative real numbers

In this section, we consider GGPMs with non-negative real number outputs. Two are based on different parameterizations of the Gamma distribution, and the other is based on the inverse Gaussian. The main difference between the likelihood functions is the amount of observation noise. In particular, the variance of the Gamma distribution is  $\phi\mu^2$ , whereas the inverse Gaussian is more dispersed, with variance  $\phi\mu^3$ .

#### 4.4.1 GAMMA DISTRIBUTION (MEAN PARAMETER, SHAPE HYPERPARAMETER)

The Gamma distribution is a model for non-negative real number observations. The distribution is parameterized by the mean  $\mu > 0$ , and the *shape* parameter  $\nu > 0$ . The exponential distribution is a special case of the Gamma distribution when  $\nu = 1$ . For the GGPM, we use  $\mu$  as the distribution parameter and  $\nu$  as the hyperparameter. Since  $\theta$  must implicitly be negative, we set the function  $\theta(\eta) = -e^{-\eta}$ , and the link function is

$$\mathbb{E}[y|\theta] = g^{-1}(\eta) = -1/\theta(\eta) = e^\eta \Rightarrow g(\mu) = \log \mu. \quad (30)$$

Hence the link function models  $\eta$  as the log-mean of the Gamma. We denote this likelihood as *Gamma-shape* (Gamma<sub>sh</sub>), since it uses the shape as the hyperparameter.

#### 4.4.2 GAMMA DISTRIBUTION (SHAPE PARAMETER, SCALE HYPERPARAMETER)

Alternatively, the Gamma distribution can be parameterized by the shape parameter  $\nu$ , and a *scale hyperparameter*  $s = \frac{\mu}{\nu}$ . Fixing the scale hyperparameter to  $s = 2$ , the Gamma distribution reduces to the Chi-square distribution. Since  $\theta$  must be positive, one candidate of  $\theta(\eta)$  is  $e^\eta$  and the link function is

$$\mathbb{E}[T(y)|\theta] = g^{-1}(\eta) = \log \phi + \psi_0(e^\eta/\phi) \Rightarrow g(\mu) = \log \psi_0^{-1}(\mu - \log \phi) + \log \phi, \quad (31)$$

where  $\psi_k(x) = \frac{\partial^{k+1}}{\partial x^{k+1}} \log \Gamma(x)$  is the polygamma function, and  $\psi_k^{-1}(z)$  is its inverse. Noting that  $\psi_0 \approx \log(x)$ , we can approximate the link function as  $g(\mu) \approx \mu = \mathbb{E}[T(y)] = \mathbb{E}[\log(y)]$ . We denote this likelihood as *Gamma-scale* (Gamma<sub>sc</sub>), since it uses the scale as the hyperparameter.

#### 4.4.3 INVERSE GAUSSIAN DISTRIBUTION

The inverse Gaussian distribution is another model for non-negative real number outputs, where  $\mu$  is the mean parameter and  $\lambda$  is the inverse dispersion. Since  $\theta$  is implicitly negative, we set  $\theta(\eta) = -e^{-\eta}$ , and the link function is

$$\mathbb{E}[y|\theta] = g^{-1}(\eta) = 1/\sqrt{2e^{-\eta}} \Rightarrow g(\mu) = 2 \log \mu + \log 2. \quad (32)$$

The link function models  $\eta$  as the log-mean of the inverse Gaussian.

### 4.5 Beta likelihood

The beta distribution is a model for output over a real interval,  $y \in [0, 1]$ , where  $\mu$  is the distribution mean and  $\nu$  is the shape parameter. To enforce the restriction  $0 < \theta < 1$ , we apply the logistic function  $\theta(\eta) = \frac{e^\eta}{1+e^\eta}$ , resulting in the link function,

$$\mathbb{E}[T(y)|\theta] = \psi_0\left(\frac{\theta}{\phi}\right) - \psi_0\left(\frac{1-\theta}{\phi}\right) \approx \log \frac{\theta}{1-\theta} = \eta \Rightarrow g(\mu) \approx \mu, \quad (33)$$

where we use the approximation to the digamma function,  $\psi_0(x) \approx \log x$ . The Beta-GGPM maps observations from the interval  $[0, 1]$  to real values in the latent space using the logit function. A similar idea has been explored in the study of estimating reflectance spectra from RGB values (Heikkinen et al., 2008), where the reflectance spectra output is regressed using a *logit-transformed*

GP. Specifically, the output values in  $[0, 1]$  are first transformed to real values using the logit function<sup>2</sup>, and a standard GP model is estimated on the transformed output. We show the relationship between this logit-transformed GP and the Beta-GGPM in Section 5.2.5.

#### 4.6 Choosing the link function

In the previous examples, several strategies have been used in selecting the link and parameter functions,  $g(\mu)$  and  $\theta(\eta)$ , to obtain a mapping from the latent space to the parameters. Using the canonical link function simplifies the calculations, but may make undesired assumptions about the mapping between latent space and the distribution mean (as in the exponential mapping for Poisson). Modifying the link function allows the desired mean trend (e.g., the linearized Poisson). When selecting the mapping via the parameter function, the main 2 hurdles are: 1) to select a function that satisfies the implicit constraints on the parameter  $\theta$  imposed by the log-partition function  $b(\theta)$ ; 2) to select a function that is defined for all values of input  $\eta \in \mathbb{R}$  to accommodate the GP prior. Figure 3 plots the log-partition functions and link functions for each model. For example, there is an implicit negative constraint on  $\theta$  for the Gamma-shape likelihood, due its the log-partition function.

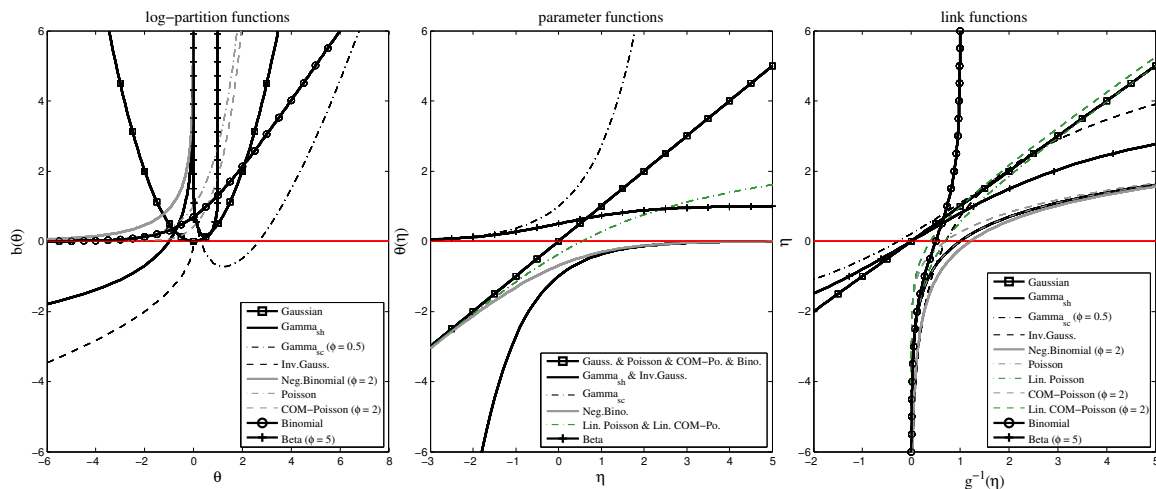


Figure 3: Log-partition, parameter, and link functions.

Finally, it is worth noting the difference between a *warped GP* (Snelson et al., 2004) and GGPMs. The warped GP learns a function to warp the output of GPR. The warping function plays a similar role as the link function in the GGPM, with one notable difference. With Snelson et al. (2004), the warping is applied directly to the output variable  $y$ ,  $z = f(y)$ , and a GPR is applied on the resulting  $z$ . As a result, the predictive distribution of  $z$  is Gaussian, whereas that of  $y = f^{-1}(z)$  is arbitrary (and perhaps multimodal). On the other hand, with GGPM, the link function applies warping between the latent value  $\eta$  and the mean parameter  $\theta$ , and hence the form of the output distribution is preserved. In addition, the warping function is learned in Snelson et al. (2004), whereas in this paper we assume the link function is fixed for a given GGPM. Certainly, in principle, the link function could be learned. However, we note that the link function and the kernel function both control the mapping between latent space and parameter space. Hence, if a link function were to be

2. Equivalently, the inverse hyperbolic tangent function ( $\text{arctanh}$ ) is applied to the data scaled to  $[-1, 1]$ .

learned, it would have to be over functions that are orthogonal to those functions learnable by the kernel function in order to avoid duplicate parameterization.

## 5. Approximate inference for GGPMs

In this section, we derive approximate inference algorithms for GGPMs based on the *general form* of the exponential family distribution in (11). One method of approximate inference is to use MCMC to draw samples from the posterior  $p(\boldsymbol{\eta}|\mathbf{X}, \mathbf{y})$ , but this can be computationally intensive (Nickisch and Rasmussen, 2008). Instead, we consider methods that approximate the posterior with a Gaussian.

We consider a closed-form approximation to inference based on a Taylor approximation, and we show that the Taylor approximation can justify common heuristics or pre-processing steps as principled inference; we prove that *label regression* (Nickisch and Rasmussen, 2008) is a Taylor approximation to GP classification (Bernoulli-GGPM), the closed-form Bayesian Poisson regression (Chan and Vasconcelos, 2009) is a Taylor approximation of a Poisson-GGPM, GP regression on *log-transformed outputs* is actually a Taylor approximation to the Gamma-GGPM, and GP regression on *logit-transformed outputs* (Heikkinen et al., 2008) is a Taylor approximation to the Beta-GGPM.

Finally, we consider several other approximate inference algorithms that have been previously proposed for various GP models, and generalize them for GGPMs.

### 5.1 Gaussian approximation to the posterior

As noted in Nickisch and Rasmussen (2008), most inference approximations on GPC work by finding a Gaussian approximation to the true posterior. Similarly, for GGPMs approximate inference also finds suitable Gaussian approximation  $q(\boldsymbol{\eta}|\mathbf{X}, \mathbf{y})$  to the true posterior, i.e.,

$$p(\boldsymbol{\eta}|\mathbf{X}, \mathbf{y}) \approx q(\boldsymbol{\eta}|\mathbf{X}, \mathbf{y}) = \mathcal{N}(\boldsymbol{\eta}|\hat{\mathbf{m}}, \hat{\mathbf{V}}) \quad (34)$$

where the parameters  $\{\hat{\mathbf{m}}, \hat{\mathbf{V}}\}$  are determined by the type of approximation. Substituting the approximation  $q(\boldsymbol{\eta}|\mathbf{X}, \mathbf{y})$  into (20), the approximate posterior for  $\eta_*$  is

$$p(\eta_*|\mathbf{X}, \mathbf{x}_*, \mathbf{y}) \approx q(\eta_*|\mathbf{X}, \mathbf{y}_*, \mathbf{y}) = \mathcal{N}(\eta_*|\hat{\mu}_\eta, \hat{\sigma}_\eta^2), \quad (35)$$

where the mean and variance are

$$\hat{\mu}_\eta = \mathbf{k}_*^T \mathbf{K}^{-1} \hat{\mathbf{m}}, \quad \hat{\sigma}_\eta^2 = k_{**} - \mathbf{k}_*^T (\mathbf{K}^{-1} - \mathbf{K}^{-1} \hat{\mathbf{V}} \mathbf{K}^{-1}) \mathbf{k}_*. \quad (36)$$

In many inference approximations,  $\{\hat{\mathbf{m}}, \hat{\mathbf{V}}\}$  take the form

$$\hat{\mathbf{V}} = (\mathbf{K}^{-1} + \mathbf{W}^{-1})^{-1}, \quad \hat{\mathbf{m}} = \hat{\mathbf{V}} \mathbf{W}^{-1} \mathbf{t}, \quad (37)$$

where  $\mathbf{W}$  is a diagonal matrix, and  $\mathbf{t}$  is a target vector. In these cases, (36) can be rewritten

$$\hat{\mu}_\eta = \mathbf{k}_*^T (\mathbf{K} + \mathbf{W})^{-1} \mathbf{t}, \quad \hat{\sigma}_\eta^2 = k_{**} - \mathbf{k}_*^T (\mathbf{K} + \mathbf{W})^{-1} \mathbf{k}_*. \quad (38)$$

Note that these are equivalent to the standard equations for GPR, but with an “effective” observation noise  $\mathbf{W}$  and target  $\mathbf{t}$  determined by the particular approximate inference algorithm.



## 5.2 Taylor approximation

In this section, we present a novel closed-form approximation to inference, which is based on applying a Taylor approximation of the likelihood term (Chan and Dong, 2011). We first define the following derivative functions of the observation log-likelihood,

$$u(\eta, y) = \frac{\partial}{\partial \eta} \log p(y|\theta(\eta)) = \frac{1}{a(\phi)} \dot{\theta}(\eta) [T(y) - \dot{b}(\theta(\eta))], \quad (39)$$

$$w(\eta, y) = - \left[ \frac{\partial^2}{\partial \eta^2} \log p(y|\theta(\eta)) \right]^{-1} = a(\phi) \left\{ \ddot{b}(\theta(\eta)) \dot{\theta}(\eta)^2 - [T(y) - \dot{b}(\theta(\eta))] \ddot{\theta}(\eta) \right\}^{-1} \quad (40)$$

For the canonical link function, these derivatives simplify to

$$u(\eta, y) = \frac{1}{a(\phi)} [T(y) - \dot{b}(\eta)], \quad w(\eta, y) = \frac{a(\phi)}{\ddot{b}(\eta)}. \quad (41)$$

### 5.2.1 JOINT LIKELIHOOD APPROXIMATION

We first consider approximating the joint likelihood of the data and latent values,

$$\log p(\mathbf{y}, \boldsymbol{\eta} | \mathbf{X}) = \log p(\mathbf{y} | \boldsymbol{\theta}(\boldsymbol{\eta})) + \log p(\boldsymbol{\eta} | \mathbf{X}). \quad (42)$$

The data likelihood term  $p(y_i | \theta(\eta_i))$  is the main hurdle for tractable integration over  $\boldsymbol{\eta}$ . Hence, we approximate the data log-likelihood term a 2nd-order Taylor expansion at the expansion point  $\tilde{\eta}_i$ ,

$$\log p(y_i | \theta(\eta_i)) \approx \log p(y_i | \theta(\tilde{\eta}_i)) + \tilde{u}_i (\eta_i - \tilde{\eta}_i) - \frac{1}{2} \tilde{w}_i^{-1} (\eta_i - \tilde{\eta}_i)^2 \quad (43)$$

where  $\tilde{u}_i = u(\tilde{\eta}_i, y_i)$  and  $\tilde{w}_i = w(\tilde{\eta}_i, y_i)$  are the derivatives evaluated at  $\tilde{\eta}_i$ . Defining  $\tilde{\mathbf{u}} = [\tilde{u}_1, \dots, \tilde{u}_n]^T$  and  $\tilde{\mathbf{W}} = \text{diag}(\tilde{w}_1, \dots, \tilde{w}_n)$ , the joint likelihood in (42) can then be approximated as (see Appendix A.1 for derivation)

$$\begin{aligned} \log q(\mathbf{y}, \boldsymbol{\eta} | \mathbf{X}) &= \log p(\mathbf{y} | \boldsymbol{\theta}(\tilde{\boldsymbol{\eta}})) - \frac{1}{2} \log |\mathbf{K}| - \frac{n}{2} \log 2\pi \\ &\quad - \frac{1}{2} \left\| \boldsymbol{\eta} - \mathbf{A}^{-1} \tilde{\mathbf{W}}^{-1} \tilde{\mathbf{t}} \right\|_{\mathbf{A}^{-1}}^2 - \frac{1}{2} \left\| \tilde{\mathbf{t}} \right\|_{\tilde{\mathbf{W}} + \mathbf{K}}^2 + \frac{1}{2} \tilde{\mathbf{u}}^T \tilde{\mathbf{W}} \tilde{\mathbf{u}} \end{aligned} \quad (44)$$

where  $\mathbf{A} = \tilde{\mathbf{W}}^{-1} + \mathbf{K}^{-1}$ ,  $\tilde{\mathbf{t}} = \tilde{\boldsymbol{\eta}} + \tilde{\mathbf{W}} \tilde{\mathbf{u}}$  is the target vector, and the individual targets are  $\tilde{t}_i = \tilde{\eta}_i + \tilde{w}_i \tilde{u}_i$ . The approximate joint log-likelihood in (44) will be used to find the approximate posterior and marginal likelihood.

### 5.2.2 APPROXIMATE POSTERIOR

Removing terms in (44) that do not depend on  $\boldsymbol{\eta}$ , the posterior of  $\boldsymbol{\eta}$  is approximately Gaussian,

$$\log q(\boldsymbol{\eta} | \mathbf{X}, \mathbf{y}) \propto \log q(\mathbf{y}, \boldsymbol{\eta} | \mathbf{X}) \propto -\frac{1}{2} \left\| \boldsymbol{\eta} - \mathbf{A}^{-1} \tilde{\mathbf{W}}^{-1} \tilde{\mathbf{t}} \right\|_{\mathbf{A}^{-1}}^2 \Rightarrow q(\boldsymbol{\eta} | \mathbf{X}, \mathbf{y}) = \mathcal{N}(\boldsymbol{\eta} | \hat{\boldsymbol{\mu}}, \hat{\mathbf{V}}), \quad (45)$$

where,  $\hat{\mathbf{V}} = (\tilde{\mathbf{W}}^{-1} + \mathbf{K}^{-1})^{-1}$ , and  $\hat{\boldsymbol{\mu}} = \hat{\mathbf{V}} \tilde{\mathbf{W}}^{-1} \tilde{\mathbf{t}}$ . These are of the form in (37), and hence, the approximate posterior of  $\eta_*$  has parameters

$$\hat{\mu}_\eta = \mathbf{k}_*^T (\mathbf{K} + \tilde{\mathbf{W}})^{-1} \tilde{\mathbf{t}}, \quad \hat{\sigma}_\eta^2 = k_{**} - \mathbf{k}_*^T (\mathbf{K} + \tilde{\mathbf{W}})^{-1} \mathbf{k}_*.$$

The Taylor approximation is a closed-form (non-iterative) approximation, that can be interpreted as performing GPR on a set of targets  $\tilde{\mathbf{t}}$  with target-specific, non-i.i.d. observation noise  $\tilde{\mathbf{W}}$ . The targets  $\tilde{\mathbf{t}}$  are a function of the the expansion point  $\tilde{\boldsymbol{\eta}}$ , which can be selected as a non-linear transformation of the observations  $\mathbf{y}$ .  $\tilde{\mathbf{W}}$  can be interpreted as a Gaussian approximation of the observation noise in the transformation space of  $\tilde{\mathbf{t}}$ , where the noise is dependent on the expansion points. For a standard GPR, this is iid noise, i.e.,  $\mathbf{W} = \sigma_n^2 \mathbf{I}$ . In other cases, the noise is dependent on the expansion points, and the particular properties of the observation likelihood. Instances of the closed-form Taylor approximation for different GP models are further explored in Section 4. One advantage with the Taylor approximation is that it is an *efficient non-iterative* method with the same complexity as standard GPR. In Section 7, we exploit its efficiency to speed up other approximate inference methods (e.g. EP) during hyperparameter estimation.

### 5.2.3 CHOICE OF EXPANSION POINT

The targets  $\tilde{\mathbf{t}}$  are a function of the the expansion point  $\tilde{\boldsymbol{\eta}}$ , which can be chosen as a non-linear transformation of the observations  $\mathbf{y}$ . Assuming that the output  $y_i$  occurs close to the mean of the distribution, a reasonable choice of the expansion point is  $\tilde{\eta}_i = g(T(y_i))$ , which we denote as the *canonical expansion point*. The derivatives and targets are then simplified to (see Appendix A.2)

$$\tilde{u}_i = u(g(T(y_i)), y_i) = 0 \quad \Rightarrow \quad \tilde{t}_i = \tilde{\eta}_i = g(T(y_i)), \quad (46)$$

$$\tilde{w}_i = w(g(y_i), y_i) = \frac{a(\phi)}{\ddot{b}(\theta(g(T(y_i))))\dot{\theta}(g(T(y_i)))^2}. \quad (47)$$

Hence, the Taylor approximation becomes GPR on the transformation of the input  $g(T(y_i))$ , with an appropriate non-i.i.d. noise term given by  $\tilde{w}_i$ .

This formulation gives some further insight on common preprocessing transformations, such as  $\log(y_i)$ , used with GPR. Using the Taylor approximation, we can show that some forms of preprocessing are actually making specific assumptions on the output noise. In addition, several heuristic methods (e.g., label regression) can be shown to be instances of approximate inference using the Taylor approximation. This is further explored for specific cases in Section 5.2.5.

Finally, it is worth noting the relationship between the GGPM Taylor approximation and warped GPs (Snelson et al., 2004). Warped GPs also apply a warping from  $y_i$  to  $t_i$ , and apply GPR on  $t_i$ . The main difference is that with warped GPs, the noise in the transformed space of  $t_i$  is modeled as i.i.d. Gaussian, resulting in an arbitrary predictive distribution of  $y_i$ . On the other hand, the Taylor approximation models the noise according to the warping function (i.e., as in  $\tilde{w}_i$ ), and hence the predictive distribution of  $y_i$  is preserved.

### 5.2.4 APPROXIMATE MARGINAL

The approximate marginal likelihood is obtained by integrating out  $\boldsymbol{\eta}$  in (44), yielding (see Appendix A.3 for derivation)

$$\log q(\mathbf{y}|\mathbf{X}) = -\frac{1}{2}\tilde{\mathbf{t}}^T(\tilde{\mathbf{W}} + \mathbf{K})^{-1}\tilde{\mathbf{t}} - \frac{1}{2}\log|\tilde{\mathbf{W}} + \mathbf{K}| + r(\phi) \quad (48)$$

where  $r(\phi) = \log p(\mathbf{y}|\theta(\tilde{\boldsymbol{\eta}})) + \frac{1}{2}\tilde{\mathbf{u}}^T\tilde{\mathbf{W}}\tilde{\mathbf{u}} + \frac{1}{2}\log|\tilde{\mathbf{W}}|$ . The approximate marginal is similar to that of standard GPR, but uses the modified targets and noise terms, as discussed earlier. There is one additional penalty term  $r(\phi)$  on the dispersion  $\phi$ , which arises from the non-Gaussianity of the observation noise. The derivatives of (48) for using conjugate gradient are derived in Appendix A.3.

## 5.2.5 TRANSFORMED GPs AS TAYLOR APPROXIMATE INFERENCE

We now show that *heuristic* methods using GPs on *transformed outputs* can be explained as Taylor approximate inference on GGPMs with specific likelihoods. The derivations, including derivative functions and targets used in Taylor approximate inference, are given in Appendix B.

**Binomial/Bernoulli** – An agnostic choice of expansion point is  $\tilde{\eta}_i = 0$ , which ignores the training classes, leading to

$$\tilde{t}_i = 4(y_i - 0.5), \quad \tilde{w}_i = 4/N. \quad (49)$$

Hence, the Taylor approximation for binomial-GGPM is equivalent to GPR in the latent space of the binomial model, with targets  $\tilde{t}_i$  scaled between  $[-2, +2]$  and an effective noise term  $\tilde{w}_i = 4/N$ . When  $y_i \in \{0, 1\}$ , the target values are  $\{-2, +2\}$ , which is equivalent to label regression (Rasmussen and Williams, 2006; Nickisch and Rasmussen, 2008; Kapoor et al., 2010), up to a scale factor. Hence, *label regression can be interpreted as a Taylor approximation to GPC inference*. The scaling of the targets ( $\pm 2$  or  $\pm 1$ ) is irrelevant when the latent space is only used for classifying based on the sign of  $\eta_*$ . However, this scaling is important when computing the actual label probabilities using the predictive distribution. The above interpretation explains why label regression tends to work well in practice, e.g., in Kapoor et al. (2010).

**Poisson** – Based on the canonical expansion point, we have  $\tilde{\eta}_i = \log(y_i + c)$ , where  $c \geq 0$  is a constant to prevent taking the logarithm of zero, and hence the target and effective noise for the Taylor approximation are

$$\tilde{t}_i = \log(y_i + c) - \frac{c}{y_i + c}, \quad \tilde{w}_i = \frac{1}{y_i + c}. \quad (50)$$

For  $c = 0$ , the Taylor approximation is exactly the closed-form approximation proposed for Bayesian Poisson regression in Chan and Vasconcelos (2009), which was derived in a different way using an approximation to the log-gamma distribution.

**Gamma (shape hyperparameter)** – Using the canonical expansion point,  $\tilde{\eta}_i = \log y_i$ , yields the target and effective noise,

$$\tilde{t}_i = \log y_i, \quad \tilde{w}_i = \frac{1}{\nu} = \phi. \quad (51)$$

Note that this is equivalent to using a standard GP on the log of the outputs (Diggle et al., 1998; Snelson et al., 2004), which is standard practice in the statistics literature when the observations are only positive values. Hence, this practice of applying a GP on log-transformed outputs is equivalent to assuming a Gamma likelihood and using Taylor approximate inference.

**Inverse Gaussian** – Using the canonical expansion point,  $\tilde{\eta}_i = \log(2y_i^2)$ , yields the target and effective noise,

$$\tilde{t}_i = \log(2y_i^2) = 2 \log y_i + \log 2, \quad \tilde{w}_i = 4\phi y_i. \quad (52)$$

This is equivalent to using a standard GP on the linear transform of log of the outputs, and the noise  $\tilde{w}_i$  is monotone in the value of output.

**Beta** – Consider an agnostic choice of the expansion point,  $\tilde{\eta}_i = 0$ , yields the targets and noise,

$$\tilde{t}_i = \frac{2\phi}{\psi_1(\frac{1}{2\phi})} \log \frac{y_i}{1-y_i}, \quad \tilde{w}_i = \frac{8\phi^2}{\psi_1(\frac{1}{2\phi})}. \quad (53)$$

Using the approximation to the trigamma function,  $\psi_1(x) \approx 1/x$ , the targets are approximately

$$\tilde{t}_i \approx \log \frac{y_i}{1-y_i}, \quad \tilde{w}_i \approx 4\phi. \quad (54)$$

Hence the GP on logit-transformed outputs of Heikkinen et al. (2008) is equivalent to using Taylor approximate inference and a Beta likelihood, with the above approximation to the trigamma function. Alternatively, another choice is the canonical expansion point,  $\tilde{\eta}_i = \log \frac{y_i}{1-y_i}$ , which we used in our experiments.

### 5.3 Laplace approximation

The Laplace approximation is a Gaussian approximation of the posterior  $p(\boldsymbol{\eta}|\mathbf{X}, \mathbf{y})$  at its maximum (mode). Hence, the Laplace approximation is a specific case of the closed-form Taylor approximation in Section 5.2, where the expansion point  $\hat{\boldsymbol{\eta}}$  is set to the maximum of the true posterior,

$$\hat{\boldsymbol{\eta}} = \underset{\boldsymbol{\eta}}{\operatorname{argmax}} \log p(\boldsymbol{\eta}|\mathbf{X}, \mathbf{y}). \quad (55)$$

The true posterior mode is obtained iteratively using the Newton-Raphson method, where in each iteration (Rasmussen and Williams, 2006),

$$\hat{\boldsymbol{\eta}}^{(new)} = \hat{\boldsymbol{\eta}} - \left[ \frac{\partial}{\partial \boldsymbol{\eta} \boldsymbol{\eta}^T} \log p(\hat{\boldsymbol{\eta}}|\mathbf{X}, \mathbf{y}) \right]^{-1} \frac{\partial}{\partial \boldsymbol{\eta}} \log p(\hat{\boldsymbol{\eta}}|\mathbf{X}, \mathbf{y}) = (\hat{\mathbf{W}}^{-1} + \mathbf{K}^{-1})^{-1} \hat{\mathbf{W}}^{-1} \hat{\mathbf{t}}, \quad (56)$$

where  $\hat{\mathbf{u}}$  and  $\hat{\mathbf{W}}$  are evaluated at  $\hat{\boldsymbol{\eta}}$ , and  $\hat{\mathbf{t}} = \hat{\mathbf{W}}\hat{\mathbf{u}} + \hat{\boldsymbol{\eta}}$ . In each iteration the expansion point  $\hat{\boldsymbol{\eta}}$  is moved closer to the maximum, and the target vector  $\hat{\mathbf{t}}$  is updated. Note that the update for  $\hat{\boldsymbol{\eta}}$  is of the same form as the mean  $\hat{\mathbf{m}}$  in the closed-form Taylor approximation. Hence, the Taylor approximation could also be considered a one-iteration Laplace approximation, using the expansion point  $\hat{\boldsymbol{\eta}}$  as the initial point.

The parameters of the approximate posterior of  $\boldsymbol{\eta}$  and  $\eta_*$  are

$$\hat{\mathbf{m}} = \hat{\boldsymbol{\eta}}, \quad \hat{\mathbf{V}} = (\hat{\mathbf{W}}^{-1} + \mathbf{K}^{-1})^{-1}, \quad (57)$$

$$\hat{\mu}_\eta = \mathbf{k}_*^T \mathbf{K}^{-1} \hat{\boldsymbol{\eta}} = \mathbf{k}_*^T \hat{\mathbf{u}}, \quad \hat{\sigma}_\eta = k_{**} - \mathbf{k}_*^T (\mathbf{K} + \hat{\mathbf{W}})^{-1} \mathbf{k}_*. \quad (58)$$

The mode is unique when the log posterior is concave, or equivalently when  $\mathbf{W}^{-1}$  is positive definite, i.e.,  $\forall y, \eta$ ,

$$\begin{aligned} w(\eta, y)^{-1} &= \frac{1}{a(\phi)} \left\{ \ddot{b}(\theta(\eta)) \dot{\theta}(\eta)^2 - \left[ T(y) - \dot{b}(\theta(\eta)) \right] \ddot{\theta}(\eta) \right\} > 0, \\ &\Rightarrow \ddot{b}(\theta(\eta)) \dot{\theta}(\eta)^2 > \left[ T(y) - \dot{b}(\theta(\eta)) \right] \ddot{\theta}(\eta). \end{aligned}$$

For a canonical link function, this simplifies to  $\ddot{b}(\eta) > 0$ , i.e., a unique maximum exists when  $b(\eta)$  is convex. Finally, the Laplace approximation for the marginal likelihood is

$$\log q(\mathbf{y}|\mathbf{X}) = \log p(\mathbf{y}|\theta(\hat{\boldsymbol{\eta}})) - \frac{1}{2}\hat{\boldsymbol{\eta}}^T \mathbf{K}^{-1} \hat{\boldsymbol{\eta}} - \frac{1}{2} \log |\hat{\mathbf{W}}^{-1} \mathbf{K} + \mathbf{I}| \quad (59)$$

$$= \log p(\mathbf{y}|\theta(\hat{\boldsymbol{\eta}})) - \frac{1}{2}\hat{\mathbf{u}}^T \mathbf{K} \hat{\mathbf{u}} - \frac{1}{2} \log |\hat{\mathbf{W}}^{-1} \mathbf{K} + \mathbf{I}|. \quad (60)$$

where the last line follows from the first-derivative condition at the maximum. Note that  $\hat{\boldsymbol{\eta}}$  is dependent on the kernel matrix  $\mathbf{K}$  and  $\phi$ . Hence, at each iteration during optimization of  $q(\mathbf{y}|\mathbf{X})$ , we have to recompute its value. Derivatives of the marginal are presented in the supplemental (Chan, 2013).

#### 5.4 Expectation propagation

Expectation propagation (EP) (Minka, 2001) is a general algorithm for approximate inference, which has been shown to be effective for GPC (Nickisch and Rasmussen, 2008). EP approximates each likelihood term  $p(y_i|\theta(\eta_i))$  with an unnormalized Gaussian  $t_i = \tilde{Z}_i \mathcal{N}(\eta_i | \tilde{\mu}_i, \tilde{\sigma}_i^2)$  (also called a site function), yielding an approximate data likelihood

$$q(\mathbf{y}|\theta(\boldsymbol{\eta})) = \prod_{i=1}^n t_i(\eta_i | \tilde{Z}_i, \tilde{\mu}_i, \tilde{\sigma}_i^2) = \mathcal{N}(\boldsymbol{\eta} | \tilde{\boldsymbol{\mu}}, \tilde{\boldsymbol{\Sigma}}) \prod_{i=1}^n \tilde{Z}_i,$$

where  $\tilde{\boldsymbol{\mu}} = [\tilde{\mu}_1, \dots, \tilde{\mu}_n]^T$  and  $\tilde{\boldsymbol{\Sigma}} = \text{diag}([\tilde{\sigma}_1^2, \dots, \tilde{\sigma}_n^2])$ . Using the site functions, the posterior approximation is

$$q(\boldsymbol{\eta}|\mathbf{X}, \mathbf{y}) = \frac{1}{Z_{EP}} \prod_{i=1}^n t_i(\eta_i) p(\boldsymbol{\eta}|\mathbf{X}) = \mathcal{N}(\boldsymbol{\eta} | \hat{\mathbf{m}}, \hat{\mathbf{V}})$$

where  $\{\hat{\mathbf{m}}, \hat{\mathbf{V}}\}$  are in the form of (37), and hence

$$\hat{\mathbf{m}} = \hat{\mathbf{V}} \tilde{\boldsymbol{\Sigma}}^{-1} \tilde{\boldsymbol{\mu}}, \quad \hat{\mathbf{V}} = (\mathbf{K}^{-1} + \tilde{\boldsymbol{\Sigma}}^{-1})^{-1}, \quad (61)$$

$$\hat{\mu}_\eta = \mathbf{k}_*^T (\mathbf{K} + \tilde{\boldsymbol{\Sigma}})^{-1} \tilde{\boldsymbol{\mu}}, \quad \hat{\sigma}_\eta^2 = k_{**} - \mathbf{k}_*^T (\mathbf{K} + \tilde{\boldsymbol{\Sigma}})^{-1} \mathbf{k}_*. \quad (62)$$

The normalization constant is also the EP approximation to the marginal likelihood (Nickisch and Rasmussen, 2008; Rasmussen and Williams, 2006),

$$\log Z_{EP} = \log q(\mathbf{y}|\mathbf{X}) = \log \int q(\mathbf{y}|\theta(\boldsymbol{\eta})) p(\boldsymbol{\eta}|\mathbf{X}) d\boldsymbol{\eta} \quad (63)$$

$$= -\frac{1}{2} \tilde{\boldsymbol{\mu}}^T (\mathbf{K} + \tilde{\boldsymbol{\Sigma}})^{-1} \tilde{\boldsymbol{\mu}} - \frac{1}{2} \log |\mathbf{K} + \tilde{\boldsymbol{\Sigma}}| + \sum_i \log \tilde{Z}_i. \quad (64)$$

Derivatives of (64) are presented in the supplemental (Chan, 2013).

##### 5.4.1 COMPUTING THE SITE PARAMETERS

Instead of computing the optimal site parameters all at once, EP works by iteratively updating each individual site using the other site approximations (Minka, 2001; Rasmussen and Williams, 2006).

In particular, to update site  $t_i$ , we first compute the *cavity distribution*, which is the marginalization over all sites except  $t_i$ ,

$$q_{\neg i}(\eta_i) = \mathcal{N}(\eta_i | \mu_{\neg i}, \sigma_{\neg i}^2) \propto \int p(\boldsymbol{\eta} | \mathbf{X}) \prod_{j \neq i} t_j(\eta_j | \tilde{Z}_j, \tilde{\mu}_j, \tilde{\sigma}_j^2) d\eta_j, \quad (65)$$

where the notation  $\neg i$  indicates the sites without  $t_i$ , and  $q_{\neg i}(\eta_i)$  is an approximation to the posterior distribution of  $\eta_i$ , given all observations except  $y_i$ . Since both terms are Gaussian, this integral can be computed in closed-form. Next, the site parameters of  $t_i$  are selected to match the moments (mean, variance, and normalization) between  $\hat{q}(\eta_i) = p(y_i | \theta(\eta_i)) q_{\neg i}(\eta_i)$  and  $t_i(\eta_i) q_{\neg i}(\eta_i)$ . This requires first calculating the moments of  $q(\eta_i) = \frac{1}{\tilde{Z}_i} p(y_i | \theta(\eta_i)) \mathcal{N}(\eta_i | \mu_{\neg i}, \sigma_{\neg i}^2)$ ,

$$\hat{\mu}_i = \mathbb{E}_q[\eta_i], \quad \hat{\sigma}_i^2 = \text{var}_q(\eta_i), \quad \hat{Z}_i = \int p(y_i | \theta(\eta_i)) q_{\neg i}(\eta_i) d\eta_i, \quad (66)$$

followed by “subtracting” the cavity distribution and then yielding the site updates.

$$\tilde{\mu}_i = \tilde{\sigma}_i^2 (\hat{\sigma}_i^{-2} \hat{\mu}_i - \sigma_{\neg i}^{-2} \mu_{\neg i}), \quad \tilde{\sigma}_i^2 = (\hat{\sigma}_i^{-2} - \sigma_{\neg i}^{-2})^{-1}, \quad (67)$$

$$\log \tilde{Z}_i = \log \hat{Z}_i + \frac{1}{2} \log 2\pi (\sigma_{\neg i}^2 + \tilde{\sigma}_i^2) + \frac{(\mu_{\neg i} - \tilde{\mu}_i)^2}{2(\sigma_{\neg i}^2 + \tilde{\sigma}_i^2)}. \quad (68)$$

EP iterates over each of the site  $t_i$ , i.e. each observation  $y_i$ , iteratively until convergence. Note that in general, EP is not guaranteed to converge. Although it is usually well behaved when the data log-likelihood  $\log p(y_i | \theta(\eta_i))$  is concave and the approximation is initialized to the prior (Nickisch and Rasmussen, 2008; Jylänki et al., 2011). Finally, these moments may not be analytically tractable (in fact,  $q(\eta_i)$  is the same form as the predictive distribution), so approximate integration is usually required. In general, the convergence of EP also depends on the accuracy of the moment approximations.

## 5.5 KL divergence minimization

In this section we discuss a variational approximation that maximizes a lower-bound of the marginal likelihood by minimizing the KL divergence between the approximate posterior and the true posterior. This type of approximate inference was first applied to robust GP regression in Manfred and Archambeau (2009), and later to GP classification in Nickisch and Rasmussen (2008). In this paper, we extend it to the GGPM.

As with other approximations, the approximate posterior is assumed to be Gaussian,

$$p(\boldsymbol{\eta} | \mathbf{X}, \mathbf{y}) \approx q(\boldsymbol{\eta} | \mathbf{X}, \mathbf{y}) = \mathcal{N}(\boldsymbol{\eta} | \mathbf{m}, \mathbf{V}) \quad (69)$$

for some  $\mathbf{m}$  and  $\mathbf{V}$ . To obtain the best approximate posterior, the KL divergence is minimized between the approximation and the true posterior,

$$\{\mathbf{m}^*, \mathbf{V}^*\} = \underset{\mathbf{m}, \mathbf{V}}{\text{argmin}} \text{KL}(\mathcal{N}(\boldsymbol{\eta} | \mathbf{m}, \mathbf{V}) \| p(\boldsymbol{\eta} | \mathbf{X}, \mathbf{y})). \quad (70)$$

As shown in Nickisch and Rasmussen (2008), minimizing the KL in (70) is equivalent to maximizing the lower bound of  $\log p(\mathbf{y} | \mathbf{X})$

$$\mathcal{L} = \log p(\mathbf{y} | \mathbf{X}) - \text{KL}(\mathcal{N}(\boldsymbol{\eta} | \mathbf{m}, \mathbf{V}) \| p(\boldsymbol{\eta} | \mathbf{X}, \mathbf{y})) \quad (71)$$

$$= f(\mathbf{m}, \mathbf{v}) + \frac{1}{2} \log |\mathbf{K}^{-1} \mathbf{V}| - \frac{1}{2} \text{tr}(\mathbf{K}^{-1} \mathbf{V}) - \frac{1}{2} \mathbf{m}^T \mathbf{K}^{-1} \mathbf{m} + \frac{n}{2}. \quad (72)$$

The function  $f(\mathbf{m}, \mathbf{v})$  is the expectation of the observation log-likelihood,

$$f(\mathbf{m}, \mathbf{v}) \equiv \int \mathcal{N}(\boldsymbol{\eta}|\mathbf{m}, \mathbf{V}) \log p(\mathbf{y}|\boldsymbol{\theta}(\boldsymbol{\eta})) d\boldsymbol{\eta} = \sum_{i=1}^n \mathbb{E}_{\eta_i|m_i, v_i} [\log p(y_i|\theta(\eta_i))], \quad (73)$$

where  $m_i = [\mathbf{m}]_i$  and  $v_i = [\mathbf{V}]_{ii}$ ,  $\mathbf{v} = \text{diag}(\mathbf{V})$ , and  $\mathbb{E}_{\eta_i|m_i, v_i}[\cdot]$  is the expectation with respect to  $\mathcal{N}(\eta_i|m_i, v_i)$ . The first term of (72) emphasizes the fit to the data (via the expectation), while remaining terms (KL divergence terms) penalize the posterior from being too different from the prior distribution.

At a local maximum of (72), the first derivative conditions yield the following constraints,

$$\hat{\mathbf{m}} = \mathbf{K}\hat{\boldsymbol{\gamma}}, \quad \hat{\mathbf{V}} = (\mathbf{K}^{-1} + \hat{\boldsymbol{\Lambda}})^{-1} \quad (74)$$

where the optimal  $\hat{\boldsymbol{\gamma}}$  and  $\hat{\boldsymbol{\Lambda}}$  satisfy

$$\hat{\boldsymbol{\gamma}} = \frac{\partial f(\mathbf{m}, \mathbf{v})}{\partial \mathbf{m}}, \quad \hat{\boldsymbol{\Lambda}} = -2 \frac{\partial f(\mathbf{m}, \mathbf{v})}{\partial \mathbf{V}} \quad (75)$$

Since the mean and covariance have the forms in (74), the optimization problem can be reformulated with the variational parameters  $\{\boldsymbol{\gamma}, \boldsymbol{\lambda}\}$ , such that

$$\mathbf{m} = \mathbf{K}\boldsymbol{\gamma}, \quad \mathbf{V} = (\mathbf{K}^{-1} + \boldsymbol{\Lambda})^{-1} = \mathbf{K}(\mathbf{I} + \boldsymbol{\Lambda}\mathbf{K})^{-1}, \quad \boldsymbol{\Lambda} = \text{diag}(\boldsymbol{\lambda}). \quad (76)$$

This parameterization also avoids inverting the kernel matrix. Substituting into (72),

$$\mathcal{L} = f(\mathbf{K}\boldsymbol{\gamma}, \mathbf{v}) + \frac{1}{2} \log |(\mathbf{I} + \boldsymbol{\Lambda}\mathbf{K})^{-1}| - \frac{1}{2} \text{tr}((\mathbf{I} + \boldsymbol{\Lambda}\mathbf{K})^{-1}) - \frac{1}{2} \boldsymbol{\gamma}^T \mathbf{K}\boldsymbol{\gamma} + \frac{n}{2}. \quad (77)$$

Finally, the optimal approximate posterior can be obtained by maximizing (77) with respect to the variational parameters  $\{\boldsymbol{\gamma}, \boldsymbol{\lambda}\}$  using standard optimization techniques (e.g., the conjugate gradient method). Note that  $\mathcal{L}$  is a lower bound on the marginal likelihood, as in (72). Hence, the model hyperparameters can also be estimated by maximizing (77). In practice, the model hyperparameters and approximate posterior can be estimated at the same time, by jointly maximizing (77) with respect to all parameters (again, e.g., using conjugate gradient).

### 5.5.1 EXPECTATION TERMS

The computation of (77) and its derivatives requires calculating  $f(\mathbf{m}, \mathbf{v})$  and its derivatives,

$$f(m_i, v_i) = \mathbb{E}_{\eta_i|m_i, v_i} [\log p(y_i|\theta(\eta_i))], \quad \frac{\partial f(m_i, v_i)}{\partial \phi} = \frac{\partial}{\partial \phi} \mathbb{E}_{\eta_i|m_i, v_i} [\log p(y_i|\theta(\eta_i))], \quad (78)$$

$$\frac{\partial f(m_i, v_i)}{\partial m_i} = \frac{\partial}{\partial m_i} \mathbb{E}_{\eta_i|m_i, v_i} [\log p(y_i|\theta(\eta_i))], \quad \frac{\partial f(m_i, v_i)}{\partial v_i} = \frac{\partial}{\partial v_i} \mathbb{E}_{\eta_i|m_i, v_i} [\log p(y_i|\theta(\eta_i))]. \quad (79)$$

Plugging in for the exponential family form, the first two terms can be rewritten as

$$f(m_i, v_i) = \frac{1}{a(\phi)} \{T(y_i) \mathbb{E}_{\eta_i|m_i, v_i} [\theta(\eta_i)] - \mathbb{E}_{\eta_i|m_i, v_i} [b(\theta(\eta_i))]\} + c(\phi, y_i), \quad (80)$$

$$\frac{\partial f(m_i, v_i)}{\partial \phi} = \frac{-\dot{a}(\phi)}{a(\phi)^2} \{T(y_i) \mathbb{E}_{\eta_i|m_i, v_i} [\theta(\eta_i)] - \mathbb{E}_{\eta_i|m_i, v_i} [b(\theta(\eta_i))]\} + \dot{c}(\phi, y_i). \quad (81)$$

Hence, the expectations  $\mathbb{E}[\theta(\eta)]$  and  $\mathbb{E}[b(\theta(\eta))]$  under a Gaussian distribution are required. Expressions of the last two terms can be obtained by directly taking the derivative,

$$\frac{\partial f(m_i, v_i)}{\partial m_i} = \int \frac{\partial \mathcal{N}(\eta_i | m_i, v_i)}{\partial m_i} \log p(y_i | \theta(\eta_i)) d\eta_i = \mathbb{E}_{\eta_i | m_i, v_i} \left[ \frac{\eta_i - m_i}{v_i} \log p(y_i | \theta(\eta_i)) \right], \quad (82)$$

$$\frac{\partial f(m_i, v_i)}{\partial v_i} = \int \frac{\partial \mathcal{N}(\eta_i | m_i, v_i)}{\partial v_i} \log p(y_i | \theta(\eta_i)) d\eta_i = \mathbb{E}_{\eta_i | m_i, v_i} \left[ \frac{(\eta_i - m_i)^2 - v_i}{2v_i^2} \log p(y_i | \theta(\eta_i)) \right]. \quad (83)$$

Hence, these two derivatives require the expectations  $\mathbb{E}[\eta^k \theta(\eta)]$  and  $\mathbb{E}[\eta^k b(\theta(\eta))]$ , where  $k \in \{1, 2\}$ . For certain likelihood and link functions (e.g., Poisson with canonical link), the above expectations have a closed form solutions. In other cases, they need to be approximated.

Alternative expressions to (82, 83) can be obtained by performing a change of variable in the expectation  $\eta = \frac{\bar{\eta} - m}{\sqrt{v}}$ ,

$$\frac{\partial f(m_i, v_i)}{\partial m_i} = \frac{\partial}{\partial m_i} \mathbb{E}_{\bar{\eta}_i | 0, 1} [\log p(y_i | \theta(\sqrt{v_i} \bar{\eta}_i + m_i))] = \mathbb{E}_{\eta_i | m_i, v_i} [u(\eta_i, y_i)], \quad (84)$$

$$\frac{\partial f(m_i, v_i)}{\partial v_i} = \frac{\partial}{\partial v_i} \mathbb{E}_{\bar{\eta}_i | 0, 1} [\log p(y_i | \theta(\sqrt{v_i} \bar{\eta}_i + m_i))] = \frac{1}{2} \mathbb{E}_{\eta_i | m_i, v_i} \left[ \frac{\eta_i - m_i}{v_i} u(\eta_i, y_i) \right]. \quad (85)$$

Hence, alternatively the expectations  $\mathbb{E}[\eta^k \dot{\theta}(\eta)]$  and  $\mathbb{E}[\eta^k \dot{b}(\theta(\eta)) \dot{\theta}(\eta)]$ ,  $k \in \{0, 1\}$ , are required under a Gaussian. The alternative forms in (84, 85) allow an intuitive comparison between the KLD method and the Laplace approximation, given in the next section.

### 5.5.2 APPROXIMATE POSTERIOR

After maximizing  $\mathcal{L}$ , resulting in optimal variational parameters  $\{\hat{\gamma}, \hat{\lambda}\}$ , the approximate posteriors have parameters

$$\hat{\mathbf{m}} = \mathbf{K} \hat{\gamma}, \quad \hat{\mathbf{V}} = (\mathbf{K}^{-1} + \hat{\mathbf{\Lambda}})^{-1}, \quad (86)$$

$$\hat{\mu}_\eta = \mathbf{k}_*^T \hat{\gamma}, \quad \hat{\sigma}_\eta^2 = k_{**} - \mathbf{k}_*^T (\mathbf{K} + \hat{\mathbf{\Lambda}}^{-1})^{-1} \mathbf{k}_*. \quad (87)$$

An interesting comparison can be made against the predictive latent distribution using the Laplace approximation in (58). In particular, with the Laplace approximation, the latent mean depends on the first derivative  $\mathbf{u}$  of the observation log-likelihood (at the mode), whereas with the variational method, the latent mean depends on the *expectation* of the first derivative,  $\hat{\gamma} = \mathbb{E}[\mathbf{u}]$ , using (84). Similarly, with the Laplace approximation, the effective noise term  $\mathbf{W}$  is the inverse of the 2nd derivative of the observation log-likelihood, and with KLD, this term depends on an estimate of the 2nd derivative by differencing the 1st derivative around  $m$ , given by (85).

## 5.6 Summary

In this section, we have studied closed-form Taylor approximation, and discussed its connections with output-transformed GPs. We also discussed other popular approximate inference methods in the context of GGPMs. Using the general EFD form for the likelihood, we can identify the specific quantities required for each algorithm in terms of parameters  $\mathcal{E}$ , as summarized in Table 3. For



example, EP requires the expectations of  $\theta(\eta)$  and  $b(\theta(\eta))$  under the approximate predictive distribution, whereas KL minimization requires these expectations under a Gaussian distribution. This result has two practical consequences: 1) the implementation of likelihood functions is simplified, since only the derivatives and expectations of simple functions in  $\mathcal{E}$  need to be implemented; 2) we elucidate the expectations that may require numerical approximation. Furthermore, different likelihood and link functions can be combined in novel ways without much additional implementation effort.

Approximation		general likelihood	GGPM likelihood
Taylor	posterior & marginal	$\frac{\partial^k}{\partial \eta^k} \log p(y \eta)$ , $k = \{1, 2\}$	$\dot{b}, \ddot{b}, \dot{\theta}, \ddot{\theta}$
	marginal derivatives	$\frac{\partial}{\partial \phi} \log p(y \eta)$	$\dot{a}, \dot{c}$
Laplace	posterior & marginal	$\frac{\partial^k}{\partial \eta^k} \log p(y \eta)$ , $k = \{1, 2\}$	$\dot{b}, \ddot{b}, \dot{\theta}, \ddot{\theta}$
	marginal derivatives	$\frac{\partial^3}{\partial \eta^3} \log p(y \eta)$ , $\frac{\partial}{\partial \phi} \frac{\partial^k}{\partial \eta^k} \log p(y \eta)$ , $k \in \{0, 2\}$	$\dot{a}, \dot{c}, \ddot{b}, \ddot{\theta}$
EP	posterior & marginal	$\log \hat{Z}_i$ , $\frac{\partial^k}{\partial \eta^k} \log \hat{Z}_i$ , $k = \{1, 2\}$	$\mathbb{E}_q[\eta_i]$ , $\text{var}_q(\eta_i)$
	marginal derivatives	$\frac{\partial}{\partial \phi} \log \hat{Z}_i$	$\dot{c}, \dot{a}, \mathbb{E}_q[\theta(\eta)], \mathbb{E}_q[b(\theta(\eta))]$
KLD	posterior & marginal	$\mathbb{E}[\eta^k \log p(y \eta)]$ , $k \in \{0, 1, 2\}$	$\mathbb{E}[\eta^k \theta(\eta)], \mathbb{E}[\eta^k b(\theta(\eta))]$ , $k \in \{0, 1, 2\}$
	marginal derivatives	$\mathbb{E}[\frac{\partial}{\partial \phi} \log p(y \eta)]$	$\dot{c}, \dot{a}$

Table 3: The required calculations of the likelihood function for approximate inference. The expectations  $\mathbb{E}_q$  and  $\text{var}_q$  can be calculated from derivatives of  $\log \hat{Z}_i$ .

## 5.7 Implementation Details

The GGPM was implemented in MATLAB by extending the GPML toolbox (Rasmussen and Nickisch, 2010) to include implementations for: 1) the generic exponential family distribution using the parameters  $\{a(\phi), b(\theta), c(y, \phi), \theta(\eta), T(y)\}$ ; 2) the closed-form Taylor approximation for inference; 3) the EP and KLD moments and the predictive distributions, approximated using numerical integration when necessary. Empirically, we found that EP was sensitive to the accuracy of the approximate integrals, and exhibited convergence problems when less accurate approximations were used (e.g. Gaussian-Hermite quadrature). Hyperparameters (dispersion and kernel parameters) were optimized by maximizing the marginal likelihood, using the existing scaled conjugate gradient method in GPML. The code will be made available<sup>3</sup>.

## 6. Comparison of approximate posteriors

In this section, we provide a theoretical and experimental comparison of the approximate posteriors from Section 5. In particular, we show that the efficacy of an approximate inference method is influenced by properties of the likelihood, evaluation metrics, and datasets.

### 6.1 Ordering of posterior means and predictive means

We first compare the latent posteriors of the Taylor, Laplace, and EP approximations for one latent variable. Consider an example using the Gamma-shape likelihood, and the corresponding true latent posterior  $p(\eta|y) \propto p(y|\eta)p(\eta)$  in Figure 4 (top-left). The first derivative of the log-posterior,

3. <http://visal.cs.cityu.edu.hk/downloads/>

$f(\eta|y) = \frac{\partial}{\partial \eta} \log p(\eta|y)$ , is plotted in Figure 4 (bottom-left). Note that the derivative of the Gamma-shape log-likelihood,  $u(\eta, y) = \nu(ye^{-\eta} - 1)$ , is convex and monotonically decreasing for all  $y > 0$ .

**Claim 1** *If the derivative of the observation log-likelihood,  $\frac{\partial}{\partial \eta} \log p(y|\eta)$ , is convex and monotonically decreasing, then the means of the 1-D approximate posteriors are ordered according to*

$$\mu_{TA} < \mu_{LA} < \mu_{EP}, \quad (88)$$

where  $\mu_{TA}$ ,  $\mu_{LA}$ , and  $\mu_{EP}$  are the latent means for the Taylor approximation, Laplace approximation, and EP, respectively. The ordering is reversed when  $\frac{\partial}{\partial \eta} \log p(y|\eta)$  is concave and decreasing.

**Proof** *The log posterior is  $\log p(\eta|y) \propto \log p(y|\eta) + \log p(\eta)$ , and the derivative is*

$$f(\eta|y) = \frac{\partial}{\partial \eta} \log p(y|\eta) + \frac{\partial}{\partial \eta} \log p(\eta) \quad (89)$$

The first term on the RHS of (89) is assumed to be convex and monotonically decreasing, while the second term is a linear function with negative slope (derivative of the Gaussian log-likelihood). Hence,  $f(\eta|y)$  is also convex and monotonically decreasing. The mean of the Laplace approximation is the mode of the true posterior, i.e., the zero crossing of  $f(\eta|y)$ , and is marked with a star (\*) in Figure 4. The Taylor approximation is equivalent to one iteration of Newton's method on  $f(\eta|y)$ , starting at the expansion point  $\tilde{\eta}$ . Hence, geometrically, the mean of the Taylor approximation is the zero-crossing of the tangent line to  $f(\eta|y)$  at the expansion point (marked with a circle (o) in Figure 4). Since  $f(\eta|y)$  is convex and monotonically decreasing, the zero-crossing point of any tangent line is always less than the zero-crossing point of  $f(\eta|y)$ . Therefore, the Taylor mean is always smaller than the Laplace mean.

Because  $f(\eta|y)$  is monotonically decreasing and convex, the posterior  $p(\eta|y)$  is skewed to the right, and its mean is larger than the mode. Since EP matches the mean of the approximation to the mean of the true posterior, the EP mean must be larger than the mode (i.e., the Laplace mean). ■

Claim 1 suggests that the posterior means follow a particular order for the 1-dimensional posterior. For the general multi-dimensional case, it is difficult to prove a similar result, since the dimensions of the latent posterior are correlated through the kernel matrix<sup>4</sup>. Nonetheless, we can empirically show that the ordering in (88) holds for multivariate posteriors on average.

To this end, we ran a synthetic experiment using the Gamma-shape likelihood, with dispersion parameter  $\phi \in [0.1, 5]$ , and RBF kernel function with scale  $K_s = 2$  and bandwidth  $K_w \in [0.1, 5]$ . For a given bandwidth  $K_w$  and dispersion  $\phi$  pair, 100 different functions are first randomly sampled from a Gamma-shape GGPM. For each function, 40 points are used for training, and the multivariate means of the approximate posteriors  $\mu_{TA}$ ,  $\mu_{LA}$ , and  $\mu_{EP}$  are calculated using Taylor, Laplace, and EP, respectively. The differences between these means are averaged over all 100 trials and plotted in Figure 5.

For all parameter settings, the ordering holds for the multivariate means on average, i.e., the TA mean is always less than the LA mean, which is always less than the EP mean. Note that, as the dispersion level increases, the difference between the three means also increases. Increasing

4. When the kernel matrix is diagonal, i.e., the kernel function is a delta function, it is easy to show that the ordering in Claim 1 will hold for each dimension.

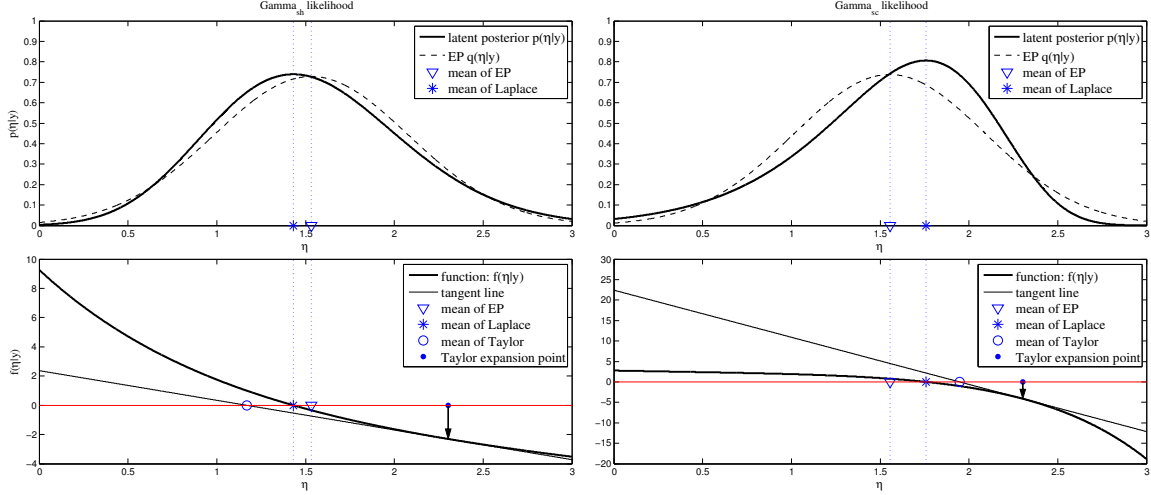


Figure 4: Comparing the approximate posterior means of Taylor, Laplace and EP methods for the Gamma-shape (left) and Gamma-scale (right) likelihood functions. The first row shows the true latent posterior  $p(\eta|y)$  and the EP approximation  $q(\eta|y)$ . The second row shows the first derivative of the log-posterior  $f(\eta|y) = \frac{\partial}{\partial \eta} \log p(\eta|y)$ . The mean of the Laplace approximation is the zero-crossing point of  $f(\eta|y)$ . The mean of the Taylor approximation is the zero-crossing of the tangent line at the expansion point (one iteration of Newton’s method).

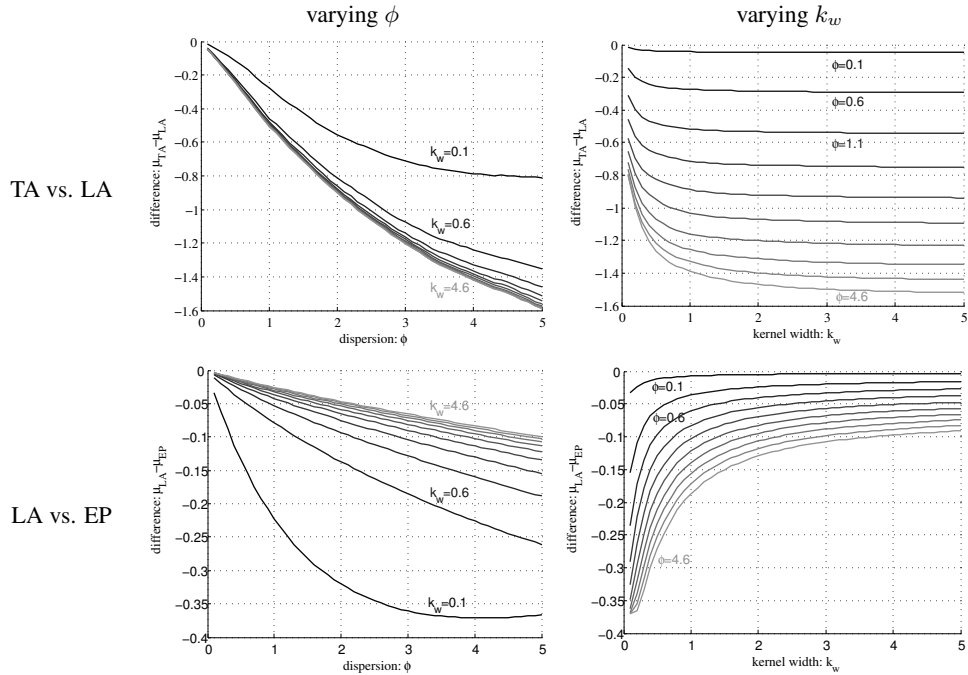


Figure 5: The difference between approximate posterior means for the Gamma-shape likelihood function. The top row compares Taylor ( $\mu_{TA}$ ) vs. Laplace ( $\mu_{LA}$ ), while the bottom row compares Laplace ( $\mu_{LA}$ ) vs. EP ( $\mu_{EP}$ ). In each row, the two plots show the difference w.r.t the dispersion parameter  $\phi$  and the RBF kernel bandwidth  $k_w$ .

the dispersion level will “stretch” the observation log-likelihood term. This will scale down its derivative, and as a result, the zero-crossing point of the tangent line ( $\mu_{TA}$ ) will move further from the zero-crossing of  $f(\eta|y)$  (i.e.,  $\mu_{LA}$ ). Similarly, “stretching” the observation log-likelihood also moves the mean further from the mode, thus increasing the difference between  $\mu_{LA}$  and  $\mu_{EP}$ . For the kernel bandwidth, increasing the bandwidth also stretches the prior. This scales down the derivatives of  $f$ , and as a result, the difference between TA and LA also increases in a similar way. On the other hand, as the bandwidth increases, the difference between LA and EP *decreases*. Increasing the bandwidth squashes the prior, making it more uniform. As a result, the prior has less influence on the mean of the posterior, compared to the likelihood term, and the EP mean converges to the mean of the likelihood term.

The ordering of the posterior means also suggest that the predictive means will follow a similar order, i.e., the predictions using TA will be less than those of LA, and the predictions using EP will always be larger than LA. This is difficult to prove theoretically, since the variance of the posterior affects the predictive mean, but has been observed empirically in toy examples, as well as in experiments on real data in Section 8. This is demonstrated in Figure 6, which uses a Gamma-shape GGPM with the four inference methods. The training samples are distributed in three distinct regions and have the similar trends to an exponential function. All the four inference methods can well capture the exponential trend. However, given an input  $x_*$ , the latent values for TA, LA, and EP exhibit the ordering of Claim 1, as seen in the second row of Figure 6(a). In addition, the predictive means also follow the ordering. KLD and EP methods have almost overlapped latent means. EP and KLD both optimize the KL divergence between the true posterior  $p$  and the approximate  $q$ . The difference is that EP optimizes  $D(p||q)$  and KLD optimizes  $D(q||p)$ . For a unimodal distribution  $p$ , minimizing either  $D(q||p)$  or  $D(p||q)$  will correctly capture the mean of  $p$ .

## 6.2 Effect on prediction error

The systematic ordering between the approximate posterior and predictive means suggests that differences in prediction accuracy between approximation methods are influenced by the distribution of the test data. If the test data has more points “below the mean curve”, then TA will have better accuracy because it systematically underpredicts. On the other hand, if there are more points “above the mean curve”, then EP will have better accuracy. This effect is illustrated in Figure 6b. Because of the configuration of the data, the predictive mean function passes above the middle points and below the extremal points. Thus TA will have the smallest prediction error for the middle region and largest error at the extremes. In contrast, EP will have lowest error on points near the ends, and largest error on the middle region. If the test data contains more points in the middle, as in Figure 6b, then the Taylor approximation will have lower average predictive error. In contrast, if the test data contains more points at the extremes, as in Figure 6a, then EP will have lower average error.

Inference	Gamma-shape				Gamma-scale			
	First Example (a)		Second Example (b)		First Example (a)		Second Example (b)	
	MAE	NLP	MAE	NLP	MAE	NLP	MAE	NLP
Taylor	0.894	1.293	<b>1.123</b>	1.429	<b>0.581</b>	1.274	0.900	1.309
Laplace	0.818	<b>1.282</b>	1.144	<b>1.424</b>	0.633	<b>1.243</b>	0.715	<b>1.241</b>
EP	<b>0.815</b>	<b>1.282</b>	1.145	<b>1.424</b>	0.636	<b>1.243</b>	<b>0.713</b>	<b>1.241</b>
KLD	<b>0.815</b>	<b>1.282</b>	1.145	<b>1.424</b>	0.636	<b>1.243</b>	<b>0.713</b>	<b>1.241</b>

Table 4: Average errors for the two 1D examples.

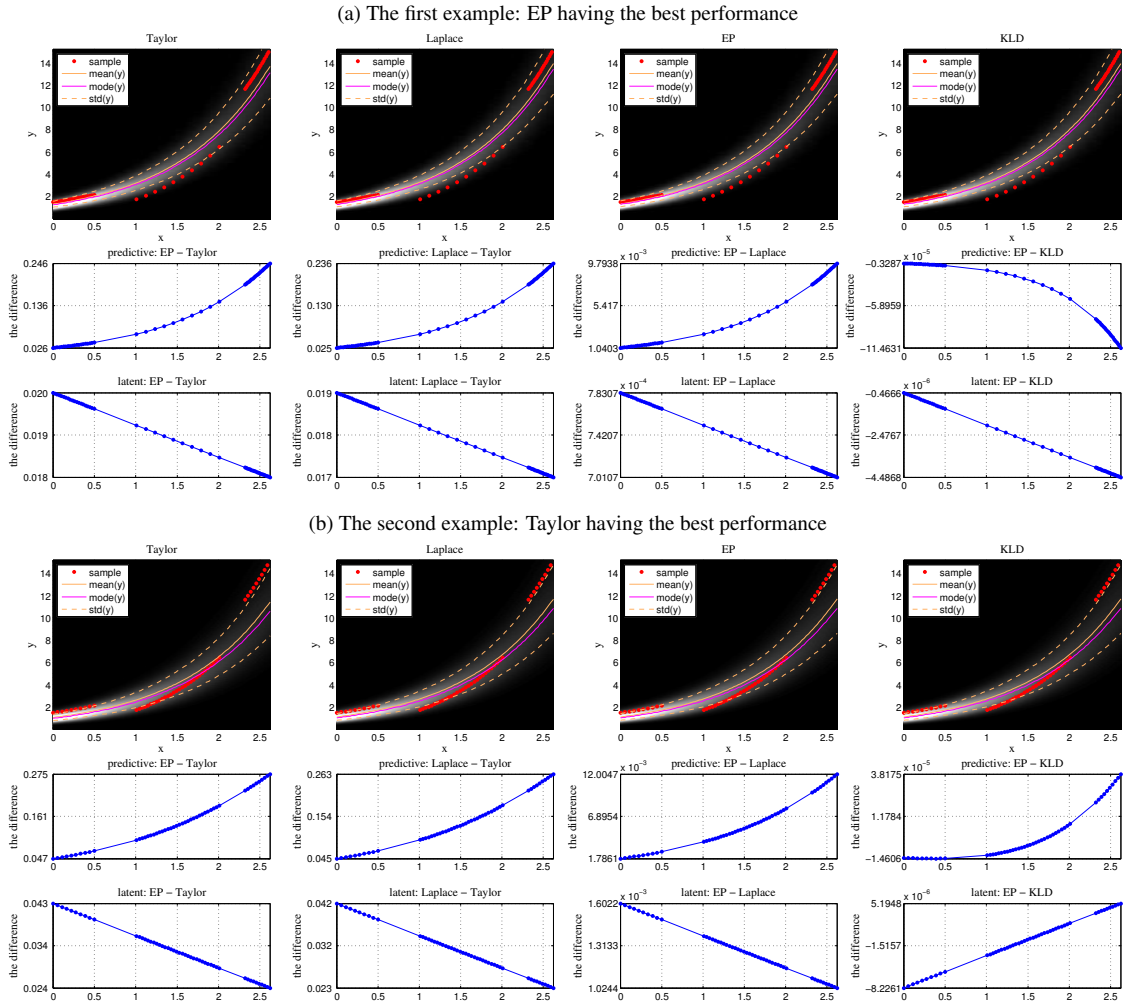


Figure 6: Two 1D examples of comparing different inference methods. In each example the top row shows the learned  $\text{Gamma}_{\text{sh}}$ -GGPM regression models with four different inference methods: Taylor, Laplace, EP, KLD. The middle row shows the difference between predictive distributions, while the bottom row shows the difference between latent functions.

To quantify this difference in predictive accuracy, a test set was generated by randomly sampling points in the neighborhood of each training point. Each inference method was evaluated using two measures: 1) the mean absolute error (MAE), which measures the goodness-of-fit; 2) the mean negative log predictive density evaluated at the test points (NLP), which measures how well the model predicts the entire density (Snelson et al., 2004). Evaluation results are presented in Table 4. For the first example (Figure 6a), there are more test points in the end regions, and EP achieves the lowest MAE of 0.815 versus 0.894 for TA. On the other hand, in the second example (Figure 6b), where most of the test data is in the middle region, TA is the most accurate among the four methods (MAE of 1.123 versus 1.145 of EP). Finally, if the likelihood is changed from Gamma-shape to Gamma-scale, the MAE results of the four inference methods are reversed for the two examples

(see Table 4 right), since the derivative of the log-likelihood of the Gamma-scale is concave. If we evaluate the results by NLP, the Taylor method always performs worse than the other three methods.

From these examples and Claim 1, it can be concluded that the performances of different inference methods are highly affected by dataset distributions, likelihood functions and evaluation metrics. The systematic ordering of the latent posterior means can affect the prediction accuracy if the test set is unbalanced or skewed. Real-life datasets are often noisy and high-dimensional, and it is unlikely for a single inference method to dominate for all datasets and metrics.

## 7. Initializing hyperparameter estimation

As with GPR, the estimation of GGPM hyperparameters by maximizing the marginal likelihood often suffers from the problem of multiple local optima. Figure 7 shows the negative log-marginal likelihood (NML), as a function of the RBF kernel width and scale hyperparameters, for the four inference methods on the rainfall dataset (see Section 8.1 for description). The NML surface for all four likelihood functions have at least two local optima, and the Laplace, EP and KLD methods produce very similar surfaces.

A common approach to hyperparameter estimation is to initialize the log-hyperparameters to zero, and then optimize using the scaled conjugate gradient method (Rasmussen and Nickisch, 2010). However, in the example in Figure 7, using the same initialization strategy leads to *different* hyperparameter estimates from each inference method. As illustrated in Figure 7, TA, KLD, and EP converge to similar local optimum on the left, whereas Laplace converges to a different local minimum on the right. Hence, a more robust initialization method is required to better explore the search space, and to ensure that a good optimum can be found for each inference method. One strategy is to run the optimization procedure many times using a large set of random initializations. However, for some inference algorithms, e.g. EP, the computational burden will be large.

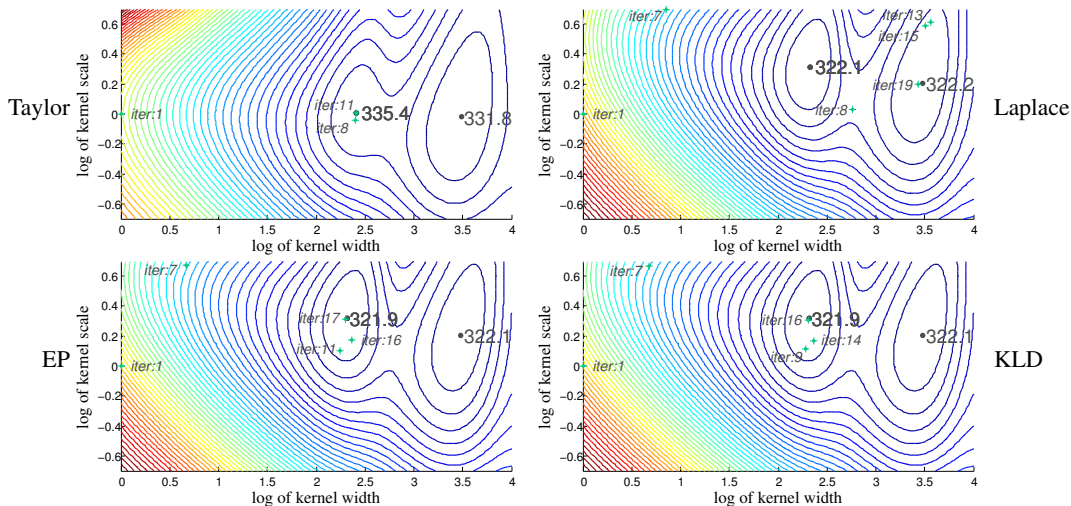


Figure 7: Contour plot of the negative log marginal likelihood as a function of the RBF kernel width and scale hyperparameters for four approximate inference methods. The iterations of scaled conjugate gradient minimization with initialization (0, 0) are plotted in green.

We propose an efficient initialization strategy that uses Taylor inference to quickly find a few good initializations for the other inference methods (Laplace, KLD, and EP). The procedure is illustrated in Figure 8. Taylor inference is used to optimize the hyperparameters using 50 random initializations (see Figure 8a), resulting in convergence to several local optima with different marginal likelihoods. The top 3 unique local optima are used as the initializations for the Laplace and EP methods, and the results are presented in Figures 8b and 8c. In both cases, the Taylor-initialized Laplace and EP can recover the same local optima as the randomly-initialized versions, but with a significant reduction in computational cost (3 times faster for Laplace, and 13 times faster for EP). The hyperparameter resulting in the largest marginal likelihood can then be selected as the estimate.

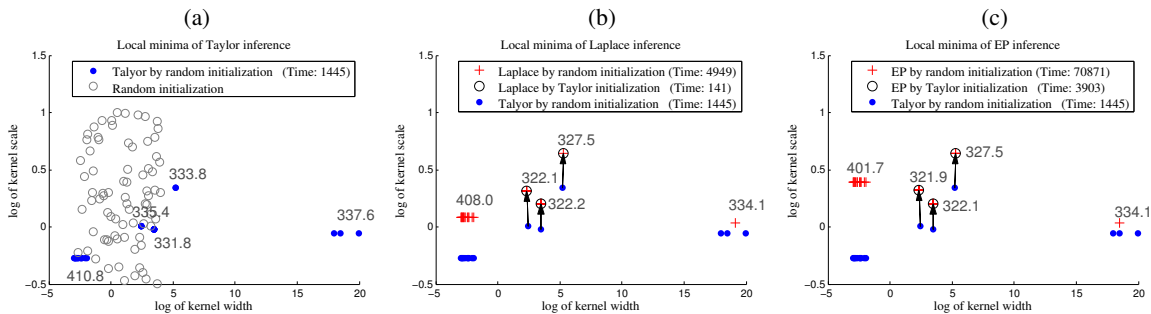


Figure 8: Illustration of using Taylor inference to initialize other inference methods for hyperparameter estimation. (a) Candidate local optima are found using Taylor method with 50 random initializations; (b) Comparison of local optima of Laplace method initialized by Taylor and 50 random points. (c) Comparison of local optima of EP method initialized by Taylor and 50 random points.

Table 5 shows the quantitative comparison between random-initialization and Taylor-initialization on three dataset (servo, auto-mpg and housing from Section 8.2). We compare the two initialization methods using the relative change in MAE,  $\Delta\text{MAE} = \frac{\text{MAE}_T - \text{MAE}_R}{\text{MAE}_R}$ , where  $\text{MAE}_T$  and  $\text{MAE}_R$  are the MAEs when using Taylor-initialization and random-initialization, respectively. The relative change in NLP is calculated in an analogous way. In all cases, the relative changes in MAE are small (within 0.002), and not statistically significant (paired  $t$ -test,  $p > 0.15$ ). A similar conclusion holds for the relative change in NLP. The Taylor-initialization yields a significant reduction in computational cost. For example, Taylor-initialized EP was about 26 times faster than random-initialized EP. Furthermore, with the help of Taylor initialization, we did not encounter any convergence problems with EP (similarly observed for the real experiments in Section 8). These experiments demonstrate that Taylor-initialization can speedup hyperparameter estimation for other inference methods, while maintaining the same quality as fully random initialization.

## 8. Experiments

In this section, we present experiments using GGPMs and inference methods on a wide variety of real-world datasets. In Section 8.1, we consider finite counting data and the Binomial-GGPM. In Section 8.2, we experiment with regression to non-negative reals (Gamma-GGPM, Inverse-

Likelihood	Laplace			EP		
	$\Delta$ MAE	$\Delta$ NLP	speedup	$\Delta$ MAE	$\Delta$ NLP	speedup
Gamma <sub>sh</sub>	0.000 $\pm$ 0.0001 ( 0.9987)	0.000 $\pm$ 0.0000 ( 0.4531)	2.97 $\pm$ 0.901	0.000 $\pm$ 0.0001 ( 0.1889)	0.000 $\pm$ 0.0023 ( 0.4090)	24.92 $\pm$ 7.566
Gamma <sub>sc</sub>	-0.002 $\pm$ 0.0127 ( 0.3474)	0.002 $\pm$ 0.0077 ( 0.2597)	3.17 $\pm$ 1.109	-0.001 $\pm$ 0.0026 ( 0.2056)	-0.001 $\pm$ 0.0019 ( 0.1270)	26.86 $\pm$ 6.487
Inv.Gauss	-0.000 $\pm$ 0.0012 ( 0.3296)	0.001 $\pm$ 0.0023 ( 0.2709)	3.44 $\pm$ 1.590	0.002 $\pm$ 0.0164 ( 0.5010)	0.013 $\pm$ 0.0534 ( 0.2103)	28.78 $\pm$ 9.861
all	-0.001 $\pm$ 0.0074 ( 0.3005)	0.001 $\pm$ 0.0046 ( 0.1567)	3.20 $\pm$ 1.236	0.000 $\pm$ 0.0095 ( 0.6372)	0.004 $\pm$ 0.0312 ( 0.2158)	26.85 $\pm$ 8.158

Table 5: Comparison between random-initialization and Taylor-initialization in terms of relative change in MAE and NLP, and the speedup factor. Parenthesis denote the  $p$  values using a paired  $t$ -test. The differences are not statistically significant.

Gaussian GGPM). Finally, Section 8.3 presents results on range data (Beta-GGPM), and Section 8.4 considers counting data and Poisson-GGPMs<sup>5</sup>.

In the following experiments, we use the Taylor initialization method from Section 7 to speed up hyperparameter estimation using the other inference methods (LA, EP, KLD). For all inference methods, the best hyperparameter is selected as the one with the largest marginal likelihood on the training set. Our results indicate that the performances of different inference methods are highly affected by likelihoods, evaluation metrics and datasets. Each inference method, even the Taylor method, can have the best performance. Furthermore, our hypothesis testing results show that the difference between EP and KLD is not statistically significant; Laplace approximation and EP often perform comparably.

### 8.1 Binomial Example

In this section we apply binomial-GGPM to the Tokyo rainfall dataset<sup>6</sup>. The dataset records the number of occurrences of rainfall over 1mm in Tokyo for every calendar day in 1983 and 1984. The rainfall occurrence for a given calendar day follow a binomial distribution. We assign the occurrence times “0”, “1”, and “2” to the outputs  $y \in \{0, 0.5, 1\}$  of the binomial model. The input feature is the calendar day (0 to 365), and the RBF kernel was used<sup>7</sup>.

As presented earlier, Figure 7 shows the negative log marginal likelihood (NML) as a function of the RBF kernel width and scale, and Figure 8 shows the results of Taylor-initialization, which yielded 5 local minima in the NML that correspond to different interpretations of the data. The best two interpretations (largest marginal likelihoods) are presented in Figures 9a and 9c, using the four inference methods. Figure 9a uses a larger kernel width, resulting in a smoother function that shows the clear seasonal pattern in Tokyo, as described by Kitagawa (1987): dry winter (Dec., Jan., and Feb.), rainy season in late June to mid-July, stable hot summer in late July through Aug., and generally fine but with an occasional typhoon in Sept. and Oct. It would be difficult to identify these trends by only looking at the original data. Finally, Figure 10 depicts the curves for the remaining

5. In this paper, we do not present results using GP regression and classification, which have been extensively studied in Rasmussen and Williams (2006); Kuss and Rasmussen (2005); Nickisch and Rasmussen (2008).

6. [http://www.stat.uni-muenchen.de/service/datenarchiv/tokio/tokio\\_e.html](http://www.stat.uni-muenchen.de/service/datenarchiv/tokio/tokio_e.html)

7. Since the input feature is the calendar day, a cyclic kernel which wraps around from 365 to 0 can be used to better model the correlation between days. In this paper, we do not adopt cyclic kernel to follow the same settings as the reference methods.



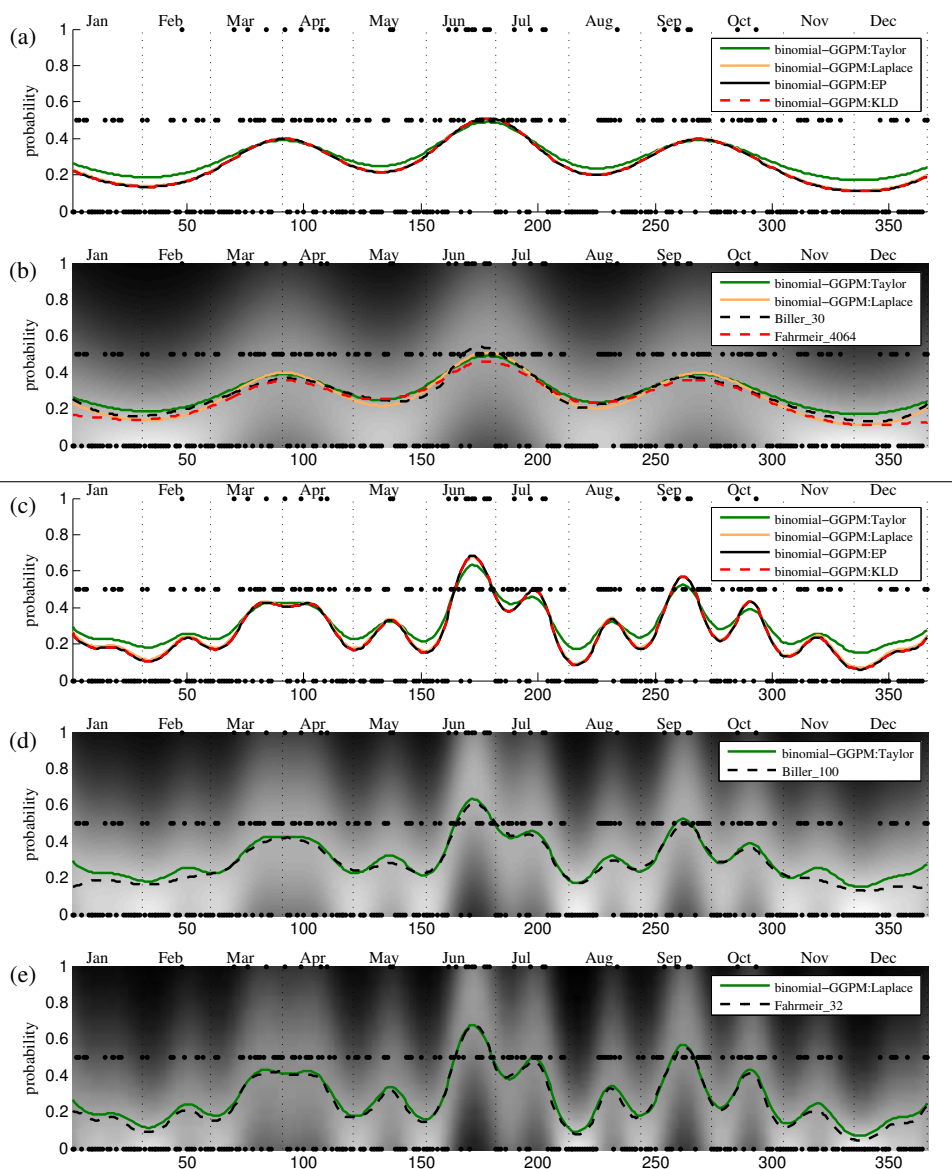


Figure 9: Two binomial-GGPM mean functions on Tokyo rainfall data, and comparisons with other methods: (a) binomial-GGPM mean function using large kernel width (smoother function), and (b) comparison to Biller (2000) and Fahrmeir et al. (1994); (c) binomial-GGPM using small kernel width (rougher function), with (d) comparison of Taylor inference to Biller (2000) and (e) comparison of Laplace inference to Fahrmeir et al. (1994).

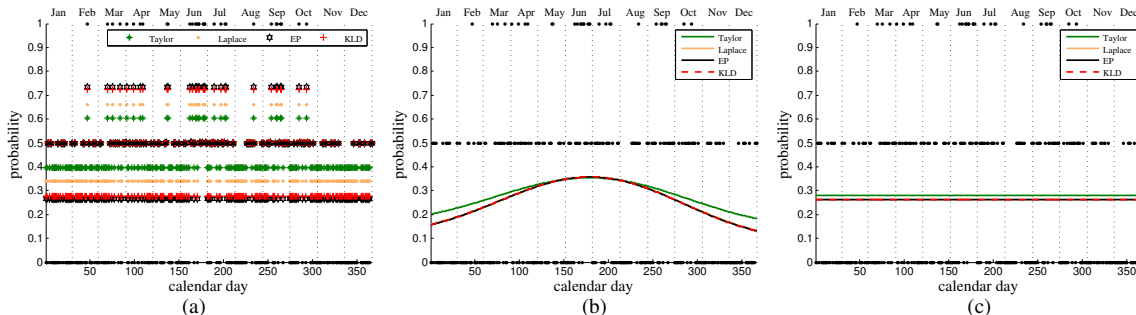


Figure 10: Estimated binomial-GGPM mean functions on Tokyo rainfall, corresponding to three bad local optima (too big or small kernel widths) as shown in Figure 8.

three bad local minima, where the kernel bandwidth is either too small or too large. The Laplace, EP and KLD methods have almost overlapped estimates for all the five local optima. The Taylor method also captures similar trends as the other three methods.

We compare the binomial-GGPMs with two spline-based regression models. The first model (Fahrmeir et al., 1994) is an extension of GLM that replaces the linear function with a cubic spline. In this model a parameter  $\lambda_S$  is used to control the tradeoff between data-fit and smoothness of the cubic function. In Fahrmeir et al. (1994),  $\lambda_S$  was estimated by cross-validation, resulting in two local minima,  $\lambda_S = 4064$  and  $\lambda_S = 32$ . The larger  $\lambda_S = 4064$  yields a relatively smoother curve, which is very close to the smoother estimate using binomial-GGPM (see Figure 9b). The curve with  $\lambda_S = 32$  is quite similar to the rougher estimate of binomial-GGPM using Laplace inference. The difference of the two local optima can be attributed to different smoothness levels.

The second model (Biller, 2000) is a fully Bayesian approach to regression splines with automatic knot placement. A Poisson distribution with parameter  $\lambda_N$  is placed over the number of knots. Experimental results (Biller, 2000) show that the rainfall dataset is very sensitive to the choice of  $\lambda_N$ . With a smaller  $\lambda_N$  the resulting function is very smooth, while increasing the value of  $\lambda_N$  allows a more flexible function. The estimate with  $\lambda_N = 100$  is similar to the rougher curve estimated by Taylor (see Figure 9d). When the value is decreased to  $\lambda_N = 30$ , the curve becomes similar to the smoother Binomial-GGPM estimate (see Figure 9b). From the two comparisons, we can see the shapes of resulted curves are highly affected by the adoption of optimal hyperparameters. If we use the negative marginal likelihood as a metric, the smoother curve will be favored by the Taylor method, while the rougher curve will be selected by the other three inference methods.

Dataset Name	$X_{dim}$	$Y_{min}$	$Y_{max}$	$N_{train}$	$N_{test}$
servo	4	0.13	7.10	70	97
auto-mpg	7	9.00	46.60	100	298
housing	12	5.00	50.00	200	306
abalone	8	1.00	29.00	1000	3177

Table 6: Datasets for non-negative real regression.

## 8.2 Non-negative Real Numbers Experiments

In this section, we perform four experiments on non-negative real numbers regression using GGPM with the Gamma and Inverse Gaussian likelihoods. We use the following four UCI datasets: 1)

		abalone dataset			housing dataset		
Lik*	Inf.	MAE	MSE	NLP	MAE	MSE	NLP
GP	Exact	1.60 ± 0.029	4.66 ± 0.232	2.19 ± 0.012	2.40 ± 0.136	11.27 ± 1.716	2.60 ± 0.047
LGP	Exact	1.47 ± 0.016	4.12 ± 0.125	2.00 ± 0.009	2.22 ± 0.141	10.39 ± 1.858	2.57 ± 0.040
WGP	Exact	1.52 ± 0.024	4.36 ± 0.169	<b>1.94 ± 0.010</b>	2.22 ± 0.138	<b>10.24 ± 1.386</b>	2.54 ± 0.191
GA <sub>sh</sub>	Taylor	1.49 ± 0.021	4.26 ± 0.238	1.99 ± 0.007	<b>2.21 ± 0.140</b>	10.46 ± 1.841	2.59 ± 0.044
GA <sub>sh</sub>	Laplace	1.55 ± 0.022	4.55 ± 0.232	2.01 ± 0.007	2.21 ± 0.144	10.41 ± 1.885	2.58 ± 0.041
GA <sub>sh</sub>	EP	1.55 ± 0.022	4.57 ± 0.237	2.01 ± 0.007	2.22 ± 0.146	10.46 ± 1.897	2.58 ± 0.040
GA <sub>sh</sub>	KLD	1.55 ± 0.022	4.53 ± 0.185	2.01 ± 0.007	2.22 ± 0.146	10.46 ± 1.891	2.58 ± 0.040
GA <sub>sc</sub>	Taylor	1.67 ± 0.023	5.10 ± 0.173	2.12 ± 0.012	2.23 ± 0.159	10.27 ± 2.282	2.52 ± 0.038
GA <sub>sc</sub>	Laplace	1.53 ± 0.024	4.41 ± 0.268	2.06 ± 0.010	2.23 ± 0.146	10.35 ± 2.104	<b>2.52 ± 0.036</b>
GA <sub>sc</sub>	EP	1.53 ± 0.025	4.39 ± 0.274	2.06 ± 0.010	2.22 ± 0.141	10.30 ± 2.046	2.52 ± 0.037
GA <sub>sc</sub>	KLD	1.53 ± 0.025	4.35 ± 0.300	2.05 ± 0.010	2.22 ± 0.142	10.29 ± 2.071	2.52 ± 0.038
INV	Taylor	<b>1.42 ± 0.022</b>	<b>4.11 ± 0.354</b>	1.99 ± 0.014	2.27 ± 0.156	11.26 ± 2.080	2.75 ± 0.069
INV	Laplace	1.54 ± 0.024	4.73 ± 0.440	1.98 ± 0.008	2.28 ± 0.163	11.05 ± 2.073	2.72 ± 0.064
INV	EP	1.55 ± 0.025	4.78 ± 0.449	1.99 ± 0.008	2.32 ± 0.171	11.39 ± 2.172	2.71 ± 0.059
INV	KLD	1.56 ± 0.019	5.04 ± 0.576	1.99 ± 0.007	2.32 ± 0.170	11.36 ± 2.149	2.71 ± 0.059

		auto-mpg dataset			servo dataset		
Lik*	Inf.	MAE	MSE	NLP	MAE	MSE	NLP
GP	Exact	2.11 ± 0.053	8.69 ± 0.349	2.48 ± 0.038	0.43 ± 0.047	0.33 ± 0.058	1.06 ± 0.033
LGP	Exact	2.10 ± 0.090	8.71 ± 0.655	2.36 ± 0.044	0.27 ± 0.035	0.18 ± 0.042	0.32 ± 0.044
WGP	Exact	<b>2.08 ± 0.061</b>	<b>8.45 ± 0.672</b>	2.39 ± 0.055	<b>0.25 ± 0.031</b>	0.18 ± 0.043	0.13 ± 0.113
GA <sub>sh</sub>	Taylor	2.09 ± 0.072	8.71 ± 0.540	2.36 ± 0.043	0.26 ± 0.035	0.20 ± 0.048	0.11 ± 0.084
GA <sub>sh</sub>	Laplace	2.09 ± 0.073	8.64 ± 0.506	<b>2.36 ± 0.040</b>	0.27 ± 0.037	0.20 ± 0.047	0.09 ± 0.072
GA <sub>sh</sub>	EP	2.09 ± 0.074	8.65 ± 0.503	2.36 ± 0.040	0.27 ± 0.037	0.20 ± 0.048	<b>0.09 ± 0.070</b>
GA <sub>sh</sub>	KLD	2.09 ± 0.075	8.66 ± 0.498	2.36 ± 0.041	0.27 ± 0.037	0.20 ± 0.048	0.09 ± 0.071
GA <sub>sc</sub>	Taylor	2.10 ± 0.076	8.73 ± 0.536	2.40 ± 0.036	0.28 ± 0.024	0.21 ± 0.041	0.19 ± 0.040
GA <sub>sc</sub>	Laplace	2.09 ± 0.064	8.74 ± 0.496	2.40 ± 0.035	0.26 ± 0.023	0.19 ± 0.033	0.18 ± 0.043
GA <sub>sc</sub>	EP	2.09 ± 0.064	8.75 ± 0.503	2.40 ± 0.036	<b>0.25 ± 0.023</b>	<b>0.18 ± 0.036</b>	0.17 ± 0.048
GA <sub>sc</sub>	KLD	2.09 ± 0.065	8.74 ± 0.495	2.40 ± 0.036	0.25 ± 0.024	0.18 ± 0.036	0.17 ± 0.048
INV	Taylor	2.11 ± 0.092	8.88 ± 0.890	2.39 ± 0.055	0.33 ± 0.045	0.34 ± 0.123	0.41 ± 0.141
INV	Laplace	2.08 ± 0.071	8.58 ± 0.624	2.36 ± 0.043	0.35 ± 0.046	0.41 ± 0.139	0.41 ± 0.155
INV	EP	2.08 ± 0.069	8.59 ± 0.589	2.36 ± 0.041	0.37 ± 0.050	0.45 ± 0.139	0.38 ± 0.146
INV	KLD	<b>2.08 ± 0.065</b>	8.59 ± 0.567	2.36 ± 0.042	0.37 ± 0.051	0.45 ± 0.147	0.40 ± 0.150

Table 7: Average errors for servo, auto-mpg, housing and abalone datasets. (\*likelihood abbreviations: **LGP** - GP on the log-transformed outputs; **WGP** - warped GP; **GA<sub>sh</sub>** - Gamma<sub>sh</sub>-GGPM; **GA<sub>sc</sub>** - Gamma<sub>sc</sub>-GGPM; **INV** - Inv. Gaussian-GGPM)

abalone<sup>8</sup> – predict the age of abalone from physical measurements; 2) housing<sup>9</sup> – predict housing values in suburbs of Boston; 3) auto-mpg<sup>10</sup> – estimate city-cycle fuel consumption in miles per gallon(mpg); 4) servo<sup>11</sup> – predict the rise time of a servo-mechanism in terms of two gain settings and two choices of mechanical linkages. The four datasets are summarized in Table 6, which lists the output range ( $Y_{min}, Y_{max}$ ), the input dimension ( $X_{dim}$ ), and the size of the training and test sets ( $N_{train}, N_{test}$ ).

In all experiments, we follow the same testing protocol. A given number of training samples are randomly selected from the dataset, and the remaining data is used for testing. This process is repeated 10 times, and the means and standard deviations of MAE and NLP reported. To test statistical significance, we use the Friedman test (Howell, 2010), which is a non-parametric test on the differences of several related samples, based on ranking. To find candidate hyperparameters in each trial, we use the Taylor-initialization procedure described in the Section 7. Then the candidate

8. <http://archive.ics.uci.edu/ml/datasets/Abalone>

9. <http://archive.ics.uci.edu/ml/datasets/Housing>

10. <http://archive.ics.uci.edu/ml/datasets/Auto+MPG>

11. <http://archive.ics.uci.edu/ml/datasets/Servo>

hyperparameters are used as the initialization for the other three inference methods. We also implemented three other typical GP models: standard GPR, GPR on the log-transformed data, and the warped GP (Snelson et al., 2004).

Experimental results are presented in Table 7. The non-negative GGPMs typically perform better than standard GPR. As expected from Section 5.2.5, the log-transformed GP performs similarly to the  $\text{Gamma}_{\text{sh}}$ -GGPM with Taylor inference. However, there are small performance differences due to the different marginal likelihoods used to estimate the hyperparameters; the former is based on the standard GP marginal in (9), while the latter is based on the Taylor marginal in (48) that includes an extra penalty term on the dispersion hyperparameter. The learned warping functions of WGP for the four datasets are also log-like, and hence WGP also has similar performance. The Inv.-Gaussian-GGPM with Taylor inference can also be viewed as using a standard GP on the log of the outputs, but with observation noise that is output dependent (see Section 5.2.5). We can benefit from this property for the auto-mpg and abalone datasets, since Inv.-Gaussian-GGPM with Taylor inference achieves the smallest fitting errors. While for the servo and housing dataset, this likelihood is worse than the  $\text{Gamma}_{\text{sh}}$  likelihood.

Next, we rank each likelihood function based on the resulting performance in either NLP or MAE, and use a Friedman test to determine significance<sup>12</sup>. Table 8 shows the average rankings and  $p$  values for various likelihood combinations. Looking at NLP, there is a best ranked likelihood function that is statistically significant in all cases except for one ( $p < 0.001$ ). For auto-mpg, the  $\text{Gamma}_{\text{sh}}$  has slightly better ranking than Inv.-Gaussian, and the difference is marginally significant ( $0.05 < p < 0.06$ ). Since each likelihood can have the smallest average rankings, all the three GGPMs should be taken into consideration when a new dataset is given.

Looking at MAE performance, there are also significant differences in ranking between likelihoods on each dataset. Note though that in many cases the difference between the top two likelihoods are not significant (e.g., housing, auto-mpg, servo). This is mainly because the relative performance of different inference methods changes between likelihood functions, e.g., on servo, Taylor inference performs better compared to the other inference methods using the  $\text{Gamma}_{\text{sh}}$ , but the ranking is reversed when using the  $\text{Gamma}_{\text{sc}}$ . Again this indicates that the effects of likelihood functions to MAE are dataset dependent, so that the choice of likelihood function is important.

(a) Using NLP as measurement													
dataset	$\text{GA}_{\text{sh}}$	$\text{GA}_{\text{sc}}$	INV	( $p$ )	$\text{GA}_{\text{sc}}$	INV	( $p$ )	$\text{GA}_{\text{sh}}$	$\text{GA}_{\text{sc}}$	( $p$ )	$\text{GA}_{\text{sh}}$	INV	( $p$ )
abalone	1.900,	3.000,	<b>1.100</b>	(0.0000)	2.000,	<b>1.000</b>	(0.0000)	<b>1.000</b> ,	2.000	(0.0000)	1.900,	<b>1.100</b>	(0.0000)
housing	2.000,	<b>1.000</b> ,	3.000	(0.0000)	<b>1.000</b> ,	2.000	(0.0000)	2.000,	<b>1.000</b>	(0.0000)	<b>1.000</b> ,	2.000	(0.0000)
auto-mpg	<b>1.400</b> ,	2.800,	<b>1.800</b>	(0.0000)	1.850,	<b>1.150</b>	(0.0000)	<b>1.050</b> ,	1.950	(0.0000)	1.350,	1.650	(0.0578)
servo	<b>1.125</b> ,	1.875,	3.000	(0.0000)	<b>1.000</b> ,	2.000	(0.0000)	<b>1.125</b> ,	1.875	(0.0000)	<b>1.000</b> ,	2.000	(0.0000)
(b) Using MAE as measurement													
dataset	$\text{GA}_{\text{sh}}$	$\text{GA}_{\text{sc}}$	INV	( $p$ )	$\text{GA}_{\text{sc}}$	INV	( $p$ )	$\text{GA}_{\text{sh}}$	$\text{GA}_{\text{sc}}$	( $p$ )	$\text{GA}_{\text{sh}}$	INV	( $p$ )
abalone	2.375,	<b>1.563</b> ,	2.063	(0.0012)	<b>1.313</b> ,	1.688	(0.0163)	1.750,	<b>1.250</b>	(0.0016)	1.625,	1.375	(0.1138)
housing	<b>1.750</b> ,	<b>1.837</b> ,	2.413	(0.0053)	<b>1.300</b> ,	1.700	(0.0114)	1.462,	1.538	(0.6310)	<b>1.288</b> ,	1.712	(0.0065)
auto-mpg	<b>1.816</b> ,	2.395,	<b>1.789</b>	(0.0117)	1.684,	<b>1.316</b>	(0.0231)	<b>1.289</b> ,	1.711	(0.0094)	1.526,	1.474	(0.7456)
servo	<b>1.528</b> ,	<b>1.472</b> ,	3.000	(0.0000)	<b>1.000</b> ,	2.000	(0.0000)	1.528,	1.472	(0.7389)	<b>1.000</b> ,	2.000	(0.0000)

Table 8: Average rankings and  $p$  values (in parenthesis) for different likelihood combinations using the Friedman test. In each grouping, bolded rankings differ significantly from non-bold rankings ( $p < 0.05$ ), but not from each other.

12. We pool trials over all inference methods.

(a) Using NLP as measurement															
Dataset	Lik	TA,	LA,	EP,	KLD	( <i>p</i> )	TA,	LA	( <i>p</i> )	LA,	EP	( <i>p</i> )	EP,	KLD	( <i>p</i> )
abalone	INV	3.050,	<b>1.650</b> ,	2.500,	2.800	(0.0683)	1.700,	1.300	(0.2059)	<b>1.200</b> ,	1.800	(0.0339)	1.400,	1.600	(0.4795)
housing	GA <sub>sc</sub>	2.200,	2.300,	2.700,	2.800	(0.6537)	1.400,	1.600	(0.5271)	1.400,	1.600	(0.5271)	1.500,	1.500	(1.0000)
auto-mpg	GA <sub>sh</sub>	3.400,	2.300,	2.050,	2.250	(0.0488)	1.800,	1.200	(0.0578)	1.600,	1.400	(0.4142)	1.450,	1.550	(0.5637)
servo	GA <sub>sh</sub>	3.050,	1.900,	2.500,	2.550	(0.2318)	1.800,	1.200	(0.0578)	1.400,	1.600	(0.5271)	1.500,	1.500	(1.0000)
all	-	2.925,	<b>2.038</b> ,	<b>2.438</b> ,	<b>2.600</b>	(0.0137)	1.675,	<b>1.325</b>	(0.0269)	1.400,	1.600	(0.1701)	1.462,	1.538	(0.5127)

(b) Using MAE as measurement															
Dataset	Lik	TA,	LA,	EP,	KLD	( <i>p</i> )	TA,	LA	( <i>p</i> )	LA,	EP	( <i>p</i> )	EP,	KLD	( <i>p</i> )
abalone	GA <sub>sc</sub>	4.000,	3.000,	<b>1.750</b> ,	<b>1.250</b>	(0.0000)	2.000,	<b>1.000</b>	(0.0016)	2.000,	<b>1.000</b>	(0.0016)	1.750,	1.250	(0.0588)
housing	GA <sub>sh</sub>	2.350,	2.050,	2.550,	3.050	(0.3411)	1.500,	1.500	(1.0000)	1.350,	1.650	(0.3173)	1.350,	1.650	(0.3173)
auto-mpg	INV	3.300,	1.800,	2.300,	2.600	(0.0694)	1.800,	1.200	(0.0578)	1.300,	1.700	(0.2059)	1.400,	1.600	(0.5271)
servo	GA <sub>sc</sub>	4.000,	3.000,	<b>1.700</b> ,	<b>1.300</b>	(0.0000)	2.000,	<b>1.000</b>	(0.0016)	2.000,	<b>1.000</b>	(0.0016)	1.700,	1.300	(0.1025)
all	-	3.413,	2.462,	<b>2.075</b> ,	<b>2.050</b>	(0.0000)	1.825,	<b>1.175</b>	(0.0000)	1.663,	<b>1.337</b>	(0.0374)	1.550,	1.450	(0.4795)

Table 9: Average rankings and  $p$  values (in parenthesis) for different inference methods using the Friedman test. Only the best performing likelihood function is considered. In each grouping, bolded rankings differ significantly from non-bolded rankings ( $p < 0.05$ ), but not from each other.

We next compare approximate inference methods for the best-performing likelihood functions (according to average rankings in Table 8) on each dataset. Table 9 shows the average rankings and the corresponding  $p$  values using a Friedman test. Looking the ranking based on NLP in Table 9a, EP and KLD have similar rankings (within 0.2) on each dataset, and any differences are not statistically significant. Similarly, LA and EP also have similar rankings (within 0.2) for each dataset except on abalone. Over all datasets, LA has the best ranking (2.038), but this result is not statistically significant, suggesting that the rank orderings of LA, EP, and KLD are not consistent. Finally, LA has a statistically better ranking than TA, when pooling over all datasets, although the difference is not large; LA outperforms TA about two-thirds of the time.

The results are similar when looking at the rankings based on MAE in Table 9b. First looking at the rankings over all datasets, as before, EP and KLD have almost identical rankings in MAE, but now EP has better MAE than LA about two-thirds of the time (statistically significant). Finally, LA typically dominates TA in MAE ranking, over all datasets. Interestingly, there are some datasets (e.g. housing, auto-mpg), where there is no significant difference between the inference algorithms. In other words, the best inference algorithm may change in each trail, based on the particular training and test set.

In summary, the performances of inference methods are highly affected by likelihoods, datasets and evaluation metrics. For a given dataset, the choice of likelihood has a large impact on the predictive density (NLP), with only one likelihood usually dominating, and less so on the prediction error (MAE), where typically more than one likelihood can achieve low error. Given the “correct” likelihood, the performance of inference methods tends to be similar, e.g., LA, EP, and KLD have similar rankings when evaluated with NLP, and EP and KLD have similar ranking for MAE. However, given the “wrong” likelihood, the performance of the inference algorithms can be highly affected by the dataset and the evaluation metrics.

### 8.3 Range Data Experiments

In this experiment, we consider conversion of device-dependent RGB values to device- and illuminant-independent reflectance spectra. In Heikkinen et al. (2008), this conversion is cast as a regularized regression problem, where the input can be RGB or HSV color values, and the output is reflectance values at sampled wavelengths. In particular, the reflectance spectra is first scaled from the  $[0 \ 1]$  interval to  $[-1 \ 1]$ , and then mapped to a real value via the inverse hyperbolic tangent (arctanh) function, then a regularized regression framework is applied. The method in Heikkinen et al. (2008) is equivalent to applying standard GPR to the logit-transformed spectral values, as discussed in Section 5.2.5. Note that the hyperparameters are fixed in Heikkinen et al. (2008), whereas using the GP interpretation, the hyperparameters can be estimated automatically using maximum marginal likelihood.

Since the regression output is constrained to the unit interval, we consider Beta-GGPM for spectra reflectance regression, and perform experiments on the Munsell dataset, consisting of 1269 RGB/spectral pairs. Following the protocol of Heikkinen et al. (2008), we used 669 for training and 600 for testing, and results are averaged over 10 trials. We also used a smaller training set, consisting of 20% of the original training set. Hyperparameters are learned using maximum marginal likelihood.

(a) Full training dataset				
Model	Inference	Avg. Error	Max. Error	Std. Error
GP	Exact	$0.0090 \pm 0.00032$	<b><math>0.0919 \pm 0.0195</math></b>	$0.0102 \pm 0.00100$
arctanh+GP	Exact	<b><math>0.0087 \pm 0.00036</math></b>	$0.0946 \pm 0.0205$	<b><math>0.0101 \pm 0.00098</math></b>
Beta-GGPM	Taylor	$0.0088 \pm 0.00037$	$0.0961 \pm 0.0195$	$0.0103 \pm 0.00098$
Beta-GGPM	Laplace	$0.0088 \pm 0.00038$	$0.0965 \pm 0.0199$	$0.0103 \pm 0.00100$
Beta-GGPM	EP	<b><math>0.0087 \pm 0.00038</math></b>	$0.0946 \pm 0.0208$	<b><math>0.0101 \pm 0.00100</math></b>
(b) Small training dataset				
Model	Inference	Avg. Error	Max. Error	Std. Error
GP	Exact	$0.0132 \pm 0.00115$	$0.0999 \pm 0.0179$	$0.0132 \pm 0.00221$
arctanh+GP	Exact	$0.0123 \pm 0.00074$	<b><math>0.0965 \pm 0.0186</math></b>	<b><math>0.0124 \pm 0.00141</math></b>
Beta-GGPM	Taylor	$0.0123 \pm 0.00080$	$0.0970 \pm 0.0170$	<b><math>0.0124 \pm 0.00147</math></b>
Beta-GGPM	Laplace	$0.0123 \pm 0.00079$	$0.0973 \pm 0.0172$	<b><math>0.0124 \pm 0.00143</math></b>
Beta-GGPM	EP	<b><math>0.0122 \pm 0.00077</math></b>	$0.0967 \pm 0.0183$	<b><math>0.0124 \pm 0.00141</math></b>

Table 10: Average errors for the Munsell dataset.

The experimental results are presented in Table 10. First, the standard GP performs worse than Beta-GGPM, due to the mismatch between output domain and actual outputs. This effect is more pronounced when less training data is available; when using the smaller training set, the average error drops around 8% for the Beta-GGPM versus the GP. Next, Beta-GGPM with Taylor inference and Gauss-GGPM+arctanh have almost the same values for the three error metrics, this is consistent to our conclusion that Beta-GGPM with Taylor inference can be viewed as using a standard GP on the logit transformation of the outputs. Finally, the three inference methods (TA, LA, EP) perform similarly for Beta-GGPM on this dataset, in terms of average error. Table 11 shows the Friedman test results for the different inference combinations. For the full training set, LA and EP have similar average rankings, with TA ranked 0.6 worse. However, the differences are not statistically significant, due to the similar average error values. For the reduced training set, EP has the best ranking, followed by TA and then LA. Again, the rankings are not statistically significant, although EP is marginally better than LA ( $0.05 < p < 0.06$ ).

(a) Full training dataset													
Metrics	TA,	LA,	EP	( $p$ )	TA,	LA	( $p$ )	TA,	EP	( $p$ )	LA,	EP	( $p$ )
Avg. Error	2.450,	1.850,	1.700	(0.0724)	1.750,	<b>1.250</b>	(0.0253)	1.700,	1.300	(0.1024)	1.600,	1.400	(0.4142)
Max. Error	1.900,	2.500,	1.600	(0.1225)	1.300,	1.700	(0.2059)	1.600,	1.400	(0.5271)	1.800,	1.200	(0.0578)
Std. Error	2.500,	2.050,	1.450	(0.0581)	1.700,	1.300	(0.2059)	1.800,	1.200	(0.0578)	1.750,	1.250	(0.0956)
(b) Small training dataset													
Metrics	TA,	LA,	EP	( $p$ )	TA,	LA	( $p$ )	TA,	EP	( $p$ )	LA,	EP	( $p$ )
Avg. Error	2.050,	2.400,	1.550	(0.1316)	1.350,	1.650	(0.3173)	1.700,	1.300	(0.2059)	1.750,	1.250	(0.0588)
Max. Error	1.800,	2.000,	2.200	(0.6703)	1.400,	1.600	(0.5271)	1.400,	1.600	(0.5271)	1.400,	1.600	(0.5271)
Std. Error	1.700,	2.350,	1.950	(0.3225)	1.250,	1.750	(0.0956)	1.450,	1.550	(0.7389)	1.600,	1.400	(0.5271)

Table 11: Beta-GGPM: Average rankings of different inference methods and  $p$  values using the Friedman test. Bolded rankings differ significantly from non-bold rankings ( $p < 0.05$ ).

## 8.4 Counting experiments

We perform two counting experiments using GGPMs with Poisson-based likelihoods. In all cases, predictions are based on the mode of the distribution for GGPMs, and the rounded, truncated mean for GPR. In the first experiment, we perform crowd counting using the UCSD crowd counting dataset<sup>13</sup> from Chan et al. (2008). The dataset contains 30-dimensional features extracted from images and the corresponding number of people in each image, for two different directions (right and left motion). The goal is to predict the number of people using just the image features. The right crowd contains more people (average of 14.69 per image) than the left crowd (average of 9.98). The dataset consists of 2000 feature/count pairs for each direction, and following Chan et al. (2008), we use 800 for training and 1200 of testing. We predict using the Poisson and COM-Poisson GGPMs and the exponential mean mapping (canonical link function), as well as the versions using the linear mean mapping (linearized link function) from Section 4.3.2. The compound linear plus RBF kernel was used for all models.

The crowd counting results are presented in Table 12. On the “right” crowd, the Poisson- and COM-Poisson-GGPMs perform better using the exponential mapping versus the linear mapping. This is due to the large number of people in the “right” crowd, which leads to a more non-linear (exponential) trend in the feature space. In contrast, the linearized link functions perform better on the “left crowd”, indicating a more linear trend in the data (due to smaller crowd sizes and fewer occlusions). Looking at the likelihood functions, the Poisson likelihood has higher accuracy on the “right” crowd, whereas the COM-Poisson is better on the “left” crowd. The main difference is that COM-Poisson provides some flexibility to control the variance of the observation noise, which helps for the “left” crowd.

To do hypothesis testing, we randomly selected 10 small training sets, consisting of 400 feature/count pairs, from the original training dataset. The learned GGPMs are evaluated on the original test dataset, and experimental results are presented in Table 13. Table 14 shows the average rankings and  $p$  values using the Friedman test for different likelihoods combinations. We can see the Poisson- and COM-Poisson-GGPMs perform significantly better than the corresponding linearized models on the “right” crowd, and vice versa, the linearized link functions perform better on the “left” crowd. This is consistent with our observations from the experiments on the original training and test datasets.

13. Data set at <http://visual.cs.cityu.edu.hk/downloads/#ucsdpedsfacts>

Likelihood	Inference	Right crowd				Left crowd			
		exponential mean		linearized mean		exponential mean		linearized mean	
		MAE	NLP	MAE	NLP	MAE	NLP	MAE	NLP
GP	Exact	-	-	1.56	2.94	-	-	0.85	1.83
Poisson	Taylor	<b>1.25</b>	<b>2.33</b>	1.36	2.34	1.03	2.20	0.88	2.18
	Laplace	1.27	2.33	1.36	2.34	1.03	2.20	0.87	2.18
	EP	1.27	2.33	1.37	2.34	1.03	2.20	0.87	2.18
COM-Poisson	Taylor	1.39	2.50	1.48	2.50	0.94	1.76	0.91	1.63
COM-Poisson	Laplace	1.39	2.54	1.49	2.51	0.94	1.77	0.85	<b>1.52</b>
COM-Poisson	EP	1.43	2.54	1.49	2.52	0.94	1.76	<b>0.83</b>	1.55

Table 12: Mean absolute errors for crowd counting with comparisons between likelihood functions, inference methods, and link functions.

Lik.	Inf.	Right crowd				Left crowd			
		exponential mean		linearized mean		exponential mean		linearized mean	
		MAE	NLP	MAE	NLP	MAE	NLP	MAE	NLP
GP	Exact	-	-	1.56 ± 0.027	2.56 ± 0.059	-	-	0.88 ± 0.022	1.69 ± 0.055
PO	TA	<b>1.31 ± 0.038</b>	2.34 ± 0.038	1.46 ± 0.036	2.35 ± 0.034	1.04 ± 0.023	2.19 ± 0.036	0.95 ± 0.024	2.17 ± 0.027
PO	LA	1.33 ± 0.033	2.34 ± 0.038	1.43 ± 0.030	2.35 ± 0.035	1.02 ± 0.019	2.19 ± 0.030	0.93 ± 0.019	2.17 ± 0.019
PO	EP	1.33 ± 0.034	2.34 ± 0.038	1.42 ± 0.032	2.35 ± 0.035	1.02 ± 0.018	2.19 ± 0.030	0.93 ± 0.018	2.17 ± 0.019
COM	TA	1.54 ± 0.076	2.61 ± 0.106	1.50 ± 0.046	2.43 ± 0.079	0.96 ± 0.038	1.83 ± 0.055	0.92 ± 0.045	1.68 ± 0.052
COM	LA	1.55 ± 0.098	2.22 ± 0.069	1.58 ± 0.037	2.43 ± 0.072	0.95 ± 0.021	1.81 ± 0.047	<b>0.86 ± 0.023</b>	1.65 ± 0.043
COM	EP	1.40 ± 0.033	<b>2.20 ± 0.057</b>	1.54 ± 0.048	2.35 ± 0.034	0.92 ± 0.016	1.75 ± 0.051	0.86 ± 0.027	<b>1.62 ± 0.049</b>

Table 13: Average errors for crowd counting dataset using reduced training set. (likelihood abbreviations: **PO** - Poisson; **COM** - COM-Poisson)

(a) Using NLP as measurement												
dataset	PO	L-PO	COM	L-COM	(p)	PO	L-PO	(p)	COM, L-COM	(p)	L-PO, L-COM	(p)
Right	<b>1.758</b>	2.788	2.030	3.424	(0.0000)	<b>1.000</b>	2.000	(0.0000)	1.333, 1.667	(0.0555)	<b>1.121</b> , 1.879	(0.0000)
Left	4.000, 3.000	2.000, <b>1.000</b>	(0.0000)	2.000, <b>1.000</b>	(0.0000)	2.000, <b>1.000</b>	(0.0000)	2.000, <b>1.000</b>	(0.0000)	2.000, <b>1.000</b>	(0.0000)	
(b) Using MAE as measurement												
dataset	PO	L-PO	COM	L-COM	(p)	PO	L-PO	(p)	COM, L-COM	(p)	L-PO, L-COM	(p)
Right	<b>1.061</b>	2.333, 3.061, 3.545	(0.0000)	<b>1.000</b>	2.000	(0.0000)	1.394, 1.606	(0.2230)	<b>1.061</b> , 1.939	(0.0000)		
Left	3.933, 2.333	2.656, <b>1.078</b>	(0.0000)	2.000, <b>1.000</b>	(0.0000)	2.000, <b>1.000</b>	(0.0000)	2.000, <b>1.000</b>	(0.0000)	1.944, <b>1.056</b>	(0.0000)	

Table 14: Average rankings and  $p$  values (in parenthesis) for different likelihood combinations using the Friedman test. Bolded rankings differ significantly from non-bold rankings ( $p < 0.05$ ). (likelihood abbreviations: **PO** - Poisson; **L-PO** - Linear Poisson; **COM** - COM-Poisson); **L-COM** - Linear COM-Poisson)



In the second experiment, the GGPM is used for age estimation of face images. We use the FG-NET dataset<sup>14</sup>, which consists of face images of 82 people at different ages (average of 12 images per person). The input vector into the GGPM is 150 facial features, which are extracted using active appearance models (Cootes et al., 2001), while the output is the age of the face. We used leave-one-person-out testing as in Zhang and Yeung (2010) to evaluate the performance of difference GGPMs. For each fold, the images of one person are used for testing, and all the other people are used as the training dataset.

The experiment results for age estimation are presented in Table 15. The linear Poisson-GGPM has the lowest MAE of 5.82 versus 6.12 for standard GPR. Table 16a shows the Friedman test results for different likelihood combinations, and results indicate that the linearized Poisson GGPM significantly better ranking than the other two GGPMs. Table 16b shows the Friedman test for different inference combinations. Although there are small differences in MAE between the inference algorithms for each likelihood, the rankings are very similar, which indicates that no inference method dominates in terms of MAE. In general, Laplace and EP perform similarly, and there is no statistically significant difference between them. Moreover, Taylor approximation can outperform the other two methods for some GGPMs, e.g. Neg. binomial-GGPM, but again the difference is not statistically significant. Finally, Figure 11 presents an example prediction on a test person.

Method	Inference	MAE
GP	Exact	6.12
Warped GP (Zhang and Yeung, 2010)	Exact	6.11
Poisson GGPM	Taylor	6.44
Poisson GGPM	Laplace	6.41
Poisson GGPM	EP	6.40
Linearized Poisson GGPM	Taylor	5.98
Linearized Poisson GGPM	Laplace	<b>5.82</b>
Linearized Poisson GGPM	EP	5.83
Neg. binomial GGPM	Taylor	6.19
Neg. binomial GGPM	Laplace	6.37
Neg. binomial GGPM	EP	6.37

Table 15: MAEs for age estimation.

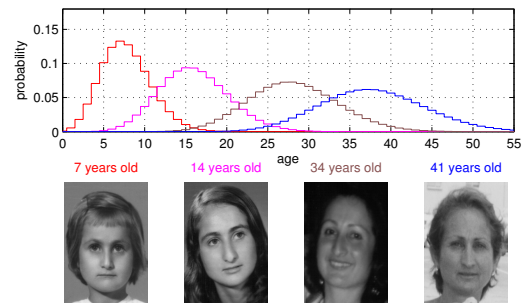


Figure 11: Examples of predicted distributions.

(a) Different likelihoods													
Inference	PO	L-PO	NB	( <i>p</i> )	L-PO	NB	( <i>p</i> )	PO	L-PO	( <i>p</i> )	PO	NB	( <i>p</i> )
all	2.193	<b>1.805</b>	2.002	(0.0001)	<b>1.433</b>	1.567	(0.0328)	1.628	<b>1.372</b>	(0.0000)	1.565	<b>1.435</b>	(0.0364)
(b) Different inference methods													
Likelihood	TA	LA	EP	( <i>p</i> )	TA	LA	( <i>p</i> )	TA	EP	( <i>p</i> )	LA	EP	( <i>p</i> )
Poisson	2.128	1.976	1.896	(0.2550)	1.555	1.445	(0.3113)	1.573	1.427	(0.1687)	1.530	1.470	(0.4233)
Lin. Poisson	2.152	1.927	1.921	(0.2094)	1.567	1.433	(0.2216)	1.585	1.415	(0.1175)	1.494	1.506	(0.8946)
Neg. binomial	1.890	2.073	2.037	(0.4013)	1.433	1.567	(0.2100)	1.457	1.543	(0.4189)	1.506	1.494	(0.8815)

Table 16: Average rankings and  $p$  values using the Friedman test. Bolded rankings differ significantly from non-bold rankings ( $p < 0.05$ ). (likelihood abbreviations: **PO** - Poisson; **L-PO** - Lin. Poisson; **NB** - Neg. binomial)

14. Data set at <http://www.fgnet.rsunit.com>

## 8.5 Summary

Our experiments have considered a variety of likelihood functions, inference methods, and datasets. In general, the choice of likelihood function is more important than the choice of approximate inference algorithm. Using a likelihood function that matches the output domain and observation noise will typically lead to better performance over the standard GP. The link function can also affect the final result, and the selection of the link function is dataset dependent, similar to the choice of the kernel function.

Looking at the inference methods, EP and KLD typically have similar performance, and Laplace inference also achieves comparable results. Taylor inference sometimes yields the smallest MAEs, while its NLP is often larger than the other three inference. This suggests that accurate estimation in terms of NLP does not always lead to smaller fitting error in terms of MAE. The performances of different inference methods are also highly affected by the distribution of training and test data, due to the systematic ordering observed in the posterior means (Section 6). Finally, on many datasets there is no dominant approximate inference algorithm, yielding mixed results and average rankings with differences that are not statistically significant.

## 9. Conclusions

In this paper, we have studied approximate inference for generalized Gaussian process models. The GGPM is a unifying framework for existing GP models, where the observation likelihood of the GP model is itself parameterized using the exponential family distribution (EFD). This allows approximate inference algorithms to be derived using the general form of the EFD. A particular GP model can then be formed by setting the parameters of the EFD, which instantiates a particular observation likelihood function for an output domain. In addition to the observation likelihood, the GGPM also has a link function that controls the mapping between the latent variable (GP prior) and the mean of the output distribution. By appropriately setting the link function, mean trends (e.g., logarithmic) can be learned that would otherwise not be possible with standard positive-definite kernel functions.

We also study an approximate inference method based on a Taylor approximation, which is non-iterative and computationally efficient. The Taylor approximation can justify many common heuristics in GP modeling (e.g., label regression, GPR on log-transformed outputs, and GPR on logit-transformed outputs) as principled inference with a particular likelihood function. We also present approximate inference for GGPMs using the Laplace approximation, expectation propagation, and KL divergence minimization. Furthermore, we demonstrate that the posterior means of the Taylor, Laplace, and EP approximations usually have a specific ordering, which are a result of the particular method of approximation. As a consequence, since the posterior means are biased in this way, the prediction error of a particular inference algorithm heavily depends on the distributions of the training and test data. Finally, we perform hyperparameter estimation using the Taylor approximation to initialize the other less-efficient approximate inference methods. Our initialization procedure can greatly increase the speed of the the learning phase, while not significantly affecting the quality of the hyperparameters. In addition, we did not notice any convergence issues of EP when using our initialization procedure.

We conduct a comprehensive set of experiments, using a variety of likelihood functions, approximate inference methods, and datasets. In our experiments, we found that the selection of the correct likelihood function has a larger impact on the prediction accuracy than the approximate inference

method. Indeed, in many cases there was no dominant inference method, and any differences in average ranking were not statistically significant. Whereas, the appropriate choice of likelihood function and link function improved accuracy significantly.

Finally, in this paper we have only considered univariate observations for the GGPM. Future work will use the multivariate exponential family distribution to form a multivariate GGPM. Such a model would encompass existing multivariate GPs, such as GP ordinal regression (Chu and Ghahramani, 2005), multi-class GP classification (Girolami and Rogers, 2006; Kim and Ghahramani, 2006; Williams and Barber, 1998), and semiparametric latent factor models (Teh et al., 2005).

## Appendix A. Closed-form Taylor Approximation

This appendix contains the derivations for the closed-form Taylor approximation in Section 5.2

### A.1 Joint likelihood approximation

Summing over (43), we have the approximation to output likelihood

$$\log p(\mathbf{y}|\boldsymbol{\theta}(\boldsymbol{\eta})) = \sum_{i=1}^n \log p(y_i|\theta(\eta_i)) \approx \sum_{i=1}^n \log p(y_i|\theta(\tilde{\eta}_i)) + \tilde{u}_i(\eta_i - \tilde{\eta}_i) - \frac{1}{2}\tilde{w}_i^{-1}(\eta_i - \tilde{\eta}_i)^2 \quad (90)$$

$$= -\frac{1}{2}(\boldsymbol{\eta} - \tilde{\boldsymbol{\eta}})^T \tilde{\mathbf{W}}^{-1}(\boldsymbol{\eta} - \tilde{\boldsymbol{\eta}}) + \tilde{\mathbf{u}}^T(\boldsymbol{\eta} - \tilde{\boldsymbol{\eta}}) + \log p(\mathbf{y}|\theta(\tilde{\boldsymbol{\eta}})). \quad (91)$$

Substituting (91) into (42), we obtain an approximation to the joint posterior,

$$\begin{aligned} \log q(\mathbf{y}, \boldsymbol{\eta}|\mathbf{X}) &= \log p(\mathbf{y}|\theta(\tilde{\boldsymbol{\eta}})) - \frac{1}{2} \log |\mathbf{K}| - \frac{n}{2} \log 2\pi \\ &\quad - \frac{1}{2}(\boldsymbol{\eta} - \tilde{\boldsymbol{\eta}})^T \tilde{\mathbf{W}}^{-1}(\boldsymbol{\eta} - \tilde{\boldsymbol{\eta}}) + \tilde{\mathbf{u}}^T(\boldsymbol{\eta} - \tilde{\boldsymbol{\eta}}) - \frac{1}{2}\boldsymbol{\eta}^T \mathbf{K}^{-1} \boldsymbol{\eta} \end{aligned} \quad (92)$$

$$\begin{aligned} &= \log p(\mathbf{y}|\theta(\tilde{\boldsymbol{\eta}})) - \frac{1}{2} \log |\mathbf{K}| - \frac{n}{2} \log 2\pi \\ &\quad \underbrace{- \frac{1}{2}(\boldsymbol{\eta} - \tilde{\boldsymbol{\eta}} - \tilde{\mathbf{W}}\tilde{\mathbf{u}})^T \tilde{\mathbf{W}}^{-1}(\boldsymbol{\eta} - \tilde{\boldsymbol{\eta}} - \tilde{\mathbf{W}}\tilde{\mathbf{u}}) - \frac{1}{2}\boldsymbol{\eta}^T \mathbf{K}^{-1} \boldsymbol{\eta} + \frac{1}{2}\tilde{\mathbf{u}}^T \tilde{\mathbf{W}}\tilde{\mathbf{u}}}_{\text{bracketed term}} \end{aligned} \quad (93)$$

Next, we note that the bracketed term in (93) is of the form

$$(\mathbf{x} - \mathbf{a})^T \mathbf{B}(\mathbf{x} - \mathbf{a}) + \mathbf{x}^T \mathbf{C}\mathbf{x} = \mathbf{x}^T \mathbf{D}\mathbf{x} - 2\mathbf{x}^T \mathbf{B}\mathbf{a} + \mathbf{a}^T \mathbf{B}\mathbf{a} \quad (94)$$

$$= \mathbf{x}^T \mathbf{D}\mathbf{x} - 2\mathbf{x}^T \mathbf{D}\mathbf{D}^{-1} \mathbf{B}\mathbf{a} + \mathbf{a}^T \mathbf{B}^T \mathbf{D}^{-1} \mathbf{B}\mathbf{a} - \mathbf{a}^T \mathbf{B}^T \mathbf{D}^{-1} \mathbf{B}\mathbf{a} + \mathbf{a}^T \mathbf{B}\mathbf{a} \quad (95)$$

$$= \|\mathbf{x} - \mathbf{D}^{-1} \mathbf{B}\mathbf{a}\|_{\mathbf{D}^{-1}}^2 + \mathbf{a}^T (\mathbf{B} - \mathbf{B}^T \mathbf{D}^{-1} \mathbf{B})\mathbf{a} = \|\mathbf{x} - \mathbf{D}^{-1} \mathbf{B}\mathbf{a}\|_{\mathbf{D}^{-1}}^2 + \|\mathbf{a}\|_{\mathbf{B}^{-1} + \mathbf{C}^{-1}}^2 \quad (96)$$

where  $\mathbf{D} = \mathbf{B} + \mathbf{C}$ , and the last line uses the matrix inversion lemma. Using this property ( $\mathbf{x} = \boldsymbol{\eta}$ ,  $\mathbf{a} = \tilde{\boldsymbol{\eta}} + \tilde{\mathbf{W}}\tilde{\mathbf{u}}$ ,  $\mathbf{B} = \mathbf{W}^{-1}$ ,  $\mathbf{C} = \mathbf{K}^{-1}$ ), the joint likelihood can be rewritten as (44).

### A.2 Special expansion point

For the case when  $\eta_i = g(T(y_i))$ , we note that

$$T(y_i) - \dot{b}(\theta(g(T(y_i)))) = T(y_i) - \dot{b}(\dot{b}^{-1}(g^{-1}(g(T(y_i)))))) = 0, \quad (97)$$

which yields (46).

### A.3 Approximate Marginal

The approximate marginal is obtained by substituting the approximate joint in (44)

$$\log p(\mathbf{y}|\mathbf{X}) = \log \int \exp(\log p(\mathbf{y}, \boldsymbol{\eta}|\mathbf{X})) d\boldsymbol{\eta} \approx \log \int \exp(\log q(\mathbf{y}, \boldsymbol{\eta}|\mathbf{X})) d\boldsymbol{\eta} \quad (98)$$

$$\begin{aligned} &= \log p(\mathbf{y}|\theta(\tilde{\boldsymbol{\eta}})) - \frac{1}{2} \log |\mathbf{K}| - \frac{n}{2} \log 2\pi \\ &\quad - \frac{1}{2} \|\tilde{\mathbf{t}}\|_{\tilde{\mathbf{W}}+\mathbf{K}}^2 + \frac{1}{2} \tilde{\mathbf{u}}^T \tilde{\mathbf{W}} \tilde{\mathbf{u}} + \log \int e^{-\frac{1}{2} \|\boldsymbol{\eta} - \mathbf{A}^{-1} \tilde{\mathbf{W}}^{-1} \tilde{\mathbf{t}}\|_{\mathbf{A}^{-1}}^2} d\boldsymbol{\eta} \end{aligned} \quad (99)$$

$$= \log p(\mathbf{y}|\theta(\tilde{\boldsymbol{\eta}})) - \frac{1}{2} \log |\mathbf{K}| - \frac{n}{2} \log 2\pi - \frac{1}{2} \|\tilde{\mathbf{t}}\|_{\tilde{\mathbf{W}}+\mathbf{K}}^2 + \frac{1}{2} \tilde{\mathbf{u}}^T \tilde{\mathbf{W}} \tilde{\mathbf{u}} + \log(2\pi)^{\frac{n}{2}} |\mathbf{A}^{-1}|^{\frac{1}{2}} \quad (100)$$

$$= \log p(\mathbf{y}|\theta(\tilde{\boldsymbol{\eta}})) - \frac{1}{2} \log |\mathbf{K}| |\mathbf{A}| - \frac{1}{2} \|\tilde{\mathbf{t}}\|_{\tilde{\mathbf{W}}+\mathbf{K}}^2 + \frac{1}{2} \tilde{\mathbf{u}}^T \tilde{\mathbf{W}} \tilde{\mathbf{u}} \quad (101)$$

Looking at the determinant term,

$$\log |\mathbf{A}| |\mathbf{K}| = \log |(\tilde{\mathbf{W}}^{-1} + \mathbf{K}^{-1})\mathbf{K}| = \log |\mathbf{I} + \tilde{\mathbf{W}}^{-1}\mathbf{K}| = \log |\tilde{\mathbf{W}} + \mathbf{K}| |\tilde{\mathbf{W}}^{-1}|. \quad (102)$$

Hence, the approximate marginal is (48). The dispersion penalty can be further rewritten as  $r(\phi) = \sum_{i=1}^n r_i(\phi)$ , where for an individual data point, we have

$$r_i(\phi) = \log p(y_i|\theta(\tilde{\eta}_i)) + \frac{1}{2} \tilde{w}_i \tilde{u}_i^2 + \frac{1}{2} \log |\tilde{w}_i|. \quad (103)$$

#### A.3.1 DERIVATIVES WRT HYPERPARAMETERS

The derivative of (48) with respect to the kernel hyperparameter  $\alpha_j$  is

$$\frac{\partial}{\partial \alpha_j} \log q(\mathbf{y}|\mathbf{X}) = \frac{1}{2} \tilde{\mathbf{t}}^T (\mathbf{K} + \tilde{\mathbf{W}})^{-1} \frac{\partial \mathbf{K}}{\partial \alpha_j} (\mathbf{K} + \tilde{\mathbf{W}})^{-1} \tilde{\mathbf{t}} - \frac{1}{2} \text{tr} \left[ (\mathbf{K} + \tilde{\mathbf{W}})^{-1} \frac{\partial \mathbf{K}}{\partial \alpha_j} \right] \quad (104)$$

$$= \frac{1}{2} \text{tr} \left[ (\mathbf{z}\mathbf{z}^T - (\mathbf{K} + \tilde{\mathbf{W}})^{-1}) \frac{\partial \mathbf{K}}{\partial \alpha_j} \right], \quad \mathbf{z} = (\mathbf{K} + \tilde{\mathbf{W}})^{-1} \tilde{\mathbf{t}}. \quad (105)$$

where  $\frac{\partial \mathbf{K}}{\partial \alpha_j}$  is the element-wise derivative of the kernel matrix with respect to the kernel hyperparameter  $\alpha_j$ , and we use the derivative properties,

$$\frac{\partial}{\partial \alpha} \mathbf{A}^{-1} = -\mathbf{A}^{-1} \frac{\partial \mathbf{A}}{\partial \alpha} \mathbf{A}^{-1}, \quad \frac{\partial}{\partial \alpha} \log |\mathbf{A}| = \text{tr}(\mathbf{A}^{-1} \frac{\partial \mathbf{A}}{\partial \alpha}). \quad (106)$$

## A.3.2 DERIVATIVE WRT DISPERSION

For the derivative with respect to the dispersion parameter, we first note that

$$\frac{\partial}{\partial \phi} \tilde{w}_i = \dot{a}(\phi) \left\{ \ddot{b}(\theta(\tilde{\eta}_i)) \dot{\theta}(\tilde{\eta}_i)^2 - \left[ T(y_i) - \dot{b}(\theta(\tilde{\eta}_i)) \right] \ddot{\theta}(\tilde{\eta}_i) \right\}^{-1} = \frac{\dot{a}(\phi)}{a(\phi)} \tilde{w}_i, \quad (107)$$

$$\frac{\partial}{\partial \phi} \tilde{\mathbf{W}} = \frac{\dot{a}(\phi)}{a(\phi)} \tilde{\mathbf{W}}, \quad (108)$$

$$\frac{\partial}{\partial \phi} \tilde{u}_i = -\frac{\dot{a}(\phi)}{a(\phi)^2} \dot{\theta}(\tilde{\eta}_i) \left[ T(y_i) - \dot{b}(\theta(\tilde{\eta}_i)) \right] = -\frac{\dot{a}(\phi)}{a(\phi)} \tilde{u}_i, \quad (109)$$

$$\frac{\partial}{\partial \phi} \tilde{w}_i \tilde{u}_i^2 = \frac{\dot{a}(\phi)}{a(\phi)} \tilde{w}_i \tilde{u}_i^2 + 2\tilde{w}_i \tilde{u}_i \left( -\frac{\dot{a}(\phi)}{a(\phi)} \tilde{u}_i \right) = -\frac{\dot{a}(\phi)}{a(\phi)} \tilde{w}_i \tilde{u}_i^2, \quad (110)$$

$$\frac{\partial}{\partial \phi} \log p(y_i | \theta(\tilde{\eta}_i)) = -\frac{\dot{a}(\phi)}{a(\phi)^2} \left[ T(y_i) \theta(\tilde{\eta}_i) - b(\theta(\tilde{\eta}_i)) \right] + \dot{c}(\phi, y_i) = -\frac{\dot{a}(\phi)}{a(\phi)} \tilde{v}_i + \dot{c}(\phi, y_i), \quad (111)$$

where  $\tilde{v}_i = \frac{1}{a(\phi)} [y_i \theta(\tilde{\eta}_i) - b(\theta(\tilde{\eta}_i))]$ , and  $\dot{c}(\phi, y_i) = \frac{\partial}{\partial \phi} c(\phi, y_i)$ . Thus,

$$\frac{\partial}{\partial \phi} r_i(\phi) = -\frac{\dot{a}(\phi)}{a(\phi)} \tilde{v}_i + \dot{c}(\phi, y_i) - \frac{1}{2} \frac{\dot{a}(\phi)}{a(\phi)} \tilde{w}_i \tilde{u}_i^2 + \frac{1}{2} \frac{1}{\tilde{w}_i} \frac{\dot{a}(\phi)}{a(\phi)} \tilde{w}_i \quad (112)$$

$$= \frac{\dot{a}(\phi)}{a(\phi)} \left( \frac{1}{2} - \tilde{v}_i - \frac{1}{2} \tilde{w}_i \tilde{u}_i^2 \right) + \dot{c}(\phi, y_i). \quad (113)$$

Summing over  $i$ ,

$$\frac{\partial}{\partial \phi} r(\phi) = \sum_i \frac{\dot{a}(\phi)}{a(\phi)} \left( \frac{1}{2} - \tilde{v}_i - \frac{1}{2} \tilde{w}_i \tilde{u}_i^2 \right) + \dot{c}(\phi, y_i) \quad (114)$$

$$= \frac{\dot{a}(\phi)}{a(\phi)} \left( \frac{n}{2} - \mathbf{1}^T \tilde{\mathbf{v}} - \frac{1}{2} \tilde{\mathbf{u}}^T \tilde{\mathbf{W}} \tilde{\mathbf{u}} \right) + \sum_{i=1}^n \dot{c}(\phi, y_i). \quad (115)$$

Also note that  $\tilde{\mathbf{t}}$  is not a function of  $\phi$ , as the term cancels out in  $\tilde{\mathbf{W}} \tilde{\mathbf{u}}$ . Finally,

$$\frac{\partial}{\partial \phi} \log q(\mathbf{y} | \mathbf{X}) = \frac{1}{2} \tilde{\mathbf{t}}^T \left( \mathbf{K} + \tilde{\mathbf{W}} \right)^{-1} \frac{\partial \tilde{\mathbf{W}}}{\partial \phi} \left( \mathbf{K} + \tilde{\mathbf{W}} \right)^{-1} \tilde{\mathbf{t}} - \frac{1}{2} \text{tr} \left( \left( \mathbf{K} + \tilde{\mathbf{W}} \right)^{-1} \frac{\partial \tilde{\mathbf{W}}}{\partial \phi} \right) + \frac{\partial}{\partial \phi} r(\phi) \quad (116)$$

$$= \frac{1}{2} \text{tr} \left[ \left( \mathbf{z} \mathbf{z}^T - \left( \mathbf{K} + \tilde{\mathbf{W}} \right)^{-1} \right) \frac{\partial \tilde{\mathbf{W}}}{\partial \phi} \right] + \frac{\dot{a}(\phi)}{a(\phi)} \left( \frac{n}{2} - \mathbf{1}^T \tilde{\mathbf{v}} - \frac{1}{2} \tilde{\mathbf{u}}^T \tilde{\mathbf{W}} \tilde{\mathbf{u}} \right) + \sum_{i=1}^n \dot{c}(\phi, y_i) \quad (117)$$

$$= \frac{\dot{a}(\phi)}{a(\phi)} \left\{ \frac{1}{2} \text{tr} \left[ \left( \mathbf{z} \mathbf{z}^T - \left( \mathbf{K} + \tilde{\mathbf{W}} \right)^{-1} \right) \tilde{\mathbf{W}} \right] + \frac{n}{2} - \mathbf{1}^T \tilde{\mathbf{v}} - \frac{1}{2} \tilde{\mathbf{u}}^T \tilde{\mathbf{W}} \tilde{\mathbf{u}} \right\} + \sum_{i=1}^n \dot{c}(\phi, y_i) \quad (118)$$

$$= \frac{\dot{a}(\phi)}{a(\phi)} \left\{ \frac{1}{2} \mathbf{z}^T \tilde{\mathbf{W}} \mathbf{z} - \frac{1}{2} \text{tr} \left[ \left( \mathbf{K} + \tilde{\mathbf{W}} \right)^{-1} \tilde{\mathbf{W}} \right] + \frac{n}{2} - \mathbf{1}^T \tilde{\mathbf{v}} - \frac{1}{2} \tilde{\mathbf{u}}^T \tilde{\mathbf{W}} \tilde{\mathbf{u}} \right\} + \sum_{i=1}^n \dot{c}(\phi, y_i) \quad (119)$$

A.3.3 DERIVATIVE WRT DISPERSION WHEN  $b_\phi(\theta)$ 

We next look at the special case where the term  $b_\phi(\theta)$  is also a function of  $\phi$ . We first note that

$$\begin{aligned} \frac{\partial}{\partial \phi} \tilde{w}_i &= \dot{a}(\phi) \left\{ \ddot{b}_\phi(\theta(\tilde{\eta}_i)) \dot{\theta}(\tilde{\eta}_i)^2 - \left[ T(y_i) - \dot{b}_\phi(\theta(\tilde{\eta}_i)) \right] \ddot{\theta}(\tilde{\eta}_i) \right\}^{-1} \\ &\quad - a(\phi) \frac{\dot{\theta}(\tilde{\eta}_i)^2 \frac{\partial}{\partial \phi} \ddot{b}_\phi(\theta(\tilde{\eta}_i)) + \ddot{\theta}(\tilde{\eta}_i) \frac{\partial}{\partial \phi} \dot{b}_\phi(\theta(\tilde{\eta}_i))}{\left\{ \ddot{b}_\phi(\theta(\tilde{\eta}_i)) \dot{\theta}(\tilde{\eta}_i)^2 - \left[ T(y_i) - \dot{b}_\phi(\theta(\tilde{\eta}_i)) \right] \ddot{\theta}(\tilde{\eta}_i) \right\}^2} \end{aligned} \quad (120)$$

$$= \frac{\dot{a}(\phi)}{a(\phi)} \tilde{w}_i - \frac{1}{a(\phi)} \tilde{w}_i^2 \left[ \dot{\theta}(\tilde{\eta}_i)^2 \frac{\partial}{\partial \phi} \ddot{b}_\phi(\theta(\tilde{\eta}_i)) + \ddot{\theta}(\tilde{\eta}_i) \frac{\partial}{\partial \phi} \dot{b}_\phi(\theta(\tilde{\eta}_i)) \right], \quad (121)$$

$$\frac{\partial}{\partial \phi} \tilde{u}_i = -\frac{\dot{a}(\phi)}{a(\phi)^2} \dot{\theta}(\tilde{\eta}_i) \left[ T(y_i) - \dot{b}_\phi(\theta(\tilde{\eta}_i)) \right] - \frac{\dot{\theta}(\tilde{\eta}_i)}{a(\phi)} \frac{\partial}{\partial \phi} \dot{b}_\phi(\theta(\tilde{\eta}_i)) = -\frac{\dot{a}(\phi)}{a(\phi)} \tilde{u}_i - \frac{\dot{\theta}(\tilde{\eta}_i)}{a(\phi)} \frac{\partial}{\partial \phi} \dot{b}_\phi(\theta(\tilde{\eta}_i)), \quad (122)$$

$$\frac{\partial}{\partial \phi} (\tilde{w}_i \tilde{u}_i^2) = \frac{\partial \tilde{w}_i}{\partial \phi} \tilde{u}_i^2 + 2\tilde{w}_i \tilde{u}_i \frac{\partial \tilde{u}_i}{\partial \phi}, \quad \frac{\partial}{\partial \phi} \tilde{t}_i = \frac{\partial}{\partial \phi} (\tilde{\eta}_i + \tilde{w}_i \tilde{u}_i) = \tilde{w}_i \frac{\partial \tilde{u}_i}{\partial \phi} + \tilde{u}_i \frac{\partial \tilde{w}_i}{\partial \phi}, \quad (123)$$

$$\frac{\partial}{\partial \phi} \log p(y_i | \theta(\tilde{\eta}_i)) = -\frac{\dot{a}(\phi)}{a(\phi)^2} [T(y_i) \theta(\tilde{\eta}_i) - b_\phi(\theta(\tilde{\eta}_i))] - \frac{1}{a(\phi)} \frac{\partial}{\partial \phi} b_\phi(\theta(\tilde{\eta}_i)) + \dot{c}(\phi, y_i) \quad (124)$$

$$= -\frac{\dot{a}(\phi)}{a(\phi)} \tilde{v}_i + \dot{c}(\phi, y_i) - \frac{1}{a(\phi)} \frac{\partial}{\partial \phi} b_\phi(\theta(\tilde{\eta}_i)). \quad (125)$$

Thus,

$$\frac{\partial}{\partial \phi} r_i(\phi) = \frac{\partial}{\partial \phi} \log p(y_i | \theta(\tilde{\eta}_i)) + \frac{1}{2} \left[ \frac{\partial \tilde{w}_i}{\partial \phi} \tilde{u}_i^2 + 2\tilde{w}_i \tilde{u}_i \frac{\partial \tilde{u}_i}{\partial \phi} \right] + \frac{1}{2} \frac{1}{\tilde{w}_i} \frac{\partial \tilde{w}_i}{\partial \phi} \quad (126)$$

For the first term in (48),

$$\frac{\partial}{\partial \phi} \left[ \tilde{\mathbf{t}}^T (\tilde{\mathbf{W}} + \mathbf{K})^{-1} \tilde{\mathbf{t}} \right] = \tilde{\mathbf{t}}^T \frac{\partial (\tilde{\mathbf{W}} + \mathbf{K})^{-1}}{\partial \phi} \tilde{\mathbf{t}} + 2\tilde{\mathbf{t}}^T (\tilde{\mathbf{W}} + \mathbf{K})^{-1} \frac{\partial \tilde{\mathbf{t}}}{\partial \phi} \quad (127)$$

$$= -\tilde{\mathbf{t}}^T (\mathbf{K} + \tilde{\mathbf{W}})^{-1} \frac{\partial \tilde{\mathbf{W}}}{\partial \phi} (\mathbf{K} + \tilde{\mathbf{W}})^{-1} \tilde{\mathbf{t}} + 2\tilde{\mathbf{t}}^T (\tilde{\mathbf{W}} + \mathbf{K})^{-1} \frac{\partial \tilde{\mathbf{t}}}{\partial \phi}. \quad (128)$$

For the second term in (48),

$$\frac{\partial}{\partial \phi} \log |\mathbf{K} + \tilde{\mathbf{W}}| = \text{tr}((\mathbf{K} + \tilde{\mathbf{W}})^{-1} \frac{\partial \tilde{\mathbf{W}}}{\partial \phi}). \quad (129)$$

Finally, we have

$$\begin{aligned} \frac{\partial}{\partial \phi} \log q(\mathbf{y} | \mathbf{X}) &= \frac{1}{2} \tilde{\mathbf{t}}^T (\mathbf{K} + \tilde{\mathbf{W}})^{-1} \frac{\partial \tilde{\mathbf{W}}}{\partial \phi} (\mathbf{K} + \tilde{\mathbf{W}})^{-1} \tilde{\mathbf{t}} - \tilde{\mathbf{t}}^T (\tilde{\mathbf{W}} + \mathbf{K})^{-1} \frac{\partial \tilde{\mathbf{t}}}{\partial \phi} \\ &\quad - \frac{1}{2} \text{tr}((\mathbf{K} + \tilde{\mathbf{W}})^{-1} \frac{\partial \tilde{\mathbf{W}}}{\partial \phi}) + \sum_i \frac{\partial}{\partial \phi} r_i(\phi). \end{aligned} \quad (130)$$

## Appendix B. Taylor approximation for specific GGPMs

This appendix contains the derivatives and target functions used to derive the special cases of Taylor approximation in Section 5.2.5.

**Binomial/Bernoulli** – The derivative functions are

$$u(\eta, y) = N\left(y - \frac{e^\eta}{1+e^\eta}\right), \quad w(\eta, y) = \frac{(1+e^\eta)^2}{Ne^\eta}.$$

Thus, for a given expansion point  $\tilde{\eta}_i$ , the target and effective noise are

$$\tilde{t}_i = \tilde{\eta}_i + \frac{(1+e^{\tilde{\eta}_i})^2}{e^{\tilde{\eta}_i}}\left(y_i - \frac{e^{\tilde{\eta}_i}}{1+e^{\tilde{\eta}_i}}\right), \quad \tilde{w}_i = \frac{(1+e^{\tilde{\eta}_i})^2}{Ne^{\tilde{\eta}_i}}.$$

**Poisson** – The derivative functions are

$$u(\eta, y) = y - e^\eta, \quad w(\eta, y) = e^{-\eta}.$$

Thus, given an expansion point  $\tilde{\eta}_i$ , the target and effective noise are

$$\tilde{t}_i = \tilde{\eta}_i + (y_i e^{-\tilde{\eta}_i} - 1), \quad \tilde{w}_i = e^{-\tilde{\eta}_i}. \quad (131)$$

**Gamma** – The derivatives of the Gamma<sub>sh</sub>likelihood (mean parameter, shape hyperparameter) are

$$u(\eta, y) = \nu e^{-\eta}(y - e^\eta) = \nu(ye^{-\eta} - 1), \quad w(\eta, y) = \frac{1}{\nu}(1 + ye^{-\eta} - 1)^{-1} = \frac{1}{\nu ye^{-\eta}}.$$

Thus, given an expansion point  $\tilde{\eta}_i$ , the target and effective noise are

$$\tilde{t}_i = \tilde{\eta}_i + \frac{1}{\nu y_i e^{-\tilde{\eta}_i}} \nu(y_i e^{-\tilde{\eta}_i} - 1) = \tilde{\eta}_i + 1 - \frac{1}{y_i e^{-\tilde{\eta}_i}}, \quad \tilde{w}_i = \frac{1}{\nu y_i e^{-\tilde{\eta}_i}}. \quad (132)$$

**Inverse Gaussian** – The derivatives of the Inverse Gaussian likelihood are

$$u(\eta, y) = \phi e^{-\eta}[y - (2e^{-\eta})^{-1/2}], \quad w(\eta, y) = \phi\{(8e^\eta)^{-1/2} + [y - (2e^{-\eta})^{-1/2}]e^{-\eta}\}^{-1}.$$

Using the canonical expansion point,  $\tilde{\eta}_i = \log(2y_i^2)$ , yields

$$u(\tilde{\eta}_i, y_i) = 0, \quad w(\tilde{\eta}_i, y_i) = 4\phi y_i. \quad (133)$$

**Beta** – Consider an agnostic choice of the expansion point,  $\tilde{\eta}_i = 0$ , and hence  $\tilde{\theta}_i = \theta(\tilde{\eta}_i) = \frac{1}{2}$ . We also have,

$$\dot{\theta}(\tilde{\eta}_i) = \frac{e^{\tilde{\eta}_i}}{(1 + e^{\tilde{\eta}_i})^2} = \frac{1}{4}, \quad \ddot{\theta}(\tilde{\eta}_i) = \frac{e^{\tilde{\eta}_i}(e^{\tilde{\eta}_i} - 1)}{(1 + e^{\tilde{\eta}_i})^3} = 0. \quad (134)$$

Looking at the 1st and 2nd derivatives of  $b(\theta)$  at  $\tilde{\theta}_i$ , we have

$$\dot{b}(\tilde{\theta}_i) = \psi_0\left(\frac{\tilde{\theta}_i}{\phi}\right) - \psi_0\left(\frac{1-\tilde{\theta}_i}{\phi}\right) = \psi_0\left(\frac{1}{2\phi}\right) - \psi_0\left(\frac{1}{2\phi}\right) = 0, \quad (135)$$

$$\ddot{b}(\tilde{\theta}_i) = \frac{1}{\phi}\psi_1\left(\frac{\tilde{\theta}_i}{\phi}\right) + \frac{1}{\phi}\psi_1\left(\frac{1-\tilde{\theta}_i}{\phi}\right) = \frac{2}{\phi}\psi_1\left(\frac{1}{2\phi}\right). \quad (136)$$

Using the above results, we can now calculate the derivative functions at  $\tilde{\eta}_i = 0$ ,

$$\tilde{u}_i = u(\tilde{\eta}_i, y_i) = \frac{1}{\phi} \dot{\theta}(\tilde{\eta}_i) \left[ T(y_i) - \dot{b}(\tilde{\theta}_i) \right] = \frac{1}{4\phi} T(y_i) = \frac{1}{4\phi} \log \frac{y_i}{1 - y_i}, \quad (137)$$

$$\tilde{w}_i = w(\tilde{\eta}_i, y_i) = \frac{\phi}{\ddot{b}(\tilde{\theta}_i) \dot{\theta}(\tilde{\eta}_i)^2 - 0} = \frac{\phi}{\frac{2}{\phi} \psi_1\left(\frac{1}{2\phi}\right) \frac{1}{4^2}} = \frac{8\phi^2}{\psi_1\left(\frac{1}{2\phi}\right)}. \quad (138)$$

which yields the targets,

$$\tilde{t}_i = \tilde{\eta}_i + \tilde{w}_i \tilde{u}_i = \frac{2\phi}{\psi_1\left(\frac{1}{2\phi}\right)} \log \frac{y_i}{1 - y_i}. \quad (139)$$

## Acknowledgements

The authors thank CE Rasmussen and CKI Williams for the GPML code (Rasmussen and Nickisch, 2010). This work was supported by City University of Hong Kong (internal grant 7200187), and by the Research Grants Council of the Hong Kong Special Administrative Region, China (CityU 110610 and CityU 123212)

## References

- J.H. Albert. Computational methods using a Bayesian hierarchical generalized linear model. *Journal of the American Statistical Association*, 83(404):1037–1044, Dec. 1988.
- Edward J. Bedrick, Ronald Christensen, and Wesley Johnson. A new perspective on priors for generalized linear models. *Journal of the American Statistical Association*, 91(436):1450–1460, December 1996.
- Clemens Biller. Adaptive Bayesian regression splines in semiparametric generalized linear models. *Journal of Computational and Graphical Statistics*, 9(1):122–140, 2000.
- Liefeng Bo and Cristian Sminchisescu. Twin Gaussian processes for structured prediction. *International Journal of Computer Vision*, 87(1):28–52, 2010.
- Gavin C. Cawley, Gareth J. Janacek, and Nicola LC Talbot. Generalised kernel machines. In *International Joint Conference on Neural Networks*, pages 1720–1725. IEEE, 2007.
- A. B. Chan. Supplemental material of “on approximate inference for generalized gaussian process models”. Technical report, City University of Hong Kong, July 2013.
- Antoni B. Chan and Daxiang Dong. Generalized Gaussian process models. In *IEEE Conf. Computer Vision and Pattern Recognition*, pages 2681–2688, 2011.
- Antoni B. Chan and Nuno Vasconcelos. Bayesian Poisson regression for crowd counting. In *IEEE Intl Conf. Computer Vision*, pages 545–551, 2009.
- Antoni B. Chan, Z. S. J. Liang, and Nuno Vasconcelos. Privacy preserving crowd monitoring: Counting people without people models or tracking. In *IEEE Conference on Computer Vision and Pattern Recognition*, pages 1–7, 2008.



- Jixu Chen, Minyoung Kim, Yu Wang, and Qiang Ji. Switching Gaussian process dynamic models for simultaneous composite motion tracking and recognition. In *IEEE Conf. Computer Vision and Pattern Recognition*, pages 2655–2662, Los Alamitos, CA, USA, 2009.
- Wei Chu and Zoubin Ghahramani. Gaussian processes for ordinal regression. *Journal of Machine Learning and Research*, 6:1019–1041, 2005.
- R. W Conway and W. L. Maxwell. A queuing model with state dependent service rates. *Journal of Industrial Engineering*, 12:132–136, 1962.
- T.F. Cootes, G.J. Edwards, and C.J. Taylor. Active appearance models. *IEEE TPAMI*, 23.6:681–685, 2001.
- Sourish Das and Dipak K. Dey. On Bayesian analysis of generalized linear models: A new perspective. Technical report, Statistical and Applied Mathematical Sciences Institute, 2007.
- Peter J. Diggle, JA Tawn, and RA Moyeed. Model-based geostatistics. *Journal of the Royal Statistical Society: Series C (Applied Statistics)*, 47(3):299–350, 1998.
- Richard O. Duda, Peter E. Hart, and David G. Stork. *Pattern Classification*. John Wiley and Sons, 2001.
- D. Ellis, E. Sommerlade, and I. Reid. Modelling pedestrian trajectory patterns with Gaussian processes. In *International Conference Computer Vision Workshops (ICCV Workshops)*, pages 1229–1234, 2009.
- Ludwig Fahrmeir, Gerhard Tutz, and Wolfgang Hennevogl. *Multivariate statistical modelling based on generalized linear models*, volume 2. Springer New York, 1994.
- Martin Fergie and Aphrodite Galata. Local Gaussian processes for pose recognition from noisy inputs. In *Proceedings of the British Machine Vision Conference*, pages 98.1–98.11. BMVA Press, 2010. ISBN 1-901725-38-3.
- Mark Gibbs and David J. C. Mackay. Variational Gaussian process classifiers. *IEEE Transactions on Neural Networks*, 11:1458–1464, 2000.
- Mark Girolami and Simon Rogers. Variational Bayesian multinomial probit regression with Gaussian process priors. *Neural Computation*, 18:1790–1817, 2006.
- Seth D. Guikema and Jeremy P. Goffelt. A flexible count data regression model for risk analysis. *Risk Analysis*, 28(1):213–223, 2008.
- Dong Han, Liefeng Bo, and Cristian Sminchisescu. Selection and context for action recognition. In *International Conference on Computer Vision*, pages 1933–1940, sep. 2009.
- Lauren A. Hannah, David M. Blei, and Warren B. Powell. Dirichlet process mixtures of generalized linear models. *Journal of Machine Learning Research*, 12:1923–1953, 2011.
- Ville Heikkinen, Reiner Lenz, Tuija Jetsu, Jussi Parkkinen, Markku Hauta-Kasari, and Timo Jääskeläinen. Evaluation and unification of some methods for estimating reflectance spectra from rgb images. *J. Opt. Soc. Am. A*, 25(10):2444–2458, Oct 2008.

- David C. Howell. *Fundamental Statistics for the Behavioral Sciences*. PSY 200 (300) Quantitative Methods in Psychology Series. Wadsworth Cengage Learning, 2010. ISBN 9780495811251.
- Pasi Jylänki, Jarno Vanhatal, and Aki Vehtari. Robust Gaussian process regression with a student-t likelihood. *J. Machine Learning Research*, 12:3227–3257, 2011.
- Ashish Kapoor, Kristen Grauman, Raquel Urtasun, and Trevor Darrell. Gaussian processes for object categorization. *International Journal of Computer Vision*, 88:169–188, 2010.
- Hyun-Chul Kim and Zoubin Ghahramani. Bayesian Gaussian process classification with the EM-EP algorithm. *IEEE Transactions on Pattern Analysis and Machine Intelligence*, 28(12):1948–1959, 2006.
- Genshiro Kitagawa. Non-Gaussian state-space modeling of nonstationary time series. *Journal of the American statistical association*, 82(400):1032–1041, 1987.
- Malte Kuss. *Gaussian Process Models for Robust Regression, Classification, and Reinforcement Learning*. PhD thesis, Technische Universität Darmstadt, 2006.
- Malte Kuss and Carl Edward Rasmussen. Assessing approximate inference for binary Gaussian process classification. *Journal of Machine Learning Research*, 6:1679–1704, 2005.
- Chen Change Loy, Tao Xiang, and Shaogang Gong. Modelling multi-object activity by Gaussian processes. In *British Machine Vision Conference*, 2009.
- Opper Manfred and Cédric Archambeau. The variational Gaussian approximation revisited. *Neural Computation*, 21(3):786–792, March 2009.
- P. McCullagh and J.A. Nelder. *Generalized linear models*. Chapman & Hall, CRC, 1989. ISBN 9780412317606.
- Thomas P. Minka. *A family of algorithms for approximate Bayesian inference*. PhD thesis, Massachusetts Institute of Technology, 2001.
- Radford M. Neal. Monte Carlo implementation of Gaussian process models for Bayesian regression and classification. Technical report, Dept. of Statistics, University of Toronto, 1997. URL [arXiv:physics/9701026v2](https://arxiv.org/abs/physics/9701026v2).
- Hannes Nickisch and Carl Edward Rasmussen. Approximations for binary Gaussian process classification. *Journal of Machine Learning Research*, 9:2035–2078, 2008.
- Hannes Nickisch and Matthias W. Seeger. Convex variational Bayesian inference for large scale generalized linear models. In *International Conference on Machine Learning*, pages 761–768, New York, NY, USA, 2009. ACM. ISBN 978-1-60558-516-1.
- Basilio Noris, Karim Benmachiche, and A. Billard. Calibration-free eye gaze direction detection with Gaussian processes. In *International Conference on Computer Vision Theory and Applications*, 2008.
- Christopher J. Paciorek and Mark J. Schervish. Nonstationary covariance functions for Gaussian process regression. In *Advances in Neural Information Processing Systems*, pages 273–280, 2004.

- Christian Plagemann, Kristian Kersting, Patrick Pfaff, and Wolfram Burgard. Gaussian beam processes: A nonparametric Bayesian measurement model for range finders. In *In Proc. of Robotics: Science and Systems (RSS)*, 2007.
- Leonid Raskin, Michael Rudzsky, and Ehud Rivlin. Tracking and classifying of human motions with Gaussian process annealed particle filter. In *Asian conference on Computer vision*, pages 442–451, Berlin, Heidelberg, 2007. Springer-Verlag. ISBN 3-540-76385-6, 978-3-540-76385-7.
- Carl Edward Rasmussen and Hannes Nickisch. Gaussian processes for machine learning (GPML) toolbox. *Journal of Machine Learning Research*, 11:3011–15, Nov 2010.
- Carl Edward Rasmussen and Christopher K. I. Williams. *Gaussian Processes for Machine Learning*. MIT Press, 2006.
- Terrance Savitsky and Marina Vannucci. Spiked Dirchlet process priors for Gaussian process models. *Journal of Probability and Statistics*, 2010, 2010.
- Terrance Savitsky, Marina Vannucci, and Naijun Sha. Variable selection for nonparametric Gaussian process priors: Models and computational strategies. *Statistical Science*, 26(1):130–149, 2011.
- Matthias Seeger. Gaussian processes for machine learning. *International Journal of Neural Systems*, 14(2):69–106, 2004.
- Matthias Seeger, Sebastian Gerwinn, and Matthias Bethge. Bayesian inference for sparse generalized linear models. In *Machine Learning: ECML 2007*, pages 298–309, 2007.
- Jian Qing Shi and Taeryon Choi. *Gaussian Process Regression Analysis for Functional Data*. CRC Press, Taylor & Francis Group, 2011.
- Galit Shmueli, Thomas P Minka, Joseph B Kadane, Sharad Borle, and Peter Boatwright. A useful distribution for fitting discrete data: revival of the conway-maxwell-poisson distribution. *Journal of the Royal Statistical Society: Series C (Applied Statistics)*, 54(1):127–142, 2005.
- F Sinz, Q Candela, GH Bakir, CE Rasmussen, and M Franz. Learning depth from stereo. In *In Pattern Recognition, Proc. 26th DAGM Symposium*, pages 245–252. Springer, 2004.
- Edward Snelson, Carl Edward Rasmussen, and Zoubin Ghahramani. Warped Gaussian processes. In *Advances in Neural Information Processing Systems*, pages 337–344. MIT Press, 2004.
- Yee Whye Teh, Matthias Seeger, and M I Jordan. Semiparametric latent factor models. In *Artificial Intelligence and Statistics*, 2005.
- Volker Tresp. The generalized Bayesian committee machine. In *ACM International conference on Knowledge discovery and data mining*, pages 130–139, New York, NY, USA, 2000. ACM.
- Raquel Urtasun and Trevor Darrell. Sparse probabilistic regression for activity-independent human pose inference. In *IEEE Conf. Computer Vision and Pattern Recognition*, pages 1–8, 2008.
- Raquel Urtasun, David J Fleet, Aaron Hertzmann, and Pascal Fua. Priors for people tracking from small training sets. In *IEEE International Conference on Computer Vision*, pages 403–410, 2005.

- Jarno Vanhatalo and Aki Vehtari. Sparse log Gaussian processes via MCMC for spatial epidemiology. In *Workshop on Gaussian Processes in Practice*, 2007.
- Jarno Vanhatalo, Pasi Jylänki, and Aki Vehtari. Gaussian process regression with Student-t likelihood. In *Neural Information Processing Systems*, 2009.
- Jarno Vanhatalo, Ville Pietiläinen, and Aki Vehtari. Approximate inference for disease mapping with sparse Gaussian processes. *Statistics in Medicine*, 29(15):1580–1607, 2010.
- Jarno Vanhatalo, Jaakko Riihimäki, Jouni Hartikainen, and Aki Vehtari. Bayesian modeling with Gaussian processes using the MATLAB toolbox GP-stuff. *submitted*, 2011.
- Jack M. Wang, David J. Fleet, and Aaron Hertzmann. Gaussian process dynamical models for human motion. *IEEE Transactions on Pattern Analysis and Machine Intelligence*, 30(2):283–298, Feb. 2008.
- Christopher K. I. Williams and David Barber. Bayesian classification with Gaussian processes. *IEEE Transactions on Pattern Analysis and Machine Intelligence*, 20(12):1342–1351, Dec. 1998.
- Oliver Williams. A switched Gaussian process for estimating disparity and segmentation in binocular stereo. In *Advances in Neural Information Processing Systems*, 2006.
- Yu Zhang and Dit-Yan Yeung. Multi-task warped Gaussian process for personalized age estimation. In *Conference on Computer Vision and Pattern Recognition*, pages 2622–2629, 2010.
- Zhihua Zhang, G. Dai, D. Wang, and M. I. Jordan. Bayesian generalized kernel models. In *Conference on Artificial Intelligence and Statistics*, volume 9, pages 972–979, 2010.
- Xu Zhao, Huazhong Ning, Yuncai Liu, and T. Huang. Discriminative estimation of 3d human pose using Gaussian processes. In *Intl Conf. Pattern Recognition*, pages 1–4, Dec. 2008.
- Jianke Zhu, Steven CH Hoi, and Michael R Lyu. Nonrigid shape recovery by Gaussian process regression. In *IEEE Conference on Computer Vision and Pattern Recognition*, pages 1319–1326, Jun. 2009.